Modeling studies of biological gas desulfurization under haloalkaline conditions

Johannes B.M. Klok

Thesis committee

Promotor
Prof. Dr A.J.H. Janssen
Special professor Biological Gas and Water Treatment
Wageningen University

Co-promotor
Dr K.J. Keesman
Associated professor, Biobased Chemistry and Technology
Wageningen University

Other members
Prof. Dr J. Molenaar, Wageningen University
Dr J. Bontsema, Wageningen University
Prof. Dr G. Muyzer, University of Amsterdam
Prof. Dr P.N.L. Lens, UNESCO-IHE, Delft

This research was conducted under the auspices of the Graduate School SENSE (Socio-Economic and Natural Sciences of the Environment)

Modeling studies of biological gas desulfurization under haloalkaline conditions

Johannes B.M. Klok

Thesis
submitted in fulfilment of the requirements for the degree of doctor
at Wageningen University
by the authority of the Academic Board,
in the presence of the
Thesis Committee appointed by the Academic Board
to be defended in public
on Tuesday 26 May 2015
at 1:30 p.m. in the Aula.

Author: Klok, Johannes Bernardus Maria
Modeling studies of biological gas desulfurization under haloalkaline conditions
172 pages.

PhD thesis, Wageningen University, Wageningen, NL (2015)
With references, with summaries in Dutch and English

ISBN 978-94-6257-298-0

Abstract

Biogas, synthesis and natural gas streams often require treatment because of the presence of gaseous hydrogen sulphide (H_2S). About 25 years ago, a biotechnological gas treatment process was developed as an alternative to the conventionally applied technologies. This process is known as the Thiopaq process and offers a number of advantages compared to the existing physical-chemical processes. Depending on the process conditions, H_2S is oxidized to elemental bio-sulfur (90-94 mol%) and sulphate (6-10 mol%). In order to enable cost effective large scale applications, the selectivity for sulfur production should be increased to more than 97 mol%. Hence, a better understanding of the combined effect of abiotic and biological reaction kinetics and the relation to hydrodynamic characteristics is required. The first part of this PhD study focuses on biological reaction kinetics and biological pathways for sulphide oxidation that occur in the process at haloalkaline conditions. It was found that two different sulfide oxidizing enzyme systems are present in haloalkaline sulfide oxidizing bacteria. It has been hypothesized that the different enzymatic routes are determined by the process conditions. Both enzyme systems were taken into account to propose and validate a new physiological mathematical model that can handle multi-substrates and multi-products. In the second part of the thesis, this model was evaluated via a normalized sensitivity method and it was demonstrated that certain key parameters affect the activity of the biomass at different substrate levels. Furthermore, from CSTR simulations it has been demonstrated that non-linear effects are of importance when scaling up from lab-scale to full-scale industrial units. Finally, the developed kinetic models have been incorporated in a full-scale biodesulfurization model that includes the effects of turbulent flow regimes and mass transfer of oxygen. This enables us to better understand the overall process. Moreover, the model can also be used as a tool to design model-based control strategies which will lead to better overall process performance, i.e. maximize sulfur production and minimize chemical consumption rates.

Contents

1 General introduction 1
1.1 Introduction 2
1.2 Biological desulfurization processes 3
1.3 Haloalkaline biological desulfurization 6
1.4 Research objectives and scope of the thesis 7
1.5 Bioprocess control 8
1.6 Modeling biochemical processes 9
1.7 Double substrate 11
1.8 Modeling biodesulfurization processes 13
1.9 Outline of the thesis 16

I Pathways & Kinetics 23

2 Pathways of sulfide oxidation by haloalkaliphilic bacteria in oxygen-limited-gas lift bioreactors 25
2.1 Introduction 26
2.2 Materials and methods 28
2.2.1 Experimental setup 28
2.2.2 Medium 28
2.2.3 Inoculum 28
2.2.4 Reactor operation 29
2.2.5 Redox control 29
2.2.6 Analysis 29
2.2.7 Biomass concentration 30
2.2.8 Growth yields 30
2.3 Results and discussion 31
2.3.1 Product Selectivity at pH 8.5 31
2.3.2 Mass balancing 32
2.3.3 Role of Limited Oxygen Route in Oxygen Balance 33
2.3.4 LOR in *Thiobacillus* species 36
2.3.5 Considerations 36

3 A physiologically based kinetic model for bacterial sulfide oxidation 43

3.1 Introduction 44
3.2 Materials and methods 45
3.2.1 Biomass source 45
3.2.2 Respiration tests 45
3.2.3 Bench scale tests 45
3.2.4 Chemicals used 46
3.3 Kinetic model 46
3.3.1 Stoichiometric relationships 46
3.3.2 The influence of the cytochrome pool 48
3.3.3 Modeling the cytochrome pool 49
3.3.4 Modeling the quinone pool 50
3.3.5 Modeling product selectivity 51
3.4 Results and discussion 52
3.4.1 Chemical oxidation 52
3.4.2 Biological oxidation 52
3.4.3 Parameter estimation 53
3.4.4 Model validation 55
3.4.5 Effect of disturbances 56
3.4.6 Physiologically based modeling in N-cycle 58
3.5 Conclusions 58

4 Temperature effects on the biological desulfurization process 65
4.1 Introduction 66
4.2 Materials and methods 67
4.2.1 Bench scale tests 67
4.2.2 Biomass respiration tests 67
4.2.3 Medium 68
4.2.4 Inoculum 68
4.3 Results and discussion 68
4.4 Conclusions 73
4.5 Acknowledgements 74

II Development of a dynamic model to describe sulfide oxidizing bioreactors 77

5 Input and parameter sensitivity analysis of a physiologically based sulfide oxidation model 79
5.1 Introduction 80
5.2 Kinetic models for sulfide oxidation 82
5.3 Materials and methods 84
5.3.1 Input and parameter sensitivity 84
5.3.2 Response surface methodology 85
5.4 Numerical results and discussion 86
5.4.1 Parameter sensitivity 86
5.4.2 Input sensitivity 89

5.4.3 Applications of sensitivity methods 93
5.5 Conclusions 93

6 Modelling of full-scale haloalkaline biodesulfurization systems 97
6.1 Nomenclature 98
6.2 Introduction 99
6.3 Development of a simulation model to describe a full-scale biodesulfurization reactor 102
6.3.1 Description of biological and abiotic kinetics 102
6.3.2 Oxygen and fluid mass transfer 104
6.3.3 Industriewater Eerbeek B.V. 105
6.4 Materials and Methods 106
6.4.1 Respiration tests 106
6.4.2 Chemicals used 107
6.5 Results and Discussion 107
6.5.1 ORP models 107
6.5.2 Full-scale model 109
6.5.3 Concluding remarks 111

III Discussions & Summary 115

7 General discussion 117
7.1 Introduction 118
7.2 Reaction pathways and kinetics 120
7.2.1 Two enzyme systems 120
7.3 Models 121
7.3.1 Physically based kinetic model 121
7.3.2 Respiration kinetics 121
7.3.3 Sensitivities and surface methodology 122
7.3.4 Dynamic models in bench and full-scale systems 123
7.3.5 Full-scale model considerations 123
7.3.6 Research objectives 124
7.4 Final considerations 125

8 Summary 131

8 Samenvatting 135

IV Appendices 139

A Non-linear least-squares estimation physiologically based model 141

B Parameter estimation results physiologically based model 145

C Thermal inactivation 147

D Sensitivity functions 151

E Meta models 153

List of publications 155

Dankwoord 157

Chapter 1

General introduction

1.1 Introduction

The biological sulfur cycle is one of the most active biological nutrient cycles [1]. Sulfur atoms occur in nine different oxidation states. Predominantly -2 (H_2S), 0 (S^0) and +6 ($SO_4{}^{2-}$) are found in nature. Sulfur can also be found in volatile organic sulfur compounds (VOSC) and makes up about 2% of the dry weight of organisms. Coenzyme A [2] and the nitrogen-fixing nitrogenase enzymes [3] are examples of natural sulfur-containing organic compounds.

The earliest form of life is attributed to cellular organization, which contained catalytic centers for the fixation of organic compounds from inorganic gasses, for instance carbon dioxide and hydrogen sulfide [4]. During an evolution of 3.5 billion years, an assortment of prebiotic molecules interacted and started to form more sophisticated compounds. At present, active complex communities of microorganisms drive nutrient cycles, such as the sulfur cycle, under a wide range of different (extreme) environmental conditions [5].

In the biological sulfur cycle, sulfur compounds are used as electron acceptors and electron donors. Whereas the pioneer bacteria were strictly **anaerobic**, later species were able to use oxygen as electron acceptor (**aerobic**). The bacteria that contribute to the global sulfur cycle use light (**phototrophs**) or oxidation of inorganic molecules (**chemotrophs**) as energy source. Chemotrophs are found in environments to which sunlight has no access, such as the deep sea and volcano fields.

A wide variety of microorganisms is capable of sulfur oxidation under a broad range of environmental conditions, displaying great metabolic diversity [6, 7, 8, 9]. The oxidation of reduced sulfur compounds yields energy, which enables bacterial maintenance and growth. On the other hand, when oxidized forms of sulfur diffuse into reducing habitats, it provides an opportunity for the reduction of sulfur-containing compounds to sulfide. An example is the dissimilatory reduction of sulfate carried out by *Desulfovibrio* and related microorganisms, used for anaerobic respiration [10]. The reduction of sulfate to sulfide also plays a role in the biosynthesis of proteins, as an assimilatory reduction process [11]. Other microorganisms carry out dissimilatory reduction of sulfite and elemental sulfur, such as thermophilic archaea [12], mycobacteria [13] and bacteria in hypersaline sediments [14]. Fig. 1.1 gives a schematic overview of the biological sulfur cycle.

Transformations in the sulfur cycle can also occur as the result of chemical reactions, i.e. in the absence of microorganisms when pH, temperature and oxidation-reduction conditions are favorable. An example is the formation of polysulfides (S_x^{2-}), stable forms of elemental sulfur at alkaline conditions (pH>8). Other sulfur compounds which can be chemically formed are inorganic elemental sulfur, thiosulfate ($S_2O_3^{2-}$) and polythionates. Chemically formed elemental sulfur has other properties than biologically formed sulfur; a major difference is that biosulfur is hydrophilic whereas inorganic sulfur is poorly dispersible in water [15].

Major sulfur reservoirs are contained in the oceans and freshwaters, on land and in the atmosphere. Sulfur is transported from the oceans to land following the release of mainly organic sulfur compounds from the sea surface [16]. In natural ecosystems, the sulfur cycle is generally in balance: equal amounts of inorganic sulfur compounds are being oxidized and

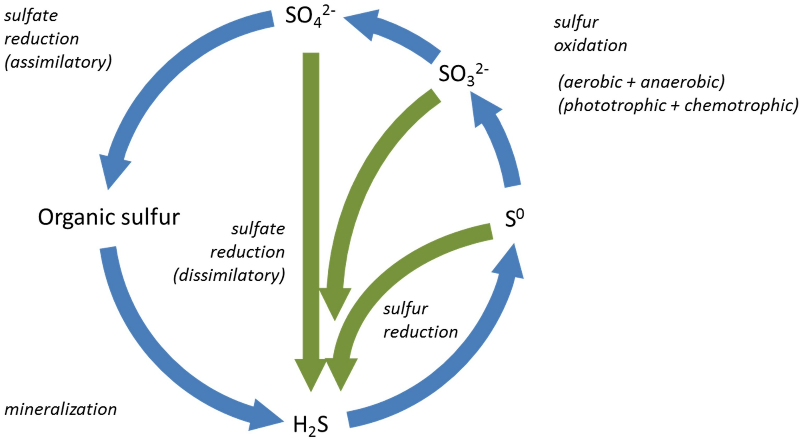

Figuur 1.1: The basic biological sulfur cycle. Green arrows indicate dissimilatory processes; blue arrows indicate assimilatory processes. Adapted from [5].

reduced. While the natural release of sulfur compounds remains important, anthropogenic emissions are taking over, primarily resulting from the burning of fossil fuels. Global sulfur dioxide (SO_2) emissions in 2008 were estimated at $97 \cdot 10^9$ kg S which anthropogenic emissions accounted for about 66% [17]. Increased SO_2 emissions to the atmosphere lead to the formation of acid compounds, which are deposited by rainfall or dry deposition [18]. This acid deposition strongly affects the environment as it induces the mobilization of toxic metals [19] and the acidification of (weakly buffered) ecosystems [20]. Hence, since the 1970s, a number of emission control strategies have been implemented to desulfurize anthropogenic waste gas streams such as flue gasses from coal-fired power plants [21].

In view of a future energy-constrained society, more effective power generation technologies will have to be developed, such as gasification of coal. Coal combustion produces roughly 27% of the world's energy and, particularly in China, the gasification of coal is becoming increasingly popular. During coal gasification, substantial amounts of S-containing pollutants are released, mainly in the form of hydrogen sulfide. At the current combustion rates, enough coal reserves are available to last more than a century. Some future energy demand models, however, predict an increase of 10% per year for the next thirty years [22]. The market for effective and cost-efficient desulfurization processes is therefore growing.

1.2 Biological desulfurization processes

Bulk removal of H_2S traditionally takes place by the application of physicochemical processes, such as the Amine-Claus-SCOT train [23]. These processes typically operate at high temperatures and pressures, and are therefore expensive, particularly in small-scale applications (i.e. H_2S loads up of to 20 tons day^{-1}). As microbiological sulfide oxidation happens at ambient temperatures and atmospheric pressures, biological desulfurization is a more cost-effective alternative [24].

In general, H_2S-containing gas or "sour" gas – is first humidified during bed irrigation, after which it is contacted with microorganisms attached to a fixed bed. Biofilters and biotrickling filters are often applied, mainly for odor removal as H_2S has an unpleasant smell [25]. A major drawback of these filters is their relative large footprint. In lab-scale setups, these filters have removal capacities of up to 300 gram H_2S m^{-3} h^{-1} [26]. A second drawback of these systems is the buildup of a pressure drop due to accumulation of biomass and S^0 formation.

In the 1980s and 1990s, the basic concept of a high-capacity biodesulfurization installation was developed at Wageningen University and Delft University of Technology in the Netherlands [27, 28]. Paques B.V. advanced this concept into a process for the treatment of biogas, which is a humid mixture mainly consisting of methane, carbon dioxide and hydrogen sulfide. The first unit for biogas desulfurization was built in 1993 [29]. Since then, more than 180 applications have been realized worldwide. Currently, the process is also used to treat high-pressure natural gas and oil refinery gasses. It is known as Thiopaq^{TM} and is commercialized by Paqell, a joint venture between Shell Global Solutions International B.V. and Paques B.V. [29].

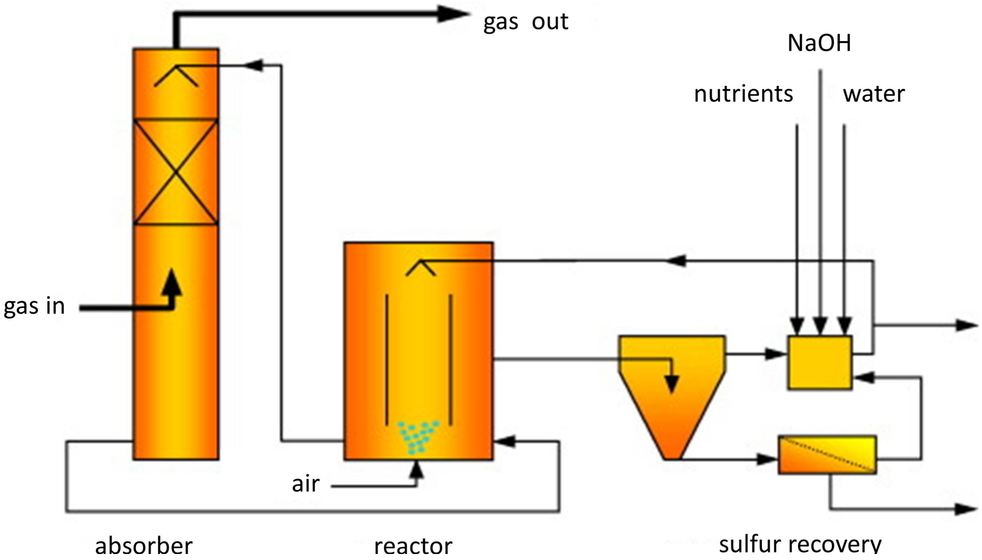

Figuur 1.2: Flow scheme of the bioscrubber process [21].

Figure 1.2 presents an overview of the process and its main (oxidation) reactions. The Thiopaq desulfurization process consists of three integrated sections [21]:

1. Absorption of H_2S into a mildly alkaline solution;
2. Sulfide oxidation to S^0, sulfate (SO_4^{2-}) and thiosulfate ($S_2O_3^{2-}$) in microaerophilic bioreactor;
3. Removal of the formed S^0 from the suspension.

Sour gas is directed to the bottom section of the **absorption column**. Hydrogen sulfide is absorbed in the alkaline washing solution (see Table 1.1, Eq. 1), thereby consuming alkalinity (see Table 1.1, Eq. 2). At the top of the absorber, the treated or "sweet"gas is sent to the gas grid for further processing, e.g. dehydration.

After absorption in the washing liquid, the dissolved sulfide (HS^{-1}) is fed to the **biological reactor**. In this reactor, bacteria (e.g. *Thioalkalivibrio* spp.) primarily oxidize the sulfide to elemental sulfur (S^0; see Table 1.1, Eq. 3). In addition, a relatively small fraction of the incoming sulfides is oxidized to SO_4^{2-} ions, typically < 10%mol (see Table 1.1, Eq. 4) [30]. Because of the greater change in the Gibbs free energy, bacteria prefer to oxidize sulfide to sulfate [27]. However, when sulfide levels are high and/or oxygen levels are becoming limiting, elemental sulfur is formed [31].

Besides biological oxidation, various abiotic oxidation processes can occur during biological desulfurization. The selectivity for product formation depends on the reactor conditions such as substrate levels, temperature and pH. $S_2O_3^{2-}$ is the main abiotically formed intermediate from the oxidation of sulfide and polysulfide (see Table 1.1, Eqs. 5-7) [32, 33].

Tabel 1.1: Main reaction equations occurring in the biological desulfurization process

	reaction	bio/chem	remarks
1	$H_2S(g) \rightleftharpoons H_2S(l)$	chem	-
2	$H_2S(l)+OH^- \rightleftharpoons HS^-+H_2O$	chem	-
3	$HS^-+\frac{1}{2}O_2 \rightarrow S^0+OH^-$	bio	-
4	$HS^-+2O_2 \rightarrow SO_4^{2-}+H^+$	bio	-
5	$2HS^-+2O_2 \rightarrow S_2O_3^{2-}+H_2O$	chem	-
6	$HS^-+(x-1)\ S^0 \rightleftarrows S_x^{2-}+H^+$	chem	pH>8.0
7	$S_x^{2-}+1\frac{1}{2}O_2 \rightarrow S_2O_3^{2-}+(x-2)\ S^0$	chem	-

The formation of elemental sulfur is preferred for several reasons. First, (thio)sulfate formation leads to the formation of protons and acidification of the medium. Furthermore, the addition of makeup water is required as (thio)sulfate can only be removed by means of a bleed stream. Second, elemental sulfur is more suitable for reuse as it can be applied for agricultural purposes. The formation of (thio)sulfate can be prevented by operating at low oxygen levels [34, 28] and at pH values between 8.0 and 9.0 [35].

Tabel 1.2: Composition natural gas and biogas

Component	Natural gas (%) [37]	Biogas from household waste (%) [38]	Biogas from WWTP sludge (%) [38]
CH_4	70 - 90	50 - 60	60 - 75
C_2H_6-C_4H_{10}	0 - 20	0	0
CO_2	0 - 8	34 - 38	19 - 33
N_2	0 - 5	0 - 5	0 - 1
H_2S	0 - 5	0.1 - 0.6	0.1 - 2.8

The reactor effluent is primary recirculated over the absorption column for H_2S removal and a much smaller flow is directed to a **gravity settler**, in which elemental sulfur particles are removed. The sulfur slurry is further dewatered in a decanter centrifuge or filter press. The purity of the recovered sulfur is 95 to 98 wt.%; the remainder consists of biomass and salts [36]. Nutrients are added to the filtrate before the stream is returned to the bioreactor.

1.3 Haloalkaline biological desulfurization

Natural gas and biogas are mixtures typically consisting of methane (CH_4) [37, 38], alkanes (C_2H_6-C_4H_{10}), carbon dioxide (CO_2), nitrogen (N_2) and hydrogen sulfide (H_2S). The proportions of these components depend on the source of the gas; see Table 1.2). High carbon dioxide partial pressures will affect the performance of the earlier described bioscrubbing process because CO_2 and H_2S compete for alkalinity. To control the pH at mildly alkaline conditions and enable H_2S absorption, elevated $NaHCO_3$ concentrations are required. Hence, increased salt concentrations (i.e. **high-salinity** conditions) will dominate.

$$CO_2(g) \rightleftharpoons CO_2(l) \quad pK = 3.6 \tag{1.1}$$

$$CO_2(l) + OH^- \rightleftharpoons HCO_3^- \quad pK = 6.3 \tag{1.2}$$

$$HCO_3^- + OH^- \rightleftharpoons CO_3^{2-} \quad pK = 10.3 \tag{1.3}$$

At higher pH levels (i.e. **alkaline** conditions), H_2S absorption is enhanced. As a result, the gas washers can be more compact so that less liquid needs to be recirculated over the absorber to treat the sour gas. Especially at high operating pressures in the absorber column, this leads to considerable savings in pumping costs. This considerably improves the applicability of the biodesulfurization process for sulfide loads of up to 100 tons per day.

In nature, such "doubly extreme" conditions of **high salinity and high alkalinity** occur in soda lakes. These lakes are climate-bound, constrained to arid and semi-arid regions such as Egypt, Central Asia and Siberia. In soda lakes, evaporation is greater than inflow, which results in salt levels exceeding those of seawater (>35 gr/L) [39]. As a result, although also depending on the type of sedimentary rock, soda lakes generally have high buffer capacities with pH values of up to 11.

Both aerobic and anaerobic sulfur metabolizers are found in soda lakes as most of these lakes have high sulfate concentrations. They also have high primary productivity. Consequently, the sulfur cycle is one of its most active element cycles, dominated by the species *Thioalkalivibrio* and *Thioalkalimicrobium* [9, 14]. *Thioalkalivibrio* strains show high activity within a broad range of salinity (0.3 to 4 M Na^+) and pH (8.5 to 10) [40, 9], and are therefore ideal candidates for use in the haloalkaline treatment process.

Recently, Wageningen University and Delft University of Technology developed a second generation of the process described in Section 1.2; it uses a mixed biomass population from sediments from soda lakes in Mongolia, southwestern Siberia and Kenya [41]. *Thioalkalivibrio* is the dominating genus [42] in these second-generation bioreactors. These are slowly growing organisms, with a high growth yield and low sulfide oxidation rates in comparison with neutrophilic bacteria used in other process types [43]. Under steady-state conditions, biomass activity still allows the formation of 0.22 kg of sulfide per m^3 reactor when the biomass concentrations are 150 mg N L^{-1} [44]. However, at these sulfide-loading rates, oxygen transfer becomes the limiting factor for the process.

1.4 Research objectives and scope of the thesis

At present, the H_2S removal efficiency in bioscrubbers reaches 99.9% sulfide removal; the maximal selectivity for sulfur production is around 90% [41, 21]. Paqell's assessment, however, is that the selectivity for sulfur production must be increased to values above 97% for large-scale application (i.e. sulfide loads of up to 100 tons per day). In principle, this can be achieved by the use of a third anaerobic process step in which the (thio)sulfate in the bleed stream is converted back to sulfide by sulfate-reducing and thiosulfate-reducing bacteria (SRB and TRB) [14, 45]. In this way, significant savings in makeup water and caustic consumption can be achieved [44]. The application of such a reductive bio-process step is, however, an expensive solution because it requires a second bioreactor and a reducing compound such as ethanol or hydrogen gas [46].

A better process control strategy for the O_2 supply to the sulfide-oxidizing bioreactor is an easier and far less expensive alternative for maximizing the sulfur production. Abiotic oxidation of sulfide becomes enhanced at higher sulfide concentrations because the biological oxidation is inhibited under these conditions [30]. Furthermore, the formation of (thio)sulfate is increased at higher oxygen levels [27, 41, 34]. This implies that fluid mixing characteristics significantly influence overall system performance. Fluid mixing is achieved by injection of air into the bioreactor, which also serves to introduce oxygen. Because of this dual function, a direct relationship exists between fluid mixing and reaction selectivity. Moreover, sulfide and oxygen **gradients** over the height of the reactor column play a role in overall reactor performance. An **optimization-based control** strategy is therefore needed that (1) avoids the formation of (thio)sulfate and (2) combines effective mixing with optimal reaction selectivity. That means that **mathematical models** are required that describe both abiotic and biotic reaction kinetics, implementing the most **recent microbiological insights** [47, 48].

Given these requirements, the objectives of this PhD research were the following:

- Development of methodology and quantitative models to describe sulfide oxidation reaction kinetics, including metabolic pathways, of biological processes that occur in gas desulfurization under haloalkaline conditions, incorporating an (i) understanding of abiotic chemistry [15], (ii) experimental data of haloalkaline processes [44] and (iii) integration of recent microbiological insights;
- Generation of a simplified mathematical model structure, by applying model reduction techniques to the model for sulfur-producing bioreactor to gain more insight in the basics of the process and improve controller design;
- Derivation of a process control strategy for optimal O_2 supply to maximize elemental sulfur production and minimize the use of any chemicals.

1.5 Bioprocess control

Over the past decades, the industrial application of biotechnological processes has become increasingly popular. Major examples can be found in treatment systems for wastewater from industries and municipalities [49], the manufacture of antibiotics and pharmaceutical agents [50], and the production of biofuels by algae [51]. The big problem that arises in these industrial applications is the requirement for monitoring and control in order to optimize the system as well as detect failure [52]. In practice, most installations are equipped with single proportional (P) or proportional-integral (PI) controllers while very few are run with (advanced) model-based control strategies that allow optimal process monitoring. Two reasons can be pointed out. First, biological processes are **complex** as they involve living microorganisms of which the characteristics are hard to grasp [53]. Selecting a model structure is an arduous process as the reproducibility of experimental work is low, which can also prevent the practical identification of parameters [54]. In addition, parameters can evolve over time as a result of adaption or natural evolution [55, 56], such as metabolic changes or unforeseeable genetic alterations in the organisms.

The second major difficulty that prevents the application of accurate model-based control is the absence of suitable **sensors** capable of monitoring the physiological functioning of the biological process. The majority of key variables in the process can only be measured by using off-line methods that rely on lab analysis. So in practice, the main control strategies used in industry are very often limited to indirect control of the process by controlling process variables such as dissolved oxygen concentration, oxidation-reduction potentials (ORP), temperature, conductivity and pH [28, 57, 58].

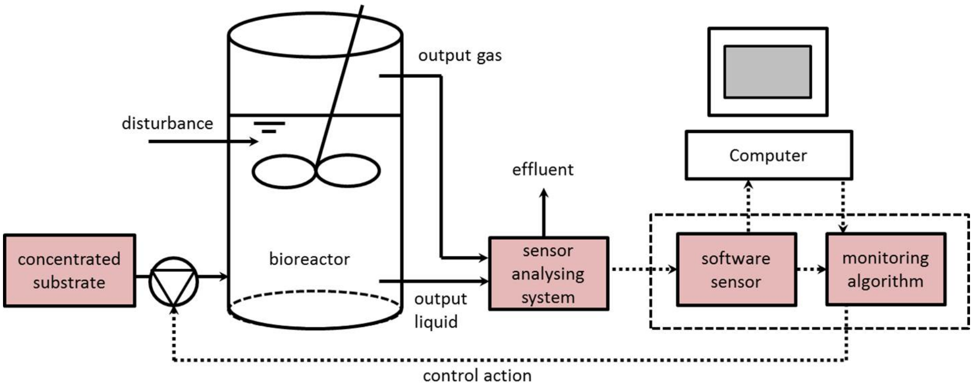

Figuur 1.3: Schematic representation of advanced bioprocess control system, adapted from [59]. Each dotted line represents an information flow.

Fig. 1.3 presents an overview of the basic concept of a bioprocess control system [59]. Typically, the substrate supply rate is a key control input parameter of a bioreactor system, in addition to temperature and pH. The substrate supply is the output of a control algorithm that uses the available process information. This information represents, on the one hand, the state of the process from online sensor measurements and, on the other hand, the available *a priori* knowledge. When control objectives are expressed in variables that cannot be measured (e.g. biomass, substrates, and products), *a priori* process knowledge is used to develop software sensors [60]. Given reliable process information and specific control objectives, accurate bioprocess control strategies can then be developed. Obviously, the more accurate the *a priori* knowledge and sensor measurements are, the more accurate the control strategy and the better the process performance. **Accurate** biochemical models are required to achieve high-performance processes.

1.6 Modeling biochemical processes

A (scientific) model is an abstract, conceptual representation of reality. Basically, models are used to understand, predict and control (complex) systems. Modeling biochemical processes is a sophisticated undertaking; physical laws (models) have been in existence for centuries (e.g. Newton's and Fick's law), but biochemical models are frequently based on empirical expressions [61].

Typically, biochemical models predict bacterial respiration behavior, which leads to bacterial growth. When growth and decay rates are known, bacterial growth curves can be predicted. Generally, four phases of bacterial growth can be distinguished in batch reactors. First, bacteria go through a lag phase in which the cells adjust to their surroundings and grow only in size, not in numbers, resulting in a **lag** time until the bacteria begin to multiply. Subsequently,

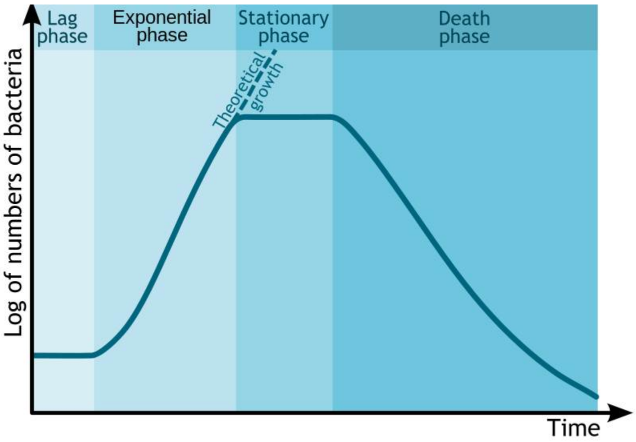

Figuur 1.4: The schematic bacterial growth curve in batch tests [62].

the increase of the bacterial population accelerates and reaches a maximum value (i.e. μ_{max} in (1/h)). This phase is called **exponential** growth phase or log phase. Next, the growth rate decreases in the so-called **stationary** phase as nutrients become scarce and/or inhibitory products are formed. Finally, bacteria run out of nutrients and die (**decay** phase). Fig. 1.4 is a schematic depiction of these growth phases. These curves are not found in continuously operating systems, as most biological treatment process are operated at low substrate levels (i.e. $\mu \ll \mu_{max}$) and fluctuating substrate and hydraulic loads. There is therefore a need to model bacterial growth and decay to predict these dynamic processes in industrial bioreactors.

Monod's empirical model is the most common expression used to describe bacterial growth rates [63]. This empirical law was derived from the enzymatic model proposed by Michaelis-Menten, following

$$\mu = \mu_{max} \frac{[S]}{K_S + [S]} \tag{1.4}$$

In this expression, μ is the growth rate (1/h), $[S]$ the substrate concentration (g/L), and K_S the half-saturation constant (g/L). Notice from Eq. 1.4 that $[S] \gg K_S$ can be approached by a zero-order model and $[S] \ll K_S$ with a first-order model. Consequently, also **zero-first order models** have been proposed [64].

Inhibition phenomena due to an excess amount of substrate are generally modeled with **Haldane's expression**. Andrews (1968) used this empirical expression by drawing parallels with enzymatic reaction kinetics, according to

$$\mu = \mu_{max} \frac{[S]}{K_S + [S] + \frac{[S]^2}{K_i}} \tag{1.5}$$

in which K_i the inhibition constant (g/L) [65]. Many relations have been established since, all based on the Monod and Haldane models. Similar approaches were used to model variations in microorganisms, temperature and pH. An example is the so-called **third-order Haldane model**; a variant of the Monod-Haldane model [66]. This model incorporates the inhibition term by a third-order term, as follows:

$$\mu = \mu_{max} \frac{[S]}{K_S + [S] + \frac{[S]^3}{K_i^2}} \tag{1.6}$$

Another factor, in addition to inhibition phenomena, is that the substrate itself can enhance the substrate removal rate. In systems biology, the effect of cooperative binding (the enhancement of the binding of a ligand to a macromolecule by the presence of other ligands) is often described by the **Hill equation** [67]

$$q = q_{max} \frac{[S]^n}{K_S + [S]^n} \tag{1.7}$$

Here, q and q_{max} stand for the consumption rate (g/h). A coefficient of $n = 1$ indicates completely independent binding. Numbers greater than 1 indicate positive cooperativity, while numbers lower than 1 indicate negative cooperativity.

Another general Monod-type model was proposed by Han and Lievenspiel (1988). This method accounts for substrate stimulation at low concentrations and substrate inhibition at high concentrations:

$$q = q_{max} \frac{\left(1 - \frac{[S]}{[S]_m}\right)^n}{[S] + K_S - \left(1 - \frac{[S]}{[S]_m}\right)^m} \tag{1.8}$$

$[S]_m$ is the critical inhibitor concentration above which the reaction stops, and m and n are constants [68]. Examples to which this model applies are nitrate oxidation by *Nitrobacter* and ammonium oxidation by *Nitrosomonas* [69].

Fig. 1.5 displays various forms of biological specific growth models; $\mu_{max} = q_{max} = 1$ h^{-1}, $K_s = 1$ g/L, $K_i = 4$ g/L, $[S]_m = 25$ g/L, $m = 4$ and $n = 4$. Notice that the further the model differentiates from the basic Monod equation (Eq. 1.4), the more parameters are introduced. Actually, Holmberg and Ranta (1982) already concluded that the Monod parameters are practically unidentifiable [70]. The following rule of thumb is usually applied: the more parameters, the better the fit, but that frequently also means that the estimation error and prediction uncertainty are greater [60].

1.7 Double substrate

In the case of aerobic processes, the co-substrate oxygen always affects bacterial growth rates as well. Frequently, the standard Monod model (Eq. 1.4) is extended with an extra Monod-

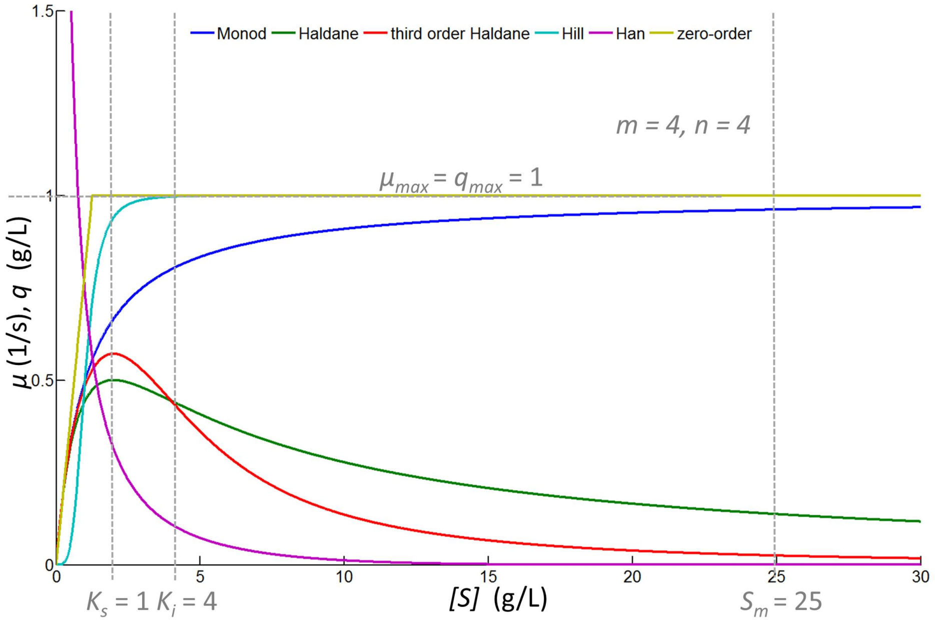

Figuur 1.5: Different forms of Monod-type of equations [63, 64, 66, 67, 68, 65].

type term, thus leading to the following equation [71]:

$$\mu = \mu_{max} \frac{[S]}{K_S + [S]} \frac{[O_2]}{K_{O_2} + [O_2]} \tag{1.9}$$

$[O_2]$ is the concentration of dissolved oxygen (g/L) and K_{O_2} the half-saturation constant of oxygen (g/L). Examples of this expression can be found in the ASM1 model, which describes processes that remove C and N [72]. The disadvantage of the extended Monod model is that data are fitted to an empirical model, which consequently loses physical interpretation. Additionally, the model accuracy over a range of both substrates is questionable. The last term in Eq. 1.9 is often omitted, under the assumption that the reactor is sufficiently aerated and that K_{O_2} is very small relative to the concentration of dissolved oxygen in the reactor.

A new form of modeling is **metabolic network modeling**. The basic principle is that genome sequences are linked to the physiology of microorganisms [73]. As biological rates are coupled to both enzyme activities and gene expression levels, an in-depth analysis of molecular mechanisms is now possible [74]. A well studied organism, with the aid of metabolic network models, is *Saccharomyces cerevisiae* (a yeast) [75]. Metabolic engineering has attained high production rates of for example ethanol [76]. Other applications of metabolic network modeling can be found in, for instance, the analysis of synthetic lethality [77] and predictions of evolutionary outcomes [78]. Metabolic network models are advanced models as they describe complete organisms. Biological sulfide oxidation, in particular by haloalkaliphilic sulfide-oxidizing bacteria (HA-SOB), has not been studied in such detail yet. The following section discusses proposed kinetic models for biological sulfide oxidation.

1.8 Modeling biodesulfurization processes

The biological and abiotic kinetics of the reaction between dissolved sulfide and oxygen have been studied extensively in the past few decades [79, 80, 34, 81, 82, 83, 31, 84, 85, 42, 86, 87, 88, 33, 89, 32, 85, 90]. As mentioned in Section 1.2, two products are formed in the biological desulfurization process, namely elemental sulfur and sulfate. The reaction kinetics of biological sulfide oxidation have been modeled for both neutral *Thiobacillus* spp. and haloalkaline *Thioalkalivibrio* spp. (see Table 1.2). Mainly maximum oxidation rates were proposed as a measure for the biological activity (with $q_{SO_4^{2-}}$ and q_{S^0} denoting the maximum oxidation rate for sulfide to sulfate and for sulfide to elemental sulfur, respectively). Generally, these rates ranges from 0.035 to 1.19 mM HS^- mg N^{-1} h^{-1}. Differences can be explained by differences in cultures and experimental setups.

In addition, some authors suggested a Monod or Monod-type model (see Table 1.3). Alcántara et al. (2004) suggested a Monod model, with substrate affinity constant $K_{SO_4^{2-}}$=0.28 mM. Roosta et al. (2011) proposed an extended model with $K_{SO_4^{2-}}$=2.524, K_{S^0}=0.106 and K_{O_2}=0.203 mM. Other authors included the inhibition of sulfide as well, by way of a Monod-Haldane model. Gonzales-Sanchez & Revah (2006) found $K_{SO_4^{2-}}$=0.07 and K_i=1.19 mM, and de Graaff et al. (2011) found $K_{SO_4^{2-}}$=0.23 and K_i=0.09 mM. Gonzales-Sanchez et al. (2009) described an extended Monod-Haldane model, in which $K_{SO_4^{2-}}$=0.01, K_{O_2}=0.028 mM and K_i=1.015 mM.

While all maximum oxidation rates are generally in the same order of magnitude, the other parameters show large differences. As a result, different models predict different behavior of the biological sulfide oxidation kinetics. These large differences arise because these black-box models have been fitted to different data sets. Especially Roosta et al. (2011) found deviating values for the affinity constants, conceivably related to the number of parameters and the dissimilar model structure.

Several studies show that oxygen and sulfide levels are key parameters in the selectivity for elemental sulfur [27, 41]. Dissolved oxygen values below 0.1 mg L^{-1} and high sulfide-loading rates lead to the biological formation of elemental sulfur [31]. However, at an industrial scale, in-line monitoring of the oxygen levels is very difficult on account of the high detection limits of the currently available oxygen sensors. To control the oxygen supply, Janssen et al. (1998) suggested the use of in-line measurements of the ORP [28]. In a bioreactor in which elemental sulfur forms, the ORP is predominately determined by the sulfide concentration. However, Van den Bosch (2008) concluded that sulfate formation is much stronger related to the sulfide concentration than to the ORP because the ORP also largely depends on the medium's pH [44]. Despite these limitations, the air-oxygen dosage in biodesulfurization systems is currently still based on in-line measurements of the ORP, combined with a

P/PI control strategy. Model-based schemes provide an alternative to P/PI control and can be used to determine the oxygen supply rate that results in better performance. Preferably, these model-based control schemes are built into simple models.

Besides biological sulfide oxidation, also chemical or abiotic oxidation takes place. The chemical oxidation of sulfide is a complex process, in which a number of reaction products can form such as sulfur, thiosulfate, sulfite and sulfate. These abiotic reactions are generally catalyzed by metal ions and the reaction product depends on conditions such as temperature, sulfide-to-oxygen ratio and salt content. Table 1.4 lists the parameters of several proposed models. These models have different substrates (i.e. sulfide, polysulfide, or total sulfide). However, all models are of the standard form suggested by O'Brien et al. [32]:

$$r = k \cdot [HS^{-}]^{\alpha} \cdot [O_2]^{\beta} \tag{1.10}$$

In this equation, the sulfide concentration may be replaced by polysulfide or a combination of sulfide and polysulfide. The kinetic parameters differ per study as they are based on different substrate concentration ranges. Generally, the abiotic oxidation of polysulfides proceeds faster than that of aqueous sulfide. The formation of polysulfide is highly dependent on the pH and on the presence of colloidal sulfur particles [33]. Typically, desulfurization processes operate at a relatively low pH (8.5). A pH of 8.5 leads to $< 4\%$ sulfide conversion to thiosulfate whereas a pH of 10 leads to $> 15\%$ sulfide conversion to thiosulfate in the overall process [35]. The models described by Kleinjan et al. (2005) and de Graaff et al. (2011) are most suitable for describing the haloalkaline biodesulfurization process.

Tabel 1.3: Overview of kinetic parameters of sulfide oxidizing bacteria

Bacteria	Reactor test	pH	$q_{SO_4^{2-}}$ (mM HS^- mg N^{-1} h^{-1})	$K_{SO_4^{2-}}$ (mM)	q_{S^0} (mM HS^- mg N^{-1} h^{-1})	K_{S^0} (mM)	K_i (mM)	K_{O_2} (mM)	Type of model	Reference
Thiobacillus sp.	chemostat	7	0.75*	0.001			1.015	0.028	extended Monod-Haldane	Gonzales-Sanchez et al., 2009 [79]
Thiobacillus denitrificans	fed-batch reactor	7.4	0.26*		0.095*				rate	McComas & Sublette, 2001 [80]
Thiobacillus	recirculation reactor	7-7.5	0.25*	0.28					Monod	Alcántara et al., 2004 [34]
Thiobacillus W5	chemostat	7.5	0.69*						rate	Visser et al., 1997 [81]
Thiobacillus thioparus	fed-batch	8	0.63*	2.524	0.93*	0.106		0.203	extended Monod	Roosta et al., 2011 [82]
Thiobacillus sp.	chemostat	8	0.94		1.9				rate	Buisman et al., 1990 [83]
Thiobacillus sp.	expanded bed reactor	8	0.15						rate	Janssen et al., 1996 [31]
Thioalkalivibrio sp.	chemostat	9	0.33						rate	van den Bosch et al., 2009 [84]
Thioalkalivibrio sp. strain K90-mix	chemostat	9.5	0.35	0.23			0.09		Monod-Haldane	de Graaff et al., 2011 [85]
Thioalkalivibrio sp.	silicon loop stirred reactor	9.5	0.035*						rate	Sorokin et al., 2008 [42]
alkaliphilic sulfide oxidizing consortium	chemostat	10	0.69*	0.07			1.19	0.02	Monod-Haldane	Gonzalez-Sanchez & Revah, 2006 [86]
Thioalkalivibrio versutus	continues chemostat	10	0.26*						rate	Banciu et al., 2004 [87]
Thioalkalivibrio thiocyanoxidans	continues chemostat	10	1.02*						rate	Sorokin et al., 2002 [88]
Thioalkalivibrio paradoxus	continues chemostat	10	0.49*						rate	Sorokin et al., 2002 [88]

* calculated assuming proteins contain 17% nitrogen

Tabel 1.4: Overview of kinetic parameters of the chemical oxidation of sulfide

Substrate	pH	T (K)	I (M)	k $L^{\alpha \cdot \beta}$ $mol^{-\alpha \cdot \beta}$ s^{-1}	α (-)	β (-)	Reference
S_x^{2-}	9	303	0.10	0.80	0.98	0.59	Kleinjan et al., 2005 [33]
HS^-	8	298	0.20	0.094	0.597	0.642	Buisman et al., 1990 [89]
HS^-	7.55	298	0.155	0.016-0.033	1.02	0.80	O'Brien et al., 1977 [32]
HS^-	7.55	298	1.78	0.06	1.02	0.80	O'Brien et al., 1977 [32]
S_{tot}^{2-}	9.5	303	0.80	0.39	0.51	*	de Graaff et al., 2011 [85]
HS^-	9.5	928	0.01	0.43	1	1	Jolley & Fortser, 1985 [90]

* $[O_2]$=0.15 mM

1.9 Outline of the thesis

Several aspects of the new biological process for natural gas desulfurization at haloalkaline conditions were investigated [41]. **Chapter 2** explores how the biological oxidation routes in the haloalkaline process were studied in lab-scale upflow bioreactors. **Chapter 3** introduces and evaluates a physiologically based model, which captures the kinetics of the identified routes in the biological desulfurization process. This model was calibrated and validated with the aid of respiration tests and (dynamic) bench-scale gas lift reactor experiments. The effects of salinity [40, 91], pH [42, 91] and oxygen/sulfide ratios [41, 35] are also discussed. Effects of temperature on reactor performance are not included. **Chapter 4** focuses on the temperature-dependent operational frame in which the haloalkaline desulfurization process shows sufficient biological activity. To obtain insight in the suggested model structure, an overall sensitivity analysis is suggested and evaluated in **Chapter 5**. Additionally, this chapter investigates system inputs, sulfide load and oxygen transfer through the development of meta-models. **Chapter 6** assesses the performance of full-scale reactors, combining models and real-time data sets. A discussion of potential optimization routes for the presented biodesulfurization process follows in **Chapter 7**. The work is summarized in the final chapter (**Chapter 8**).

References

[1] M.A. Kertesz. Riding the sulfur cycle - metabolism of sulfonates and sulfate esters in gram-negative bacteria. *FEMS Microbiology Reviews*, 24(2):135–175, 2000.

[2] J. Baddiley, E. M. Thain, G. D. Novelli, and F. Lipmann. Structure of coenzyme a. *Nature*, 171, 1953.

[3] O. Einsle, F. A. Tezcan, S. L. A. Andrade, B. Schmid, M. Yoshida, J. B. Howard, and D. C. Rees. Nitrogenase MoFe-protein at 1.16 A resolution: A central ligand in the FeMo-cofactor. *Science*, 297(5587):1696–1700, 2002.

[4] D. Wacey, M. R. Kilburn, M. Saunders, J. Cliff, and M. D. Brasier. Microfossils of sulphur-metabolizing cells in 3.4-billion-year-old rocks of Western Australia. *Nature Geoscience*, 4(10):698–702, 2011.

[5] J. Willey, L. Sherwood, and C. Woolverton. *Prescott's Microbiology*. McGraw-Hill, 2001.

[6] D. P. Kelly, J. K. Shergill, W. P. Lu, and A. P. Wood. Oxidative metabolism of inorganic sulfur compounds by bacteria. *Antonie van Leeuwenhoek, International Journal of General and Molecular Microbiology*, 71(1-2):95–107, 1997.

[7] A. S. Engel, M. L. Porter, L. A. Stern, S. Quinlan, and P. C. Bennett. Bacterial diversity and ecosystem function of filamentous microbial mats from aphotic (cave) sulfidic springs dominated by chemolithoautotrophic "Epsilonproteobacteria". *FEMS Microbiology Ecology*, 51(1):31–53, 2004.

[8] B. B. Jørgensen. Ecology of the bacteria of the sulphur cycle with special reference to anoxic-oxic interface environments. *Philosophical transactions of the Royal Society of London. Series B: Biological sciences*, 298(1093):543–561, 1982.

[9] D. Y. Sorokin, G. J. Kuenen, and G. Muyzer. The microbial sulfur cycle at extremely haloalkaline conditions of soda lakes. *Frontiers in Microbiology*, 2(44), 2011.

[10] L. L. Barton and G. D. Fauque. Biochemistry, physiology and biotechnology of sulfate-reducing bacteria. *Advances in Applied Microbiology*, 68:41–98, 2009.

[11] G. Muyzer and A. J. M. Stams. The ecology and biotechnology of sulphate-reducing bacteria. *Nature Reviews Microbiology*, 6(6):441–454, 2008.

[12] A. Kletzin, T. Urich, F. Müller, T. M. Bandeiras, and C. M. Gomes. Dissimilatory oxidation and reduction of elemental sulfur in thermophilic archaea. *Journal of Bioenergetics and Biomembranes*, 36(1):77–91, 2004.

[13] R. Pinto, J. S. Harrison, T. Hsu, W. R. Jacobs Jr., and T. S. Leyh. Sulfite reduction in mycobacteria. *Journal of Bacteriology*, 189(18):6714–6722, 2007.

[14] D. Y. Sorokin, E. E. Zacharova, N. V. Pimenov, T. P. Tourova, A. N. Panteleeva, and G. Muyzer. Sulfidogenesis in hypersaline chloride-sulfate lakes of Kulunda steppe (Altai, Russia). *FEMS Microbiology Ecology*, 79(2):445–453, 2012.

[15] W. E. Kleinjan. *Biologically produced sulfur particles and polysulfide ions Effects on a biotechnological process for the removal of hydrogen sulfide from gas streams.* Ph.D. thesis, Wageningen University, Wageningen, The Netherlands, 2005.

[16] J. E. Lovelock, R. J. Maggs, and R. A. Rasmussen. Atmospheric dimethyl sulphide and the natural sulphur cycle. *Nature*, 237(5356):452–453, 1972.

[17] J. A. Fisher, D. J. Jacob, Q. Wang, R. Bahreini, C. C. Carouge, M. J. Cubison, J. E. Dibb, T. Diehl, J. L. Jimenez, E. M. Leibensperger, Z. Lu, M. B. J. Meinders, H. O. T. Pye, P. K. Quinn, S. Sharma, D. G. Streets, A. van Donkelaar, and R. M. Yantosca. Sources, distribution, and acidity of sulfate-ammonium aerosol in the Arctic in winter-spring. *Atmospheric Environment*, 45(39):7301–7318, 2011.

[18] G. E. Likens, R. F. Wright, J. N. Galloway, and T. J. Butler. Acid rain. *Scientific American*, 221(4):43–51, 1979.

[19] S. Goidanich, J. Brunk, G. Herting, M. A. Arenas, and I. Odnevall Wallinder. Atmospheric corrosion of brass in outdoor applications. patina evolution, metal release and aesthetic appearance at urban exposure conditions. *Science of the Total Environment*, 412-413:46–57, 2011.

[20] D. J. Monticello and W. R. Finnerty. Microbial desulfurization of fossil fuels. *Annual Review of Microbiology*, 39:371–389, 1985.

[21] A. J. H. Janssen, P. N. L. Lens, A. J. M. Stams, C. M. Plugge, D. Y. Sorokin, G. Muyzer, H. Dijkman, E. Van Zessen, P. Luimes, and C. J. N. Buisman. Application of bacteria involved in the biological sulfur cycle for paper mill effluent purification. *Science of the Total Environment*, 407(4):1333–1343, 2009.

[22] D. Shindell and G. Faluvegi. The net climate impact of coal-fired power plant emissions. *Atmospheric Chemistry and Physics*, 10(7):3247–3260, 2010.

[23] A. J. H. Janssen, R. C. Van Leerdam, P. L. F. Van den Bosch, E. Van Zessen, G. Van Heeringen, and C. J. N. Buisman. Development of a family of large-scale biotechnological processes to desulphurise industrial gases, 2nd international congress on biotechniques for air pollution control, A Coruña, Spain. 2007.

[24] A. J. H. Janssen, R. Ruitenberg, and C. J. N. Buisman. Industrial applications of new sulphur biotechnology. *Water Science and Technology*, 44(8):85–90, 2001.

[25] M. de Graaff. *Biological treatment of sulfidic spent caustics under haloalkaline conditions using soda lake bacteria*. Ph.D. thesis, Wageningen University, Wageningen, The Netherlands, 2012.

[26] C. Rattanapan, P. Boonsawang, and D. Kantachote. Removal of h2s in down-flow gac biofiltration using sulfide oxidizing bacteria from concentrated latex wastewater. *Bioresource Technology*, 100(1):125–130, 2009.

[27] C. J. N. Buisman, B. G. Geraats, P. IJspeert, and G. Lettinga. Optimization of sulphur production in a biotechnological sulphide-removing reactor. *Biotechnology and Bioengineering*, 35(1):50–56, 1990.

[28] A. J. H. Janssen, S. Meijer, J. Bontsema, and G. Lettinga. Application of the redox potential for controling a sulfide oxidizing bioreactor. *Biotechnol. Bioeng.*, 60(2):147–155, 1998.

[29] Paqell. website paqell, March 2012.

[30] A. J. H. Janssen, R. Sleyster, C. van der Kaa, J. Bontsema, , and G. Lettinga. Biological sulphide oxidation in a fed-batch reactor. *Biotechnol. Bioeng.*, 47(3):327–333, 1995.

[31] A. J. H. Janssen, S. C. Ma, P. Lens, and G. Lettinga. Performance of a sulfide-oxidizing expanded-bed reactor supplied with dissolved oxygen. *Biotechnol. Bioeng.*, 53(1):32–40, 1996.

[32] D. J. O'Brien and F. B. Birkner. Kinetics of oxygenation of reduced sulfur species in aqueous solution. *Environmental Science and Technology*, 11(12):1114–1120, 1977.

[33] W. E. Kleinjan, A. De Keizer, and A. J. H. Janssen. Kinetics of the chemical oxidation of polysulfide anions in aqueous solution. *Water Research*, 39(17):4096–4100, 2005.

[34] S. Alcántara, A. Velasco, A. Muñoz, J. Cid, S. Revah, and E. Razo-Flores. Hydrogen sulfide oxidation by a microbial consortium in a recirculation reactor system: Sulfur formation under oxygen limitation and removal of phenols. *Environmental Science and Technology*, 38(3):918–923, 2004.

[35] P. L. F. Van den Bosch, D. Y. Sorokin, C. J. N. Buisman, and A. J. H. Janssen. The effect of pH on thiosulfate formation in a biotechnological process for the removal of hydrogen sulfide from gas streams. *Environmental Science and Technology*, 42(7):2637–2642, 2008.

[36] C. Cline, R. Hoksberg, R. Abry, and A. J. H. Janssen. Biological process for H_2S removal from gas streams. The Shell-Paques/Thiopaq gas desulfurization process. *Laurence Reid gas conditioning conference, Norman, Oklahoma*, 2003.

[37] NaturalGas. website naturalgas, October 2012.

[38] Biogaz Europe. website biogas renewable energy, October 2012.

[39] B. E. Jones, W. D. Grant, A. W. Duckworth, and G. G. Owenson. Microbial diversity of soda lakes. *Extremophiles*, 2(3):191–200, 1998.

[40] D. Y. Sorokin and J. G. Kuenen. Haloalkaliphilic sulfur-oxidizing bacteria in soda lakes. *FEMS Microbiol. Rev.*, 29(4):685–702, 2005.

[41] P. L. F. Van den Bosch, O. C. Van Beusekom, C. J. N. Buisman, and A. J. H. Janssen. Sulfide oxidation at halo-alkaline conditions in a fed-batch bioreactor. *Biotechnology and Bioengineering*, 97(5):1053–1063, 2007.

[42] D. Y. Sorokin, P. L. F. Van Den Bosch, B. Abbas, A. J. H. Janssen, and G. Muyzer. Microbiological analysis of the population of extremely haloalkaliphilic sulfur-oxidizing bacteria dominating in lab-scale sulfide-removing bioreactors. *Appl. Microbiol. Biotechnol.*, 80(6):965–975, 2008.

[43] D. Y. Sorokin, H. Banciu, M. Van Loosdrecht, and J. G. Kuenen. Growth physiology and competitive interaction of obligately chemolithoautotrophic, haloalkaliphilic, sulfur-oxidizing bacteria from soda lakes. *Extremophiles*, 7:195–203, 2003.

[44] P. L. F. Van den Bosch. *Biological sulfide oxidation by natron-alkaliphilic bacteria Application in gas desulfurization*. PhD thesis, Wageningen University, Wageningen, The Netherlands, 2008.

[45] P.N.L. Lens, A. Visser, A. J. H. Janssen, L. W. Hulshoff Pol, and G. Lettinga. Biotechnological treatment of sulfate-rich wastewaters. *Critical Reviews in Environmental Science and Technology*, 28(1):41–88, 1998.

[46] R. T. Van Houten, H. van der Spoel, A. C. van Aelst, L.W. Hulshoff Pol, and G. Lettinga. Biological sulfate reduction using synthesis gas as energy and carbon source. *Biotechnol Bioeng.*, 50(2):136–144, 1996.

[47] G. Muyzer, D. Y. Sorokin, K. Mavromatis, A. Lapidus, A. Clum, N. Ivanova, A. Pati, P. d'Haeseleer, T. Woyke, and N. C. Kyrpides. Complete genome sequence of "thioalkalivibrio sulfidophilus"hl-ebgr7. *Standards in Genomic Sciences*, 4:23–35, 2011.

[48] G. Muyzer, D. Y. Sorokin, K. Mavromatis, A. Lapidus, B. Foster, H. Sun, N. Ivanova, A. Pati, P. D'haeseleer, T. Woyke, and N. C. Kyrpides. Complete genome sequence of thioalkalivibrio sp. k90mix. *Standards in Genomic Sciences*, 5, 2011.

[49] H. Spanjers, G. G. Patry, and K. J. Keesman. Respirometry-based on-line model parameter estimation at a full-scale WWTP. *Water Science and Technology*, 45(4-5):335–343, 2002.

[50] F. Zepp. Principles of vaccine design-lessons from nature. *Vaccine*, 28(3):C14–C24, 2010.

[51] Wijffels R. H. and Barbosa M.J. An outlook on algal biofuels. 2010.

[52] P. A. Vanrolleghem, U. Jeppsson, J. Carstensen, B. Carlsson, and G. Olsson. Integration of wastewater treatment plant design and operation - A systematic approach using cost functions. *Water Science and Technology*, 34(3-4 -4 pt 2):159–171, 1996.

[53] D. U. Hooper, F. S. Chapin III, J. J. Ewel, A. Hector, P. Inchausti, S. Lavorel, J. H. Lawton, D. M. Lodge, M. Loreau, S. Naeem, B. Schmid, H. Setala, A. J. Symstad, J. Vandermeer, and D. A. Wardle. Effects of biodiversity on ecosystem functioning A consensus of current knowledge. *Ecological Monographs*, 75(1):3–35, 2005.

[54] K. J. Keesman and J. D. Stigter. Optimal parametric sensitivity control for the estimation of kinetic parameters in bioreactors. *Mathematical Biosciences*, 179(1):95–111, 2002.

[55] K. J. Keesman. State and parameter estimation in biotechnical batch reactors. *Control Engineering Practice*, 10(2):219 – 225, 2002.

[56] P. A. Vanrolleghem and K. J. Keesman. Identification of biodegradation models under model and data uncertainty. *Water Science and Technology*, 33(2):91–105, 1996.

[57] S. E. Oh, S. Van Ginkel, and B. E. Logan. The relative effectiveness of ph control and heat treatment for enhancing biohydrogen gas production. *Environmental Science and Technology*, 37(22):5186–5190, 2003.

[58] P. Gonzalez-Contreras, J. Weijma, and C. J. N. Buisman. Bioscorodite crystallization in an airlift reactor for arsenic removal. *Crystal Growth and Design*, 12(5):2699–2706, 2012.

[59] D. Dochain. *Automatic control of bioprocesses*. ISTE Ltd, London, 2008.

[60] K. J. Keesman. *System Identification an Introduction*. Springer Verlag London, 2011.

[61] E. Zitzler, K. Deb, and L. Thiele. Comparison of multiobjective evolutionary algorithms: empirical results. *Evolutionary computation*, 8(2):173–195, 2000.

[62] Wikipedia. website wikipedia, October 2012.

[63] J. Monod. The growth of bacterial cultures. *Annual Review of Micrbiology*, 3:371, 1949.

[64] H. Spanjers and K. Keesman. Identification of wastewater biodegradation kinetics. volume 2, pages 1011–1016, 1994.

[65] J. F. Andrews. A mathematical model for the continuous culture of microorganisms utilizing inhibitory substance. *Biotechnology and Bioengineering*, 10:707–723, 1968.

[66] T. Yano and S. Koga. Dynamic behaviour of the chemostat subject to substrate inhibition. *Biotechology and Bioengineering*, 11(2):139–153, 1969.

[67] J. N. Weiss. The Hill equation revisited: Uses and misuses. *FASEB Journal*, 11(11):835–841, 1997.

[68] K. Han and O. Levenspiel. Extended monod kinetics for substrate, product and cell inhibition. *Biotechnol. Bioeng.*, 32(4):430–437, 1988.

[69] E. H. Edwards. The influence of high substrate concentrations on microbial kinetics. *Biotechnol. Bioeng.*, 12(5):679–712, 2070.

[70] A. Holmberg and J. Ranta. Procedures for parameter and state estimation of microbial growth process models. *Automatica*, 18(2):181–193, 1982.

[71] R. D. McGee and J. F. Drake. Studies in intermicrobial symbiosis, *Saccharomyces cerevisiae* and *Lactobacillus casei. Can. J. Microbiol.*, 18:1733–1742, 1972.

[72] U. Jeppsson. *Modelling aspects of wastewater treatment processes*. Ph.D. thesis, Lund Institute of Technology, Lund, 1996.

[73] S. H. Strogatz. Exploring complex networks. *Nature*, 410(6825):268–276, 2001.

[74] J. J. Heijnen. Approximative kinetic formats used in metabolic network modeling. *Biotechnology and Bioengineering*, 91(5):534–545, 2005.

[75] M. R. Mashego, W. M. Van Gulik, and J. J. Heijnen. Metabolome dynamic responses of saccharomyces cerevisiae to simultaneous rapid perturbations in external electron acceptor and electron donor. *FEMS Yeast Research*, 7(1):48–66, 2007.

[76] J. L. DeRisi, V. R. Iyer, and P. O. Brown. Exploring the metabolic and genetic control of gene expression on a genomic scale. *Science*, 278(5338):680–686, 1997.

[77] M. Costanzo, A. Baryshnikova, J. Bellay, Y. Kim, E. D. Spear, C. S. Sevier, H. Ding, J. L. Y. Koh, K. Toufighi, S. Mostafavi, J. Prinz, R. P. St. Onge, B. Vandersluis, T. Makhnevych, F. J. Vizeacoumar, S. Alizadeh, S. Bahr, R. L. Brost, Y. Chen, M. Cokol, R. Deshpande, Z. Li, Z. Y. Lin, W. Liang, M. Marback, J. Paw, B. J. S. Luis, E. Shuteriqi, A. H. Y. Tong, N. Van Dyk, I. M. Wallace, J. A. Whitney, M. T. Weirauch, G. Zhong, H. Zhu, W. A. Houry, M. Brudno, S. Ragibizadeh, B. Papp, C. Pal, F. P. Roth, G. Giaever, C. Nislow, O. G. Troyanskaya, H. Bussey, G. D. Bader, A. C. Gingras, Q. D. Morris, P. M. Kim, C. A. Kaiser, C.L. Myers, B. J. Andrews, and C. Boone. The genetic landscape of a cell. *Science*, 327(5964):425–431, 2010.

[78] S. S. Fong, J. Y. Marciniak, and B. A. Palsson. Description and interpretation of adaptive evolution of *Escherichia coli* K-12 MG1655 by using a genome-scale in silico metabolic model. *Journal of Bacteriology*, 185(21):6400–6408, 2003.

[79] A. Gonzalez-Sanchez, M. Tomas, A. D. Dorado, X. Gamisans, A. Guisasola, J. Lafuente, and D. Gabriel. Development of a kinetic model for elemental sulfur and sulfate formation form the autotrophic sulfide oxidation using respirometric techniques. *Water Science and Technology*, 59:1323–1329, 2009.

[80] C. McComas and K. L. Sublette. Characterization of a noval biocatalyst system for sulfide oxidation. *Biotechnology Progress*, 17:439–446, 2001.

[81] J. M. Visser, L. A. Robertson, H. W. Van Verseveld, and J. G. Kuenen. Sulfur production by obligately chemolithoautotrophic thiobacillus species. *Applied and Environmental Microbiology*, 63(6):2300–2305, 1997.

[82] A. Roosta, A. Jahanmiri, D. Mowla, and A. Niazi. Mathematical modeling of biological sulfide removal in a fed batch bioreactor. *Biochemical Engineering Journal*, 58:50–56, 2011.

[83] C. J. N. Buisman, P. IJspeert, A. Hof, A. J. H. Janssen, R. Ten Hagen, and G. Lettinga. Kinetic parameters of a mixed culture oxidizing sulfide and sulfur with oxygen. *Biotechnology and Bioengineering*, 38(8):813–820, 1990.

[84] P. L. F. Van den Bosch, M. Fortuny-Picornell, and A. J. H. Janssen. Effects of methanethiol on the biological oxidation of sulfide at natron-alkaline conditions. *Environmental Science and Technology*, 43(2):453–459, 2009.

[85] M. de Graaff, J. B. M. Klok, M. F. M. Bijmans, G. Muyzer, and A. J. H. Janssen. Application of a 2-step process for the biological treatment of sulfidic spent caustics. *Water Research*, 46(3):723 – 730, 2012.

[86] A. Gonzalez-Sanchez and S. Revah. The effect of chemical oxidation on the biological sulfide oxidation by an alkaliphilc sulfoxidizing bacterial consortium. *Enzeme and Microbial Technology*, 40:292–298, 2006.

[87] H. Banciu, D. Y. Sorokin, R. Kleerebezem, G. Muyzer, E. A. Galinski, and J. G. Kuenen. Growth kinetics of haloalkaliphilic, sulfur-oxidizing bacterium *Thioalkalivibrio versutus* strain ALJ 15 in continuous culture. *Extremophiles*, 8(3):185–192, 2004.

[88] D. Y. Sorokin, T. P. Tourova, A. M. Lysenko, L. L. Mitushina, and J. G. Kuenen. Thioalkalivirbio thiocyanoxidans sp. nov. and Thioalkalivibrio paradoxus sp. nov., novel alkaliphilic, obligately autotrophic, sulfur-oxidizing bacteria capable of growth on thiocyanate, from soda lakes. *International Journal of Systematic and Evolutionary Microbiology*, 52:657–664, 2002.

[89] C. J. N. Buisman, P. IJspeert, A. J. H. Janssen, and G. Lettinga. Kinetics of chemical and biological sulphide oxidation in aqueous solutions. *Water Research*, 24(5):667–671, 1990.

[90] R. A. Jolley and C. F. Forster. The kinetics of sulphide oxidation. *Environmental Technology Letters*, 6(1):1–10, 1985.

[91] D. Y. Sorokin, H. Banciu, L. A. Robertson, J. G. Kuenen, M. S. Muntyan, and G. Muyzer. The prokaryotes - prokaryotic physiology and biochemisry. 2013.

Part I

Pathways & Kinetics

Chapter 2

Pathways of sulfide oxidation by haloalkaliphilic bacteria in oxygen-limited-gas lift bioreactors[1]

Abstract Physicochemical processes, such as the Lo-cat and Amine-Claus process, are commonly used to remove hydrogen sulfide from hydrocarbon gas streams such as landfill gas, natural gas, and synthesis gas. Bio-desulfurization offers environmental advantages, but still requires optimization and more insight in the reaction pathways and kinetics. We carried out experiments with gas lift bioreactors inoculated with haloalkaliphilic sulfide-oxidizing bacteria. At oxygen-limiting levels, i.e., below an O_2/H_2S mole ratio of 1, sulfide was oxidized to elemental sulfur and sulfate. We propose that the bacteria reduce NAD^+ without direct transfer of electrons to oxygen and that this is most likely the main route for oxidizing sulfide to elemental sulfur which is subsequently oxidized to sulfate in oxygen-limited bioreactors. We call this pathway the limited oxygen route (LOR). Biomass growth under these conditions is significantly lower than at higher oxygen levels. These findings emphasize the importance of accurate process control. This work also identifies a need for studies exploring similar pathways in other sulfide oxidizers such as *Thiobacillus* bacteria.

---

[1] This chapter has been published as: Klok JBM, van den Bosch PLF, Buisman CJN, Stams AJM, Keesman KJ and Janssen AJH. Pathways of sulfide oxidation by haloalkaliphilic bacteria in limited-oxygen gas lift bioreactors. *Environ. Sci. Technol.* 2012

2.1 Introduction

Hydrogen sulfide (H_2S) is present in many hydrocarbon gas streams such as landfill gas, biogas, natural gas, refinery gases and synthesis gas. Bulk removal of this toxic, corrosive compound commonly proceeds by physicochemical processes, such as the Lo-cat and Amine-Claus process [1]. These processes consume chemicals or are operated at high temperatures (up to 850°C) and pressures. An alternative, the bio-desulfurization process, offers environmental advantages as it operates at ambient temperatures (40°C) and pressures and consumes considerable less chemicals than the Lo-cat process [2, 3]. Moreover, bio-sulfur can be used as a soil fertilizer or fungicide. Currently, more than 150 applications, typically treating 100 to 10,000 kilograms of H_2S per day, are in use worldwide [4]. The utilization potential of the bio-desulfurization process is much greater, as the search for new natural gas reservoirs continues and the exploitation often requires biodesulfurizaton. Bio-desulfurization of gas streams is usually carried out in bubble column bioreactors which limits the application scope due to poor oxygen mass transfer. To be able to scale up, we need more insight into the kinetics and stoichiometry. The objective of the study described in the present paper was to improve our understanding of the reaction stoichiometry of biological sulfide oxidation in gas lift bioreactors.

During bio-desulfurization, the H_2S first dissolves, releasing a proton to the caustic. In low-redox and oxygen-limiting conditions, the sulfide is then mostly oxidized into elemental sulfur (S^0). However, part of the sulfide (typically less than 10%) is oxidized to sulfate (SO_4^{2-}) by a mixed population of sulfur-oxidizing bacteria (SOB) [5]. It is important to keep sulfate formation as low as possible, to prevent having to adjust the pH and having to remove the sulphate from the system.

Traditionally, the overall biological reactions are given as follows [5, 3]:

$$2\,HS^- + O_2 \rightarrow 2\,S^0 + 2\,OH^- \tag{2.1}$$

$$2\,HS^- + 4\,O_2 \rightarrow 2\,SO_4^{2-} + 2\,H^+ \tag{2.2}$$

Additionally, chemical oxidation of sulfide may occur, leading to the formation of thiosulfate ($S_2O_3^{2-}$) [6] (also unwanted).

$$2\,HS^- + 2\,O_2 \rightarrow S_2O_3^{2-} + H_2O \tag{2.3}$$

The pH and sodium content of the medium are important factors in the process. At a relatively high pH (>8.5) and at high salt concentrations (2M), the uptake of H_2S is enhanced and the sodium and potassium carbonate levels buffer the uptake of carbon dioxide. The bacteria used in haloalkaline biodesulfurization are adapted to these conditions; they are predominantly haloalkaliphilic sulfur-oxidizing bacteria (HA-SOB) belonging to the genus *Thioalkalivibrio* [7]. The complete genome of *Thioalkalivibrio sulfidophilus* was recently published, and suggests the availability of several enzymes for the oxidation of sulfide to S^0 and SO_4^{2-} [8, 9].

The electrons derived from the sulfide oxidation enter the respiration chain at the level of c-type cytochromes with the aid of flavocytochrome c oxidoreductase (FCC) [8, 10, 9, 7].

This enzyme is a part of the respiratory system, and oxidizes HS^- to S^0 with cytochrome c as electron acceptor [11].

Another well known enzyme associated with sulfide oxidation is sulfide:quinone oxidoreductase (SQR) [12]. The FCC and SQR are related, having a common ancestor and a similar catalytic (flavin) domain [13]. Based upon the measured decyl-ubiquinone-dependent oxidation of sulfide, activity of SQR in haloalkaliphilic SOB has been suggested [7]. The genomic sequence of several *Thioalkalivibrio* species revealed indeed the presence of several ubiquinone dependent enzymes. However, the genes encoding for SQR were not identified [8, 9]. Therefore, we hypothesize that because of the absence of SQR, some variants of FCC might act as SQR, i.e. donates electrons to ubiquinone instead of cytochrome c.

The reduced electron acceptors, cytochrome c and ubiquinone, can be subsequently oxidized by using oxygen via an oxidase complex, such as cytochrome c oxidase (CCO) and quinol oxidase (QO) [14, 11]. Eq. 2.1 describes the overall reaction for the oxidation of H_2S to S^0.

In addition to the route for the oxidation of the reduced quinone pool in *Thioalkalivibrio sulfidophilus*, a route has been proposed that is based on the reduction of NAD^+ via NADH dehydrogenase, with ubiquinone as electron donor [8]. Hypothetically, sulfide can be oxidized without transfer of electrons to oxygen, as NAD^+ can be regenerated by carbon fixation, e.g. for osmolyte synthesis. A consequence of increased levels of osmolyte synthesis would be a decrease in growth rate [15]. Also, the hypothetical route via the reduction of NAD^+ is energetically less favorable because the midpoint potential of S^0/H_2S couple is less negative than that of the $NAD^+/NADH$ couple. It would require energy to transport electrons from sulfide to NAD^+ [12]. This implies that this route is not feasible without another energy-yielding process, i.e. further oxidation of S^0 to SO_4^{2-}. Oxidation of S^0 to SO_4^{2-} is believed to proceed via a reversed dissimilatory sulfite reductase pathway and sulfite dehydrogenase [8]. The overall equation is given as follows [16, 17]:

$$S^0 + 1.5\ O_2 + H_2O \rightarrow SO_4^{2-} + 2\ H^+ \tag{2.4}$$

As this NADH route will consume less oxygen, an increase in oxygen supply to the biodesulfurization reactor will lead to a higher SO_4^{2-} formation rate than follows from Eq. 2.2. For large-scale process applications, this route would imply higher costs as formation of sulfuric acid requires neutralization by addition of caustic. Therefore, there is a need to explore the sulfide and oxygen balance and determine the predominant routes for the biological desulfurization process at S^0-forming conditions.

Van den Bosch et al. described the electron balance for sulfide oxidation at haloalkaline conditions (pH 10) in a fed-batch reactor [5]. Their experiments led to the conclusion that product formation (i.e. S^0, $S_2O_3^{2-}$, SO_4^{2-} and biomass) and oxygen consumption do not fully balance. Therefore, new experiments were performed under haloalkaline conditions at different O_2/H_2S supply ratios to investigate the relation between product formation and the electron balance for sulfide and oxygen with an enriched bacterial community originating from hypersaline soda lakes.

Previous studies have indicated that formation of unwanted $S_2O_3^{2-}$ increases with increasing pH values [6]. Hence, we carried out our reactor experiments at pH 8.5 as this is the lowest pH at which the HA-SOB still show reasonable activity [7].

2.2 Materials and methods

2.2.1 Experimental setup

The reactor experiments were performed in two identical gas lift reactors with a wet volume of 4.7 L each, as described by Van den Bosch et al. [5]. The same types of analytical and bench scale equipment (pH and redox electrodes, water baths, H_2S, O_2 and N_2 gas and mass flow controllers) was used. In addition, the dissolved oxygen (DO) concentration was monitored via a DO sensor (PSt3 and PSt6, Presens Precision Sensing GmbH, Regensburg, Germany) with a detection limit of 30 nM. The gas flow (300 L h^{-1}) was completely recycled to create a closed reactor system and reach low oxygen levels in the gas and liquid phase. To prevent water vapor condensation and subsequent damage to the compressor, the recycle gas was dried through cooling at 5±1°C. The system contained a water lock to allow any excess gas to be released to a safe location, e.g. in the event of an unforeseen pressure buildup. Whenever the pressure dropped below atmospheric levels, N_2 gas was added to restore the original pressure. The reactors were operated at 35±1°C using a thermostat bath. No biomass support material was supplied.

2.2.2 Medium

The mineral medium consisted of a mixture of a 2M bicarbonate (pH 8.3, 19L) and a 2M carbonate (pH 12.3, 1L) solution. Both solutions contained 0.66 mol L^{-1} Na^+ and 1.34 mol L^{-1} K^+. Furthermore, the medium contained 1.0 g L^{-1} K_2HPO_4, 0.6 g L^{-1} urea, 6.0 g L^{-1} NaCl and 0.20 g L^{-1} $MgCl_2 \cdot 6\ H_2O$ (all in demineralized water). Trace elements solution was added as described by Pfennig and Lippert [18]. After addition of all compounds, the pH of the medium was 8.5-8.6.

2.2.3 Inoculum

The reactors were inoculated with biomass taken from a sulfide-oxidizing gas lift bioreactor [7]. The original inoculum consisted of a mixture of sediments from hypersaline soda lakes in Mongolia, southwestern Siberia and Kenya and was obtained from Delft University of Technology. An overview of the physiology of the SOB present in the inoculum is given elsewhere in the literature (pH range 8.8 - 10.1; 2 M carbonate buffer) [19, 20].

2.2.4 Reactor operation

First the reactors were filled with medium after which the biomass was added (around 20 mg N L^{-1}). After temperature stabilization (35°C), sulfide addition was started at a volumetric load of 2.13 mmol L^{-1} h^{-1}. During startup (48 h), biomass growth was stimulated by operating the reactor at relative high oxidation reduction potential (ORP) levels, i.e. between -100 and 20 mV (Ag/AgCl). After the start phase, the oxygen supply rate was set to a constant value, which was different for the various experimental runs. The sulfide loading rate was kept constant throughout all experiments; the O_2/H_2S supply ratio (mol/mol) was varied by changing the oxygen supply rate. As the medium was highly buffered, the pH remained constant at 8.5-8.6. The selectivity of the process was determined over a period of at least 55 hours at stable reactor conditions.

2.2.5 Redox control

The ORP was maintained between -360 and -420 mV. The measured ORP is mainly determined by the dissolved sulfide concentration [21]. At a constant oxygen and sulfide load, a decreasing ORP corresponds to an accumulation of H_2S. From previous work, it is known that when the ORP becomes more negative than -420 mV (Ag/AgCl), biological inhibition occurs due to too high sulfide concentrations. If this occurred, we interrupted the reactor run by shutting off the sulfide addition and increasing the oxygen concentration. This enabled the removal of sulfide through chemical oxidation to $S_2O_3^{2-}$.

2.2.6 Analysis

The sulfide was measured as total sulfide (S_{tot}^{2-}), being the sum of the concentrations of H_2S, HS^-, S^{2-}, H_2S_x, HS_x^- and S_x^{2-}. The sulfide detection method was based on a modified methylene blue method as described by Van den Bosch et al. [5]. Ion chromatography (Dionex DX-600 model 50, Salt Lake City, USA) was applied to determine the concentrations of SO_4^{2-} and $S_2O_3^{2-}$. An IonPac AS19 column was used at 30±1°C and a flow rate of 1.5 ml min^{-1}. The high carbonates were bypassed with a carbonate trap. The injection volume was 25µL. The eluent was generated by an eluent generator (EG40, Dionex, Salt Lake City, USA) equipped with a KOH cartridge, and carried by deionized water. Detection of the ions was based on conductivity; we used an ASES-ULTRA suppressor to suppress eluent conductivity.

As the formed sulfur particles have a tendency to attach to the reactor wall, it was not possible to calculate the S^0 production rate from the S^0 analysis. No other products than S^0, SO_4^{2-} and $S_2O_3^{2-}$ were identified, so we calculated the production rate of S^0 from the following mass balance:

$$P_{S^0} = I_{H_2S} - P_{SO_4{}^{2-}} - P_{S_2O_3{}^{2-}} \tag{2.5}$$

Here, P_{S^0}, $P_{SO_4{}^{2-}}$ and $P_{S_2O_3{}^{2-}}$ are the production rates of S^0, SO_4^{2-}, and $S_2O_3^{2-}$, respectively, in mmol L^{-1} h^{-1} and I_{H_2S} is the volumetric H_2S influent in mmol L^{-1} h^{-1}.

2.2.7 Biomass concentration

The biomass concentration was measured as the amount of total N-organic, based on the absorbance of nitrophenol at 370 nm, with the Lange cuvette test LCK338 (Hache Lange, Germany). The difference between filtered medium (cellulose acetate filter, Schleicher & Schuell OE66) and non-filtered medium indicates the total amount of N present in the biomass. Van den Bosch et al. [5] have carried out a study to compare this method against a traditional destruction method, with good results.

2.2.8 Growth yields

The overall mass balance of oxygen depends on both assimilation and product formation. In order to quantify the electrons used for bacterial growth on sulfide, consider the following stoichiometric equation for the HA-SOB [15]:

$$H_2S + HCO_3^- + 0.2\ NH_3 + 0.95\ O_2 \rightarrow CH_{1.8}O_{0.5}N_{0.2} + SO_4^{2-} + 0.4\ H_2O + H^+ \tag{2.6}$$

As no biomass growth was observed when SO_4^{2-} formation was below 5 mol %, it was concluded that the electron mass balance is only compensated for growth when SO_4^{2-} is formed [5], as follows:

$$O_2^{SO_4^{2-}} = \alpha_{H2S} \cdot O_2^{as} + (1 - \alpha_{H2S}) \cdot O_2^{dis} \tag{2.7}$$

Here, $O_2^{SO_4^{2-}}$ is the oxygen cost of the overall mass balance to form SO_4^{2-} in mmol mmol^{-1}, and O_2^{as} and O_2^{dis} are the oxygen costs in mmol mmol^{-1} for the assimilation and dissimilation processes of the biomass. Given the stoichiometry in Eq. 2.6, the fraction of sulfide used for assimilation (α_{H2S}) is calculated as follows:

$$\alpha_{H2S} = \frac{Y}{0.2 \cdot u_N} \tag{2.8}$$

Here, u_N is the molar mass of nitrogen in mg mmol^{-1} and Y is the growth yield on SO_4^{2-} in mg N mmol^{-1}.

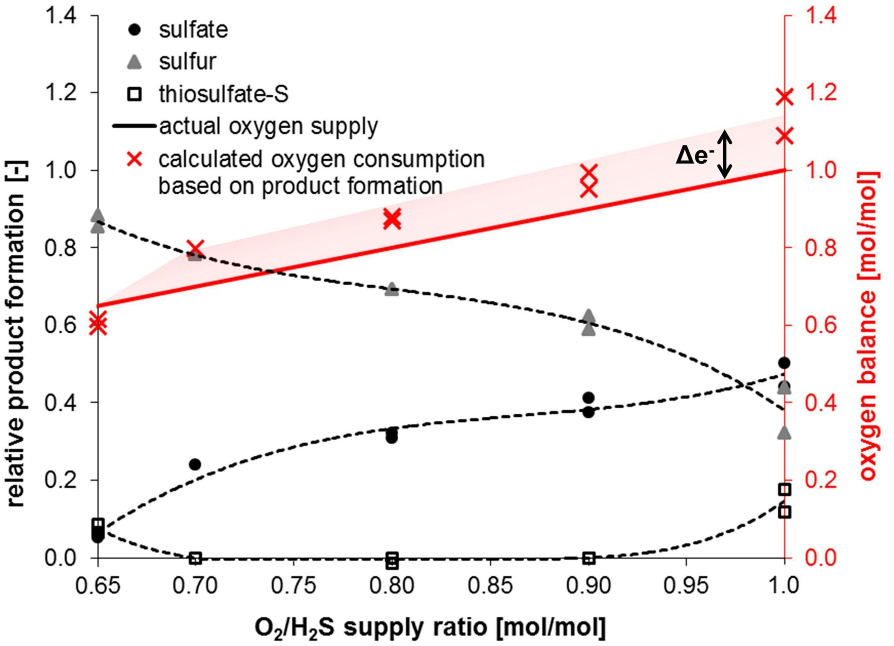

Figuur 2.1: Measured product selectivity at different molar O_2/H_2S supply ratios for haloalkaliphilic bioreactors at pH 8.5. The solid line represents the actual O_2 supply and the crosses represent the calculated oxygen consumption according to Eqs. 2.1-2.3 and 2.6, and show a structural discrepancy. The dotted lines are polynomials fitted to the measured data.

2.3 Results and discussion

2.3.1 Product Selectivity at pH 8.5

A series of experiments was carried out at O_2/H_2S dosing ratios of 0.6, 0.65, 0.7, 0.8, 0.9 and 1.0 mol/mol, all at pH 8.5. All experiments, except those at a ratio of 0.7 mol/mol, were performed in duplicate. Figure 2.1 presents the results. It can be seen that an increase in the O_2/H_2S ratio resulted in a decrease of S^0 formation as already shown in several previous studies [22, 23, 5]. For a O_2/H_2S ratio of 0.65 mol/mol, the selectivity for S^0 formation amounted to 85-88 mol% whereas at a ratio of 1.0 mol/mol, only 31-44 mol% of S^0 was formed. The term selectivity is generally applied in chemical engineering to describe the mole fractions of products that are formed from a substrate. An explanation for the results in Figure 2.1 is that more oxygen was available at higher O_2/H_2S dosing ratios and thus more SO_4^{2-} was formed. $S_2O_3^{2-}$ was only formed at a O_2/H_2S dosing ratio of 0.65 mol/mol, 1.0 mol/mol and during the startup phase (data not shown). An explanation for this observation is that in these circumstances, the biological oxidation capacity is a limiting factor. $S_2O_3^{2-}$

formation can be attributed to a number of factors, e.g. abiotic (poly)sulfide oxidation and S^0 hydrolysis [24]. At O_2/H_2S ratios between 0.7 and 0.9 mol/mol, the biological oxidation rate of $S_2O_3^{2-}$ appears to be higher than the chemical formation rate. HA-SOB are able to oxidize $S_2O_3^{2-}$ to S^0 and SO_4^{2-} [25]. However, as $S_2O_3^{2-}$ has a higher oxidation state than S^0, its formation will always lead to sulfate formation and is therefore unwanted.

At increasing pH values, the rate of chemical $S_2O_3^{2-}$ formation increased [6]. This resulted in a higher abiotic oxygen consumption which rendered less oxygen available as electron acceptor for biological sulfide oxidation and as a consequence, the SO_4^{2-} production rate declined. At a O_2/H_2S ratio of 0.8 mol/mol, 30.8-32.1 mol% of SO_4^{2-} was formed (at pH 8.5), whereas others have found a selectivity for SO_4^{2-} production of 23.0-29.0 mol% for pH 10 [5]. At O_2/H_2S ratios of 0.6 mol/mol, the system was not stable. Within 15 minutes, the ORP decreased to values below −420 mV as a result of sulfide accumulation. This implies the occurrence of biological inhibition. Several attempts to obtain a stable system at this supply ratio failed.

2.3.2 Mass balancing

To describe the oxygen balance based on sulfur product formation and oxygen consumption, oxygen used for biological assimilation is included in the calculations using Eq. 2.7. The growth yield under full oxidation of sulfide to SO_4^{2-} was found to be around 0.9 mg N / mmol H_2S [5]. Use of Eqs. 2.2 and 2.6 through Eq. 2.8 produced a value of 1.66 for $O_2^{SO_4^{2-}}$. According to the stoichiometry of 2.2, this implies that 17% of the electrons from sulfide oxidation are required for biomass synthesis.

Figure 2.1 displays the actual oxygen supply (mol/mol) and the oxygen consumption ratio according to Eqs. 2.1, 2.3 and 2.7 versus the different O_2/H_2S ratios, for our pH value of 8.5. As can be seen, the calculated oxygen consumption is higher than the actual dosing rate supply for O_2/H_2S supply ratios above 0.70 mol/mol. Apparently, other oxidants were active in the system such as dissolved CO_2 and bicarbonates. Previous studies have produced similar results for pH 10 [5]. Any oxidation of sulfide with nitrate or nitrite as electron acceptor is unlikely because of the use of urea as nitrogen source. Furthermore, hydrolysis of urea does not play a role in the overall electron balance of the process as it would cover less than 0.5 % of the overall electron balance.

When the electron gap (Δe^-) is entirely attributed to biomass synthesis (Eq. 2.7), i.e. when we subtract the chemical oxidation routes to $S_2O_3^{2-}$ from the overall electron balance, around 33% of the liberated electrons are needed for biomass formation (at O_2/H_2S ratios of 1.0 mol/mol). This is unrealistic as it has been known for more than fifty years that approximately 15% of the total electrons from oxidized sulfur compounds are used for cell assimilation [26]. Therefore, an additional route of electrons must be considered.

Via the quinone pool, the bacteria are able to reduce NAD^+ without direct transfer of electrons

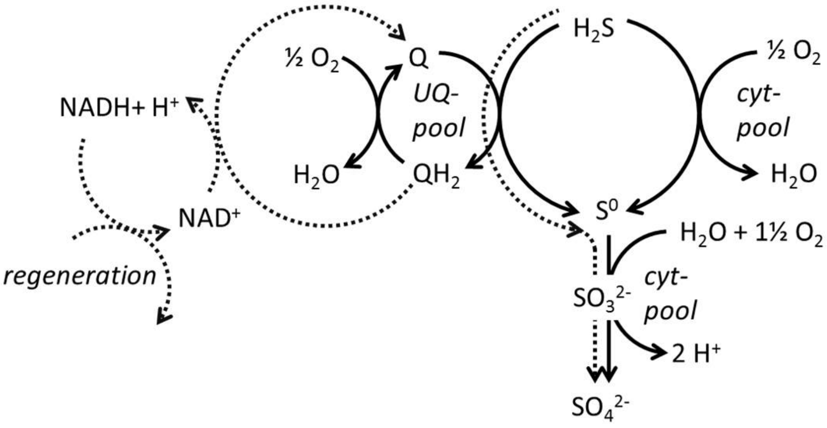

Figuur 2.2: Proposed reaction pathways that lead to the formation of S^0 and SO_4^{2-} from the biological oxidation of sulfide [8, 12, 14, 11, 16, 17]. The dotted line represents the limited oxygen route (LOR) and the solid lines represent the full oxygen route (FOR). Respectively 17% and 5.2% of all the electrons from sulfide oxidation end up in biomass synthesis via the FOR and LOR. These electron routes are not shown in this scheme. The UQ-pool = ubiquinone pool, Q/QH$_2$ = oxidized/reduced quinones, cyt-pool = cytochrome pool.

to oxygen. At oxygen-limiting conditions, this is most likely the main route for oxidizing sulfide via S^0 to SO_4^{2-}. Hereafter, we will call this route the limited oxygen route (LOR) and the route summarized by the overall Eq. 2.2 the full oxygen route (FOR). Evidence of this existence has been demonstrated by many authors [23, 27, 28]. Figure 2.2 gives a schematic representation of the possible overall biological routes. The LOR produces less energy and the growth yield is therefore also smaller than for the FOR. In the LOR, only 1.5 mol of oxygen is reduced to form 1 mol of SO_4^{2-}, and the growth yields are around 0.4 mg N / mmol H_2S [5]. According to Eq. 2.7, $O_2^{SO_4^{2-}} = 1.42$ and thus only 5.2% of the electrons from sulfide oxidation via the LOR end up in biomass synthesis.

2.3.3 Role of Limited Oxygen Route in Oxygen Balance

For Figure 2.3, we calculated the mass balance for oxygen by taking both the LOR and FOR into account. The results show the actual oxygen supply and the calculated oxygen consumption for pH 8.5 and pH 10. The calculated oxygen consumption is in good agreement with the actual dosing rate, when the LOR is taken into account. Apparently, any SO_4^{2-} was not formed via the FOR as an electron gap between measured an calculated electron balance (Δe^-) was found.

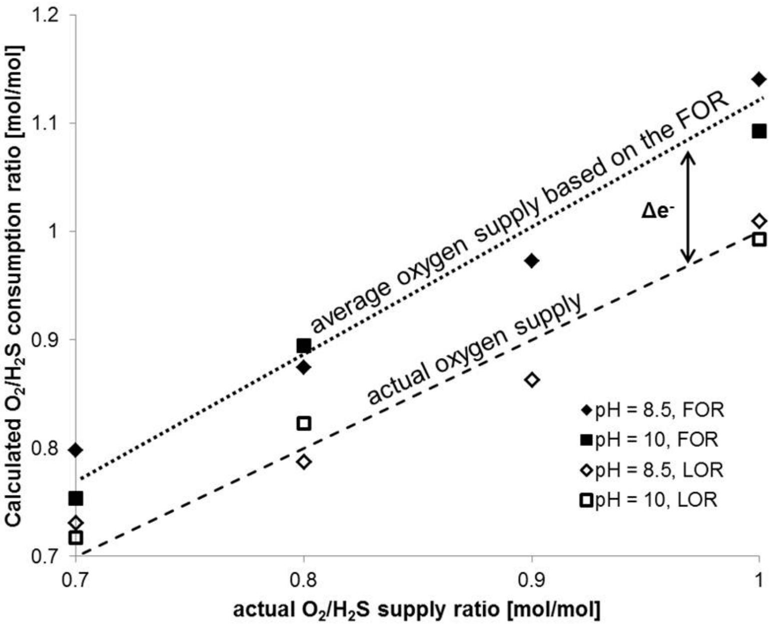

Figuur 2.3: Calculated O_2/H_2S consumption ratio based on product formation via the LOR, FOR and synthesis of biomass. As the ratio O_2/H_2S increases, more oxygen is available and thus more SO_4^{2-} is formed. The dashed line represents the actual oxygen supply (measured). The difference between the dotted and dashed line represents the average electron gap when the electron balance is calculated via the FOR. The data for pH 10 were calculated using the results of Van den Bosch et al. [5].

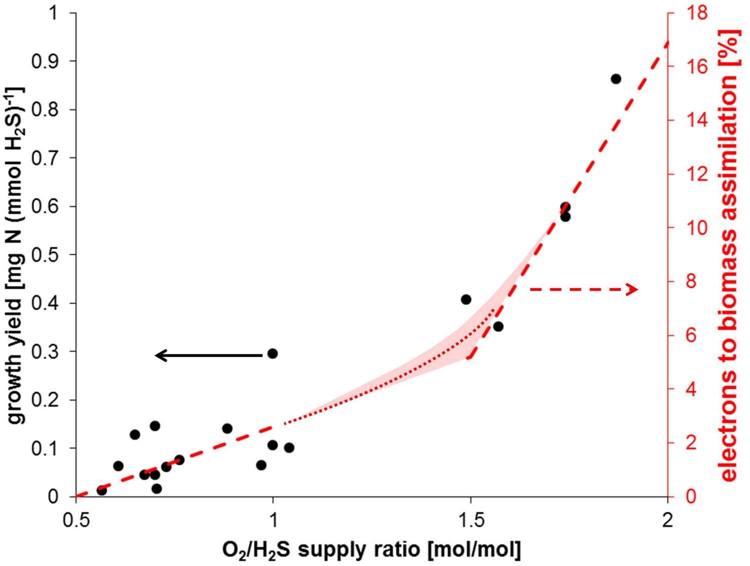

Figuur 2.4: Growth yields in mg N per mmol oxidized H_2S for a haloalkaliphilic system in relation to the O_2/H_2S supply ratio, calculated from the growth rates reported by Van den Bosch et al. [5] for pH 10. For comparative reasons, the hypothetical amounts of electrons are shown by the dashed line. Between a O_2/H_2S ratio of 1.0 and 2.0 mol/mol, the transition area between S^0 formation and SO_4^{2-} formation via LOR and FOR is indicated with dotted line, as this area can not be quantified on the basis of the performed experiments. At higher O_2/H_2S ratios, the FOR will be the main sulfide oxidation route.

As the bacteria gain less energy from the LOR than from the FOR, biomass growth yields can be indicative of the used pathway. A linear increase in oxygen consumption should theoretically lead to a linear increase of the formation of SO_4^{2-} and thus of biomass. Furthermore, biomass yield on the formation of SO_4^{2-} via the FOR should be higher than when the LOR is active. Figure 2.4 shows the calculated biomass growth yields, based on the oxidation of sulfide and using biomass growth rates determined in previous research [5] with a haloalkaliphilic reactor system operating at pH 10. A gradual increase of the growth yield can be seen at O_2/H_2S ratios of 0.5 up to 1.0 mol/mol. Below a ratio of 0.5 mol/mol, no biomass growth was detected. Above the ratio of 1.50 mol/mol, a larger increase of the growth yield is visible. The measured growth yield triples between an O_2/H_2S ratio of 1.50 and 2.0 mol/mol. This corresponds to the assumption that a pathway shift occurs towards the FOR. Via the FOR, more electrons are used for assimilation processes. For comparative reasons, Figure 2.3 shows the hypothetical amounts of electrons. It is assumed that 100 mol% S^0 formation takes place at an O_2/H_2S ratio of 0.5 mol/mol. Furthermore, no energy is assumed available for biomass growth at this ratio. As the electron balance could only be closed via the LOR at O_2/H_2 ratios below 1.0 mol/mol, we take this as an indication that at ratio of 1.5 mol/mol, sulfide is mainly oxidized via the LOR (5.2% of electrons end up in biomass). Between a ratio of 1.0 and 2.0 mol/mol, a gradual transition occurs from the LOR to the FOR; at a ratio of 2.0 mol/mol, all sulfide is oxidized via the FOR (17% of electrons go into biomass).

2.3.4 LOR in *Thiobacillus* species

When the bioreactor was run at O_2/H_2S ratios around 0.65 mol/mol, formation of SO_4^{2-} was low due to low levels of oxygen and/or high sulfide concentrations. Our experimental results show that mainly S^0 (more than 80 mol%) was formed (see Figure 2.1). We found that it is not possible to achieve stable operating conditions at O_2/H_2S ratios of 0.60 mol/mol or lower with haloakaliphilic biomass at pH 8.5.

However, systems incubated with a mixture of non-halophilic *Thiobacillus* species were able to oxidize sulfide completely at O_2/H_2S ratios as low as 0.35 mol/mol and pH 8.0 [21]. An explanation can be found in the higher maintenance requirements of the haloalkaliphilic system; more energy is required to maintain homeostasis. Carbon fixation [29] explains the fact that O_2/H_2S consumption ratios below 0.5 mol/mol are found for *Thiobacillus*. It could be an indication that these bacteria partly oxidize sulfide to S^0 by NAD^+ reduction, similar as presented in Figure 2.2. Moreover, Alcántara et al. presented experimental results that provide evidence for the existence of an alternative electron route [23]. At O_2/H_2S supply ratios of 1.0 mol/mol, the selectivity for SO_4^{2-} formation was around 60 mol% in their system, whereas a value of 33 mol% would be expected according to Eqs. 2.1 and 2.2. In that study, a reactor system was operating at pH 7.0 to 7.5, incubated with strains of *Thiobacillus*, with various O_2/H_2S supply ratios. These results could be an indication that *Thiobacillus* bacteria are able to oxidize sulfide via a route similar to the LOR. Further research should be conducted to confirm this hypothesis.

2.3.5 Considerations

Our experiments show that haloalkaliphilic sulfur-oxidizing bacteria in bench-scale gas lift reactors are able to oxidize sulfide to SO_4^{2-} via several respiration routes. One of the routes, the LOR, features at limiting oxygen levels. We hypothesize that sulfide is oxidized to S^0 via a variant of FCC acting as SQR (i.e. donating electrons to ubiquinone instead of cytochrome c) in which the electron acceptor is not oxygen, but NAD^+. As a consequence, 25% less oxygen is consumed for the formation of one mole of SO_4^{2-} relative to oxidation with oxygen as the sole electron acceptor. These results may have an impact on process optimization as at limiting oxygen levels, relatively more SO_4^{2-} may be formed, which is undesirable. Furthermore, the activity range of the haloalkaliphilic biomass prevents optimization of biological S^0 formation at pH values of less than 8.5. At higher pH values, this biomass shows more activity at lower O_2/H_2S ratios. These results emphasize the importance of accurate process control to secure a high S^0 selectivity at haloalkaliphilic conditions.

Acknowledgements

The authors thank Di Fang for assistance with the oxidation measurements, Dimitry Y. Sorokin and Gerard Muyzer for stimulating discussions.

References

[1] A. J. H. Janssen, R. C. Van Leerdam, P. L. F. Van den Bosch, E. Van Zessen, G. Van Heeringen, and C. J. N. Buisman. Development of a family of large-scale biotechnological processes to desulphurise industrial gases, 2nd international congress on biotechniques for air pollution control, A Coruña, Spain. 2007.

[2] A. J. H. Janssen, R. Ruitenberg, and C. J. N. Buisman. Industrial applications of new sulphur biotechnology. *Water Science and Technology*, 44(8):85–90, 2001.

[3] A. J. H. Janssen, P. N. L. Lens, A. J. M. Stams, C. M. Plugge, D. Y. Sorokin, G. Muyzer, H. Dijkman, E. Van Zessen, P. Luimes, and C. J. N. Buisman. Application of bacteria involved in the biological sulfur cycle for paper mill effluent purification. *Science of the Total Environment*, 407(4):1333–1343, 2009.

[4] Paqell. website paqell, March 2012.

[5] P. L. F. Van den Bosch, O. C. Van Beusekom, C. J. N. Buisman, and A. J. H. Janssen. Sulfide oxidation at halo-alkaline conditions in a fed-batch bioreactor. *Biotechnology and Bioengineering*, 97(5):1053–1063, 2007.

[6] P. L. F. Van den Bosch, D. Y. Sorokin, C. J. N. Buisman, and A. J. H. Janssen. The effect of pH on thiosulfate formation in a biotechnological process for the removal of hydrogen sulfide from gas streams. *Environmental Science and Technology*, 42(7):2637–2642, 2008.

[7] D. Y. Sorokin, P. L. F. Van Den Bosch, B. Abbas, A. J. H. Janssen, and G. Muyzer. Microbiological analysis of the population of extremely haloalkaliphilic sulfur-oxidizing bacteria dominating in lab-scale sulfide-removing bioreactors. *Appl. Microbiol. Biotechnol.*, 80(6):965–975, 2008.

[8] G. Muyzer, D. Y. Sorokin, K. Mavromatis, A. Lapidus, A. Clum, N. Ivanova, A. Pati, P. d'Haeseleer, T. Woyke, and N. C. Kyrpides. Complete genome sequence of "thioalkalivibrio sulfidophilus"hl-ebgr7. *Standards in Genomic Sciences*, 4:23–35, 2011.

[9] G. Muyzer, D. Y. Sorokin, K. Mavromatis, A. Lapidus, B. Foster, H. Sun, N. Ivanova, A. Pati, P. D'haeseleer, T. Woyke, and N. C. Kyrpides. Complete genome sequence of thioalkalivibrio sp. k90mix. *Standards in Genomic Sciences*, 5, 2011.

[10] D. Y. Sorokin, G. A. H. de Jong, L. A. Robertson, and G. J. Kuenen. Purifcation and characterization of sufide dehydrogenase from alkaliphilic chemolithoautotrophic sulfur-oxidizing bacteria. *FEBS letters*, 427(1), 1998.

[11] M. Griesbeck, C. ans Schütz, T. Schödl, S. Bathe, L. Nausch, N. Mederer, M. Vielreicher, and G. Hauska. Mechanism of sulfide-quinone reductase investigated using site-directed mutagenesis and sulfur analysis. *Biochemistry*, 2002.

[12] C. Griesbeck, G. Hauska, and M. Schutz. Biological sulfide oxidation: Sulfide-quinone reductase (sqr), the primary reaction. *Recent Research Developments in Microbiology*, 4:179–203, 2000.

[13] U. Theissen, M. Hoffmeister, M. Grieshaber, and W. Martin. Single eubacterial origin of eukaryotic sulfide:quinone oxidoreductase, a mitochondrial enzyme conserved from the early evolution of eukaryotes during anoxic and sulfidic times. *Molecular Biology and Evolution*, 20(9):1564–1574, 2003.

[14] I. Belevich and M. I. Verkhovsky. Molecular mechanism of proton translocation by cytochrome c oxidase. *Antioxidants and Redox Signaling*, 10(1):1–29, 2008.

[15] H. Banciu, D. Y. Sorokin, R. Kleerebezem, G. Muyzer, E. A. Galinski, and J. G. Kuenen. Growth kinetics of haloalkaliphilic, sulfur-oxidizing bacterium *Thioalkalivibrio versutus* strain ALJ 15 in continuous culture. *Extremophiles*, 8(3):185–192, 2004.

[16] D. P. Kelly. Thermodynamic aspects of energy conservation by chemolithotrophic sulfur bacteria in relation to the sulfur oxidation pathways. *Archives of Microbiology*, 171(4):219–229, 1999.

[17] F. J. Steward, O. Dmytrenko, E. F. DeLong, and C. M. Cavanaugh. Metatranscriptomic analysis of sulfur oxidation genes in the endysymbiont of *Solemya velum*. *Frontiers in Microbiology*, 2, 2011.

[18] N. Pfennig and K.D. Lippert. Über das vitamin B12-bedürfenis phototropher schwefelbakterien. *Archives of Microbiology*, 55(3):245–256, 1966.

[19] D. Y. Sorokin and J. G. Kuenen. Haloalkaliphilic sulfur-oxidizing bacteria in soda lakes. *FEMS Microbiol. Rev.*, 29(4):685–702, 2005.

[20] D. Y. Sorokin, H. Banciu, M. Van Loosdrecht, and J. G. Kuenen. Growth physiology and competitive interaction of obligately chemolithoautotrophic, haloalkaliphilic, sulfur-oxidizing bacteria from soda lakes. *Extremophiles*, 7:195–203, 2003.

[21] A. J. H. Janssen, S. Meijer, J. Bontsema, and G. Lettinga. Application of the redox potential for controling a sulfide oxidizing bioreactor. *Biotechnol. Bioeng.*, 60(2):147–155, 1998.

[22] A. J. H. Janssen, R. Sleyster, C. van der Kaa, J. Bontsema, , and G. Lettinga. Biological sulphide oxidation in a fed-batch reactor. *Biotechnol. Bioeng.*, 47(3):327–333, 1995.

[23] S. Alcántara, A. Velasco, A. Muñoz, J. Cid, S. Revah, and E. Razo-Flores. Hydrogen sulfide oxidation by a microbial consortium in a recirculation reactor system: Sulfur formation under oxygen limitation and removal of phenols. *Environmental Science and Technology*, 38(3):918–923, 2004.

[24] W. E. Kleinjan, A. De Keizer, and A. J. H. Janssen. Kinetics of the chemical oxidation of polysulfide anions in aqueous solution. *Water Research*, 39(17):4096–4100, 2005.

[25] D. Y. Sorokin, G. J. Kuenen, and G. Muyzer. The microbial sulfur cycle at extremely haloalkaline conditions of soda lakes. *Frontiers in Microbiology*, 2(44), 2011.

[26] H. G. Trüper and H. G. Schlegel. Sulphur metabolism in *Thiorhodaceae* i. quantitative measurements on growing cells of *Chromatium okenii*. *Antonie van Leeuwenhoek*, 1964.

[27] P.N.L. Lens, A. Visser, A. J. H. Janssen, L. W. Hulshoff Pol, and G. Lettinga. Biotechnological treatment of sulfate-rich wastewaters. *Critical Reviews in Environmental Science and Technology*, 28(1):41–88, 1998.

[28] P. L. F. Van den Bosch, M. Fortuny-Picornell, and A. J. H. Janssen. Effects of methanethiol on the biological oxidation of sulfide at natron-alkaline conditions. *Environmental*

Science and Technology, 43(2):453–459, 2009.

[29] G. C. Stefess, R. A. M. Torremans, R. De Schrijver, L. A. Robertson, and J. G. Kuenen. Quantitative measurement of sulphur formation by steady-state and transient-state continuous cultures of autotrophic *Thiobacillus* species. *Applied Microbiology and Biotechnology*, 45(1-2):169–175, 1996.

Chapter 3

A physiologically based kinetic model for bacterial sulfide oxidation[1]

Abstract In the biotechnological process for hydrogen sulfide removal from gas streams, a variety of oxidation products can be formed. Under natron-alkaline conditions, sulfide is oxidized by haloalkaliphilic sulfide oxidizing bacteria via flavocytochrome c oxidoreductase. From previous studies, it was concluded that the oxidation-reduction state of cytochrome c is a direct measure for the bacterial end-product formation. Given this physiological feature, incorporation of the oxidation state of cytochrome c in a mathematical model for the bacterial oxidation kinetics will yield a physiologically based model structure. This paper presents a physiologically based model, describing the dynamic formation of the various end-products in the biodesulfurization process. It consists of three elements: 1) Michaelis-Menten kinetics combined with 2) a cytochrome c driven mechanism describing 3) the rate determining enzymes of the respiratory system of haloalkaliphilic sulfide oxidizing bacteria. The proposed model is successfully validated against independent data obtained from biological respiration tests and bench scale gas-lift reactor experiments. The results demonstrate that the model is a powerful tool to describe product formation for haloalkaliphilic biomass under dynamic conditions. The model predicts a maximum S^0 formation of about 98 mol%. A future challenge is the optimization of this bioprocess by improving the dissolved oxygen control strategy and reactor design.

---

[1] This chapter has been published as: Klok JBM, de Graaff M, van den Bosch PLF, Boelee NC, Keesman KJ and Janssen AJH. A physiologically based kinetic model for bacterial sulfide oxidation. *Wat Res* 2012

3.1 Introduction

Hydrogen sulfide is present in natural and synthetic hydrocarbon gas streams. Bulk removal conventionally proceeds by applying physicochemical processes, such as the amine-Claus process [1]. These processes typically perform at high temperature and pressure, and are therefore expensive particularly for small scale applications (i.e. H_2S loads up to 100 tons day^{-1}). As microbiological sulfide oxidation proceeds at ambient temperatures and atmospheric pressure, biological desulfurization is considered as a cost-effective alternative to the existing technology [2].

In biological gas desulfurization, dissolved sulfide is oxidized by a mixed population of chemolithoautotrophic haloalkaliphilic sulfide oxidizing bacteria (HA-SOB) into elemental sulfur (S^0) under oxygen-limited conditions, whilst a part (typically less than 10%) is oxidized to sulfate (SO_4^{2-}) [3, 4]. Additionally, a fraction of the dissolved sulfide is oxidized abiotically to thiosulfate ($S_2O_3^{2-}$) [5]. In this process, the formation of S^0 is preferred, as $S_2O_3^{2-}$ and SO_4^{2-} formation will increase the process costs significantly, because of an increased caustic consumption rate.

In order to scale-up the process up to 100 tons of sulfide per day, more insight in the relation between the associated biological kinetics and hydraulic phenomena is needed. Hence as a first step, it is essential that bacterial end product formation and growth can be estimated accurately. Bacterial growth kinetics are commonly described by Monod kinetics [6], while substrate inhibition can, for instance, be described by a Haldane model. A drawback of these mono-substrate kinetic models is the disability to describe the formation of multiple end-products. Furthermore, these empirical relationships do not give complete insight into complex biological processes such as the biological desulfurization process.

The process selectivity (i.e. the relative formation of different end-products) of biological desulfurization depends on various substrate levels, such as oxygen, sulfide and polysulfides ($S_x{}^{2-}$) [3, 5]. For the description of the biological formation of S^0 and $SO_4{}^{2-}$ via a Monod-Haldane model, at least 12 empirical parameters have to be estimated. This would make the accuracy of such a model over a range of substrate concentrations questionable. Furthermore, as multiple products can be formed by the HA-SOB, a Monod-Haldane model does not give insight into the mechanism of the underlying biological processes. Hence, there is a need for a novel mechanistic description of the process kinetics.

In this study, the concept of combined Michaelis-Menten cytochrome kinetics, based upon the respiratory enzymes of HA-SOB, is introduced in a mathematical model to describe the biological sulfide oxidation chain up to $SO_4{}^{2-}$. The resulting model is validated against biological oxygen respiration tests with a mixture of HA-SOB. The validated model is subsequently used to predict the product selectivity in bench scale gas-lift reactor experiments.

3.2 Materials and methods

3.2.1 Biomass source

HA-SOB were obtained from a bench scale gas-lift reactor inoculated with a mixture of sediments obtained from hypersaline soda lakes in Mongolia, southwestern Siberia and Kenya that where kindly provided by Delft University of Technology. An overview of the physiology of the SOB present in the inoculum is given elsewhere [7, 8].

The bench scale gas-lift reactors were operated for more than a year at pH 8.6 under oxygen limiting conditions to maximize S^0 formation. Before washing the biomass, the reactor samples were stored for at least 7 days to secure the settling of S^0. Subsequently, bacterial cells were separated from the medium by steps of centrifugation (5000 rpm), washing and resuspension in a (bi)carbonate buffer, resulting in a cell suspensions with a final concentration of 1570 mg N L^{-1}.

The biomass concentration was measured as the amount of total N-organic, based on the absorbance of nitrophenol at 370 nm, with the Lange cuvette test LCK338 (Hache Lange, Germany). Van den Bosch et al. (2007) have carried out a study to compare this method against a traditional destruction method [3]. This method was tested by standard addition of urea and nitrate to reactor samples as well as fresh medium, with and without the presence of biologically produced sulfur. Presence of biologically produced sulfur did not affect the results.

3.2.2 Respiration tests

Respiration tests were performed in a thermostated 4 mL glass chamber mounted on a magnetic stirrer and closed off with a dissolved oxygen (DO) sensor (PSt3, PreSens Precision Sensing GmbH, Regensburg, Germany). A small opening allowed injection of substrate. A schematic representation of the setup is shown elsewhere [9]. While the solution was saturated with oxygen by sparging air for at least 5 minutes, cell suspension was added to a final concentration of 15 mg N L^{-1}. Experiments commenced by injection of 16 - 230 μL of sulfide substrate stock solutions. The decrease of DO concentration was measured with a sampling time of 5 seconds and the initial slope was used as a measure of the oxidation rate. The maximum oxygen solubility in the buffer at 35 °C was found to be 0.15 mmol L^{-1}. The biomass oxidation rates were determined in triplicate, controls were performed in duplicate with buffer solution only. Oxygen consumption rates were obtained for different sulfide concentrations, ranging from 0 up to 5 mM.

3.2.3 Bench scale tests

The results of the bench scale tests were obtained with the same bioreactor set-up as described elsewhere [3, 10]. Also, the same analytical equipment, start-up and analysis were applied.

The mode of the reactor (i.e. fed-batch or continuous, with or without pH control), sulfide supply rates as well as concentrations of biomass, SO_4^{2-}, $S_2O_3^{2-}$ and S^0 may vary for various reactor runs. The oxygen supply rate follows from a proportional controller using the total sulfide concentration (based on oxidation reduction potential (ORP), (Ag/AgCl)).

3.2.4 Chemicals used

Carbonate buffer was prepared by mixing sodium and potassium (1:2) bicarbonate (pH 8.3) and carbonate (pH 12.3) buffer solutions. For the respiration tests, a final pH of 8.5 was obtained. For the fed-batch reactor experiments, the final pH range was between 8.3 and 10.2. Furthermore, the medium for the fed-batch experiments was enriched with macro nutrients and trace elements similar to previous research [3]. Both buffers contained 1.67 M K^+, 0.33 M Na^+ as (bi)carbonate.

Sodium sulfide stock solutions for the respiration tests (2.5/15/100 mM) were freshly prepared by dissolution of $Na_2S{\cdot}9H_2O$ crystals in de-aerated water by flushing with nitrogen gas. The sulfide concentrations of the stock solutions were experimentally validated.

3.3 Kinetic model

3.3.1 Stoichiometric relationships

The biological oxidation of sulfide to S^0 and SO_4^{2-} is assumed to proceed according to a number of subsequent reaction steps [11]. A wide range of enzyme mechanisms are identified in a variety of SOB, e.g. FCC [12, 13], sulfur oxidizing system (SOX) [14, 15] and sulfite dehydrogenase (SOR) [13, 16].

HA-SOB are able to oxidize a number of sulfur species, preferred by the reduction potential of the component [17]. However, in this paper, the only sulfur containing substrate of the SOB is sulfide. It is assumed that the performed respiration tests are solely based on sulfide oxidation, because of the absence of any other sulfur species such as S^0 and S_x^{2-}.

In a previous study, it was suggested that haloalkaliphilic SOB contain FCC and some variant of FCC (FQ), oxidize sulfide to intermediate S^0 via electron transfer to cytochromes and quinones respectively [10]. Further oxidation of S^0 is possible via several routes in which both reductases and dehydrogenases have been identified [13]. Several enzymes are involved in the oxidation of S^0, all based on the transfer of electrons to cytochrome c [14, 18, 13]. A schematic overview of the modeled enzymatic processes is shown in Figure 3.1. In this scheme, a clear distinction is made between the cytochrome system and the non-cytochrome system (i.e. quinone system). FCC catalyzes electron transfer from hydrogen sulfide to oxidized cytochrome c (cyt^+), according to [19]:

$$H_2S + 2\,cyt^+ \rightarrow S^0 + 2\,cyt + 2\,H^+ \tag{3.1}$$

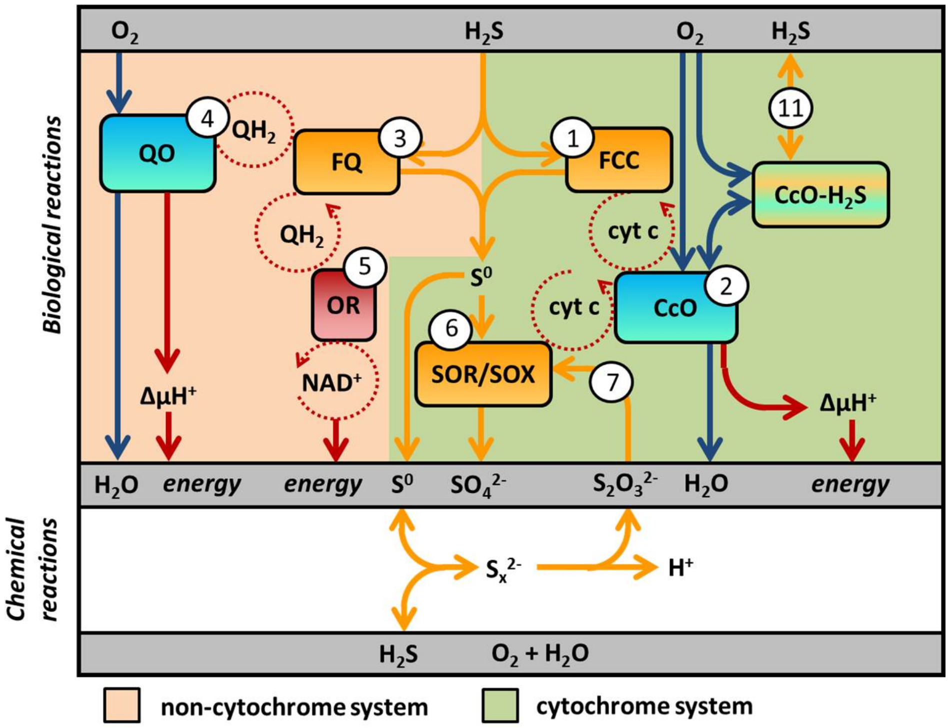
Biological reactions
Chemical reactions
O2
H2S
O2
H2S
QO
4
QH2
FQ
3
1
FCC
11
CcO-H2S
QH2
cyt c
5
OR
S0
cyt c
CcO
2
6
SOR/SOX
NAD+
7
ΔμH+
ΔμH+
H2O
energy
energy
S0
SO4 2-
S2O3 2-
H2O
energy
Sx 2-
H+
H2S
O2 + H2O
non-cytochrome system
cytochrome system

Figuur 3.1: Reaction pathways that lead to the (biological and chemical) formation of S^0, $S_2O_3^{2-}$ and SO_4^{2-} from the oxidation of hydrogen sulfide. Numbers inside circles refer to reaction equation numbers mentioned in the text. Notice that biomass growth is not included in this figure.

Reduced cytochrome c (cyt) is oxidized via the reduction of oxygen to water by the enzyme cytochrome c oxidase (CcO), according to [20]:

$$4\text{cyt} + 4\,\text{H}^+ + \text{O}_2 \rightarrow 4\,\text{cyt}^+ + 2\,\text{H}_2\text{O} \tag{3.2}$$

The reduction of oxygen yields a proton gradient ($\Delta\mu\text{H}^+$) that enables bacteria to obtain energy for maintenance and growth [21]. At moderate concentrations, sulfide inhibits CcO. A functional model has been suggested in [22]. According to this model, it can be derived that activity of the FCC system is suppressed due to a lack of cyt^+ at higher concentrations of sulfide.

FQ catalyzes the hydrogen sulfide dependent reduction of quinones (Q) [10], according to [19]

$$\text{H}_2\text{S} + \text{Q} \rightarrow \text{S}^0 + \text{QH}_2 \tag{3.3}$$

Two possible routes were hypothesized in which the bacteria are able to oxidize the quinones: the 'low oxygen route' (LOR) and the 'full oxygen route' (FOR) [10]. Via the FOR, bacteria transfer the electrons to oxygen via quinol oxidase (QO) [19].

$$\mathrm{QH_2} + \frac{1}{2}\,\mathrm{O_2} \rightarrow \mathrm{Q} + \mathrm{H_2O} \tag{3.4}$$

Via the LOR, quinones transfer electrons directly to NAD^+ via a NADH-oxidoreductase (OR) [10].

$$\mathrm{QH_2} + \mathrm{NAD^+} \rightarrow \mathrm{Q} + \mathrm{NADH} + \mathrm{H^+} \tag{3.5}$$

There are two options to regenerate NAD^+, namely via the electron chain and via fixation of CO_2. This last route yields less energy than the FOR and is therefore not preferred by the bacteria; formation of NADH via the couple H_2S/S^0 costs energy [19]. The advantage of the quinone system is that it is less susceptible to sulfide intoxication as compared to the cytochrome system. At higher sulfide levels, it is thus expected that the major oxidation route of hydrogen sulfide is via FQ. However, the quinone system does not sustain complete oxidation of (poly)sulfide to SO_4^{2-} [23].

In the subsequent oxidation from S^0 to SO_4^{2-}, several enzymatic routes are involved [13]. We consider the following overall equation describing the oxidation of S^0 to SO_4^{2-}.

$$\mathrm{S^0} + 6\,\mathrm{cyt^+} + 4\mathrm{H_2O} \rightarrow \mathrm{SO_4^{2-}} + 6\,\mathrm{cyt} + 8\,\mathrm{H^+} \tag{3.6}$$

Furthermore, as haloalkaliphilic SOB are only able to grow when SO_4^{2-} is formed [3], part of the reduced cytochromes is oxidized via the formation of biomass.

The haloalkaliphilic SOB are also able to oxidize $S_2O_3^{2-}$ via the SOX route [13]. To give a complete overview, the oxidation of $S_2O_3^{2-}$ is included as well. Hence, [14]

$$\mathrm{S_2O_3^{2-}} + 8\,\mathrm{cyt^+} + 5\,\mathrm{H_2O} \rightarrow 2\,\mathrm{SO_4^{2-}} + 8\,\mathrm{cyt} + 10\,\mathrm{H^+} \tag{3.7}$$

3.3.2 The influence of the cytochrome pool

The work in [24] suggests that the bacterial end-product of neutrophilic *Thiobacillus* species is determined by the reduction degree of the cytochrome pool (F), where F is given by

$$F = \frac{\mathrm{cyt}}{\mathrm{cyt} + \mathrm{cyt^+}} \tag{3.8}$$

and $0 \leq F \leq 1$. In what follows, the oxidation rate of sulfide is directly related to F and thus to the selectivity of end-products. The relation between F and the selectivity for product formation $P(F)$ is visualized in Figure 3.2. In this figure, information on sulfide loads, sulfur-compound production and cytochrome reduction degree from Visser et al. [24] are arbitrarily converted to 'selectivity'-curves for the formation of SO_4^{2-} ($P_{SO_4^{2-}}$) and S^0 (P_{S^0}) as function of F.

In the figure, F_1 is introduced to indicate the 'switch' points of selectivity for product formation. For $F \leq F_1$, no O_2 limitation occurs, resulting in a complete oxidation to SO_4^{2-}. For $F > F_1$, the electron transport capacity becomes limiting, resulting in an interruption of the oxidation chain. The interruption leads to formation of S^0. When $F = 1$, i.e. beyond the sulfide oxidation capacity of FCC, no SO_4^{2-} formation occurs. Consequently, bacterial growth will be strongly limited, as only the FQ system remains available for electron channeling.

The product formation function for S^0 (P_{S^0}) is found from the difference between the (normalized) sulfide oxidation and sulfate formation rates. This seems an appropriate assumption as no other sulfur products from biological origin have been identified [24]. Consequently,

$$P_{S^0}(F) = 1 - P_{SO_4^{2-}}(F) \tag{3.9}$$

where $0 \leq P_{SO_4^{2-}} \leq 1$.

3.3.3 Modeling the cytochrome pool

The sulfide oxidation rate for FCC (q_{FCC}) and the total cyt oxidation rate (q_{CcO}) are introduced in the following *combined Michaelis-Menten-cytochrome* equations.

$$q_{FCC} = q_{FCC,max}\,(1 - F)\,\frac{[HS^-]}{K_{FCC} + [HS^-]} \tag{3.10}$$

$$q_{CcO} = q_{CcO,max} F \frac{[O_2]}{K_{CcO} + [O_2]}\frac{K_i}{K_i + [HS^-]} \tag{3.11}$$

in which $q_{FCC,max}$ and $q_{CcO,max}$ represent the maximal reaction rates (mmol mg N^{-1} s^{-1}), K_{FCC} and K_{CcO} the affinity constants (mmol L^{-1}) and $[HS^-]$ the total sulfide concentration, which is determined by the sum of the concentration of sulfide and S_x^{2-} [3, 25]. The inhibition term $\frac{K_i}{K_i+[HS^-]}$ is included, according to simplifications to the proposed functional model by Collman et al. [22]. It should be noted that the terms for the reaction rates include the total cytochrome content of the bacteria, as F denotes a fraction of cytochromes.

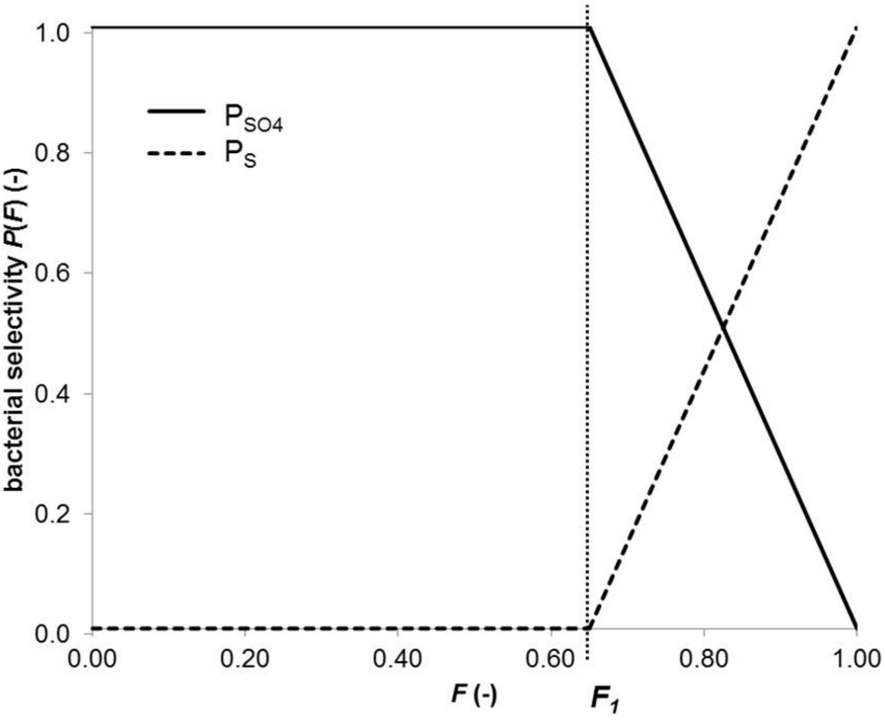

Figuur 3.2: The relative product formation as function of the reduction degree of the cytochrome pool F. The vertical dashed line represent the boundary conditions (F_1) for the selectivity. These curves are derived from the results of Visser et al. [24].

3.3.4 Modeling the quinone pool

In the oxidation of sulfide via the FQ, the quinone pool is involved. The reduction degree of the quinone pool (Q) is defined similarly as F in Eq. 3.8. The reduction and oxidation reactions of Q are given by

$$q_{FQ} = q_{FQ,max}\,(1 - Q)\,\frac{[HS^-]}{K_{FQ} + [HS^-]} \tag{3.12}$$

$$q_{FQox} = q_{FQox,max} Q \frac{[O_2]}{K_{FQox} + [O_2]} \tag{3.13}$$

with $q_{FQ,max}$ and $q_{FQox,max}$ the maximal reaction rates (mmol s^{-1} mg N^{-1}), K_{FQ} and K_{FQox} the affinity constants (mmol L^{-1}). In what follows, it is assumed that the quinone pool changes instantaneously according to the sulfide and oxygen levels, and thus at quasi-steady state conditions [26] holds:

$$\frac{dQ}{dt} = q_{FQ} - q_{FQox} = 0 \tag{3.14}$$

This equation determines the equilibrium of Q ($Q^{\dagger}$) for given sulfide and oxygen concentrations. After substituting Eqs. 3.12 and 3.13 in the equation mentioned above, $Q^{\dagger}$ can be determined. Substituting $Q^{\dagger}$ in Eq. 3.12 leads to the overall equation of sulfide oxidation by FQ.

$$q_{FQ} = \frac{q_{FQ,max}[HS^-]}{\frac{q_{FQ,max}}{q_{FQox,max}}\left(\frac{[O_2]+K_{FQox}}{[O_2]}\right)[HS^-] + [HS^-] + K_{FQ}} \tag{3.15}$$

In respiration tests oxygen levels are high (close to 100%), $K_{FQox} \ll [O_2]$ and thus we can simplify Eq. 3.15 to

$$q_{FQ} = \frac{q_{FQ,max}[HS^-]}{\frac{q_{FQ,max}}{q_{FQox,max}}[HS^-] + [HS^-] + K_{FQ}} \tag{3.16}$$

When both oxygen and sulfide are not limiting (i.e. $K_{FQox} \ll [O_2]$ and $K_{FQ} \ll [HS^-]$) , Eq. 3.16 can be further simplified to

$$q_{FQ} = \frac{q_{FQ,max}\, q_{FQox,max}}{q_{FQ,max} + q_{FQox,max}} = \left(\frac{1}{q_{FQ,max}} + \frac{1}{q_{FQox,max}}\right)^{-1} \tag{3.17}$$

which can be interpreted in the context of a serial network.

3.3.5 Modeling product selectivity

The overall oxidation rate of sulfide to S^0 (q_{tot}) is determined by the activity of both FQ and FCC see Figure 3.1. Thus,

$$q_{tot} = q_{FCC} + q_{FQ} \tag{3.18}$$

The reduced cytochrome pool is directly related to the product selectivity, such that

$$q_{SO_4^{2-}} = P_{SO_4^{2-}}(F)\, q_{tot} \tag{3.19}$$

and

$$q_{S^0} = P_{S^0}(F)\, q_{tot} = 1 - P_{SO_4^{2-}}(F)\, q_{tot} = q_{tot} - q_{SO_4^{2-}} \tag{3.20}$$

with $P_{SO_4^{2-}}(F)$ and P_{S^0} as in Figure 3.2. According to this kinetic model, the cytochrome pool determines the model-state for end-product formation. Given the rates q_{FCC}, $q_{SO_4^{2-}}$ and q_{CcO}, the rate of the cytochrome reactions (q_F) can be described by

$$q_F = 2q_{FCC} + (6 - Y)q_{SO_4^{2-}} - q_{CcO} \tag{3.21}$$

The rationale behind this relationship is that two mol cyt$^+$ are reduced to form 1 mol of S^0 (Eq. 3.1), 6 mol cyt are reduced to form 1 mol of SO_4^{2-} (Eq. 3.6) and 4 mol cyt are oxidized with 1 mol O_2 (Eq. 3.2). Furthermore, Y is the number of electrons that is used by the bacteria for growth. At high oxygen levels (FOR) $Y = 1.36$, at limiting oxygen conditions (LOR) $Y = 0.32$ [10].

3.4 Results and discussion

3.4.1 Chemical oxidation

In the respiration test, the chemical oxidation of sulfide is determined in the absence of biomass, as shown in Figure 3.3. The general rate equation given by O'Brien and Birkner [27],

$$\frac{d[O_2]}{dt} = -k_{S_2O_3^{2-}}[HS^-]^{\delta_1}[O_2]^{\delta_2} \tag{3.22}$$

is fitted to the data. As the respiration tests were evaluated at saturated oxygen levels, δ_2 can not be identified. Therefore, δ_2 is assumed to be 0.8, as found in previous research by [27]. The unknown parameters $k_{S_2O_3^{2-}}$ and δ_1 were found from the data in Figure 3.3. This figure also shows the identified chemical curve with $k_{S_2O_3^{2-}} = 2.91 \cdot 10^{-4}$ mmol L^{-1} s^{-1} and $\delta_1 = 1.02$ (see appendix A for details of the parameter estimation routine).

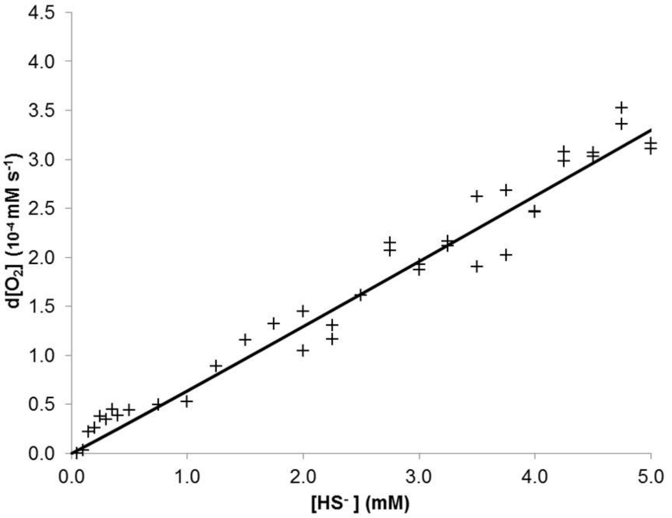

Figuur 3.3: Chemical oxidation rate in respiration tests (line represents model fit).

3.4.2 Biological oxidation

The reduction rates of oxygen in the respiration tests were measured and corrected for chemical activity for a range of sulfide concentrations, see Figure 3.4. It appears that the activity rapidly increases for sulfide concentrations between 0 and 0.15 mM. At sulfide levels of 0.15 up to 0.30 mM an optimum of around 100 nmol O_2 mg N^{-1} s^{-1} is found for the reduction rate of oxygen. This corresponds well with the rate of 97 nmol O_2 mg N^{-1} s^{-1}, which was

Tabel 3.1: Estimated parameters with corresponding bounds or standard deviations

parameter	unit	estimate	σ
$k_{S_2O_3^{2-}}$	mM s^{-1}	$2.91 \cdot 10^{-4}$	$2.32 \cdot 10^{-5}$
δ_1	-	1.02	$5.93 \cdot 10^{-2}$
$q_{FCC,max}$	mmol mg N^{-1} s^{-1}	$1.35 \cdot 10^{-4}$	$6.26 \cdot 10^{-6}$
$q_{CcO,max}$	mmol mg N^{-1} s^{-1}	$6.71 \cdot 10^{-4}$	$1.70 \cdot 10^{-4}$
$q_{FQ,max}$	mmol mg N^{-1} s^{-1}	$1.23 \cdot 10^{-4}$	$1.82 \cdot 10^{-6}$
$q_{FQox,max}$	mmol mg N^{-1} s^{-1}	$2.15 \cdot 10^{-4}$	-**
K_{FCC}	mM	$5.0 \cdot 10^{-2}$	$4.0 \cdot 10^{-2}$ - $6.0 \cdot 10^{-2}$*
K_{CcO}	mM	$2.3 \cdot 10^{-3}$	0 - $4.5 \cdot 10^{-3}$*
K_i	mM	$6.18 \cdot 10^{-2}$	$1.72 \cdot 10^{-2}$
K_{FQ}	mM	1.8	1.6 - 2.0*
K_{FQox}	mM	-**	-**

* bounds of the graphically determined parameter

** not identifiable on basis of respiration tests

found by de Graaff et al. [28]. For sulfide concentrations of 0.30 up to 10 mM, the respiration activity gradually decreases. This could be an indication of inhibition of CcO/FCC and thus sulfide intoxication of the bacteria [22]. Surprisingly, from 1.0 to 5.0 mM sulfide, the bacterial respiration increases, most likely as a result of adaptation of the bacteria to high sulfide levels. This sulfide removal activity can be dedicated to the FQ system which is less susceptible for high levels of sulfide. As sulfide concentrations of 5.0 mM and higher only occur in heavily overloaded bioreactors, higher concentrations were not tested.

3.4.3 Parameter estimation

Given the proposed model structure and experimental data, a parameter estimation routine is used to calibrate and validate the model structure (see [29, 30] and appendix A for details). All unknown parameters ($q_{FCC,max}$, $q_{CcO,max}$, $q_{FQ,max}$, $q_{FQox,max}$, K_{FCC}, K_{CcO}, K_i, K_{FQ} and K_{FQox}) were estimated from the average oxygen respiration for each specific sulfide concentration. As we mentioned above, it is assumed that F, as Q, changes instantly according to the sulfide and oxygen levels. The resulting model fit with optimized parameters appeared to be satisfactorily. However, an eigenvalue decomposition of the accompanying covariance matrix revealed large uncertainties in specific parameter combinations. For instance, the substrate affinity constants and corresponding maximal growth rates were practically unidentifiable, as already shown in [31]. Therefore K_{FCC} and K_{FQ} were determined graphically on the basis of the maximal rate for the enzymes FCC and FQ, physiologically interpreted from Figure 3.4. For FCC this is K_{FCC}=0.05±0.01mM, for FQ this is K_{FQ}=1.8±0.2mM. To obtain the maximal overall oxidation capacity of FQ, its parameter is extrapolated around the value 240 ± 3 nM H_2S mg N^{-1} s^{-1} and thus, given the estimate for $q_{FQ,max}$, $q_{FQox,max}$ can be determined via Eq. 3.17, as $K_{FQox} \ll [O_2]$ and $K_{FQ} \ll [HS^-]$. On the basis of the respiration tests only, K_{CcO} and K_{FQox} are not identifiable, as these experiments take place at approximately 100% DO levels. These parameters should therefore be determined via dynamic reactor experiments at

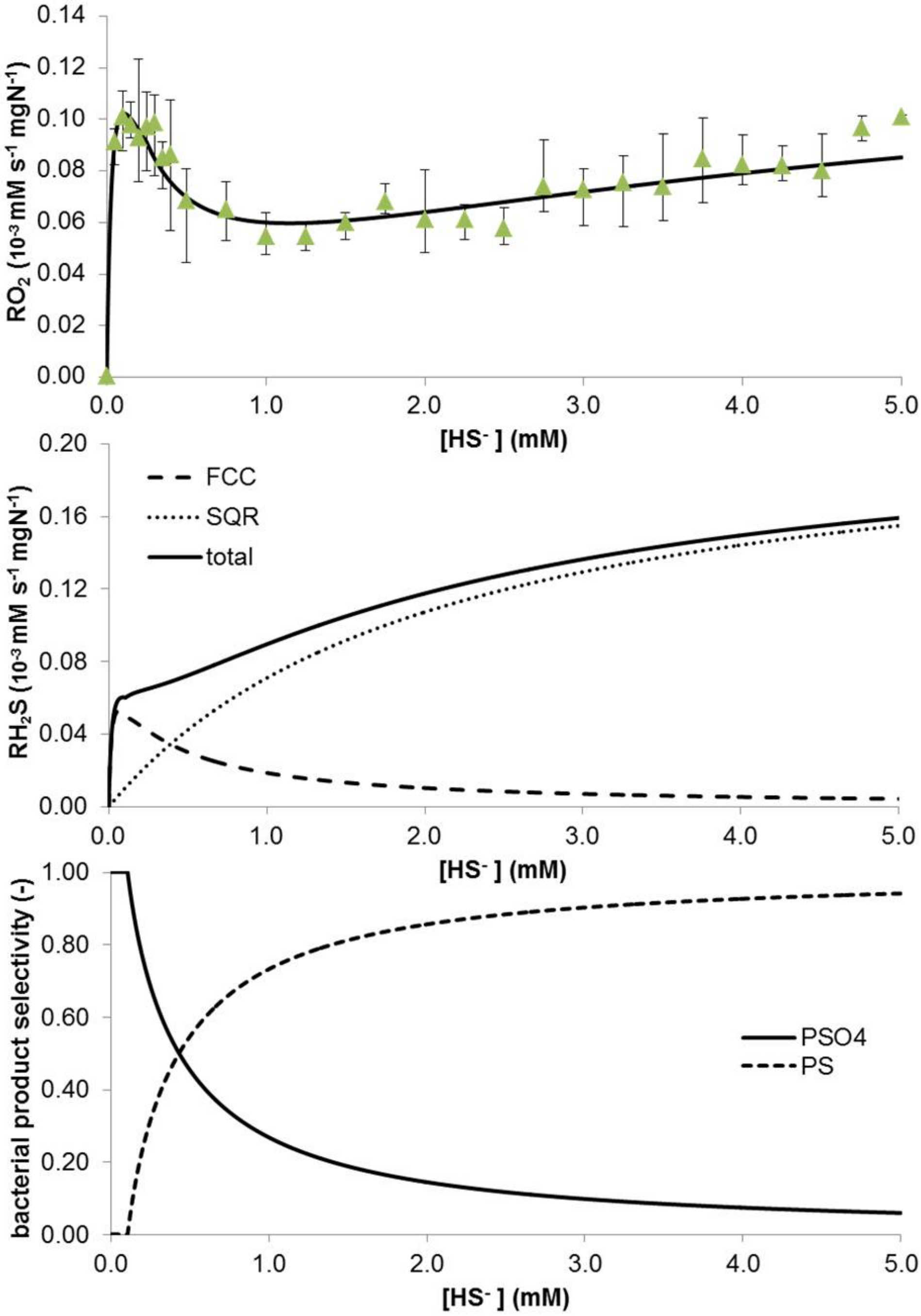

Figuur 3.4: Biological respiration rates RO_2 (oxygen removal) and RH_2S (sulfide oxidation) in respiration tests A and model predictions A, B & C. In figure A, the average measured oxygen consumption rate is indicated with triangles and the range of measurements with error bars. Figures B and C are solely based on model predictions.

limiting oxygen concentrations. However, still the magnitude can be roughly estimated from the respiration test. For instance, when the DO concentration at the respiration test dropped below (data not shown) 4.5 µM with an initial sulfide concentration of 0.54 mM, oxygen removal dramatically decreases. As the cytochrome system, and thus CcO, is active at these sulfide concentrations, it can be concluded that the K_{CcO} should be around 2.3 µM. For K_{FQox}, the same procedure gives unreliable results as this parameter should be determined at higher sulfide concentrations. At these concentrations, the curves are heavily influenced by the chemical oxidation. For the prediction of selectivity of the bacteria, however, this parameter is not of influence, as the quinone system only forms S^0. Following these physiological based assumptions, only four parameters ($q_{FCC,max}$, $q_{CcO,max}$, $q_{FQ,max}$ and K_i) out of nine were estimated. After reparameterization of the model, the second set of parameters appeared to be largely uncorrelated and less uncertain (see Table 3.1 and appendix B).

The model results, using the estimated parameter values from Table 3.1 and Appendix B are shown in Figure 3.4 A. Over the whole range of sulfide concentrations, it appears that with the proposed model it is possible to estimate the independent data set. This suggests that the model structure is defined properly.

In Figure 3.4 B, the total sulfide removal according to the model prediction is shown for the individual oxidation systems FCC and FQ and the total sulfide removal. At low concentrations of sulfide, the major respiratory system of the HA-SOB is FCC whereas at higher concentrations, FQ is the product determining system.

In Figure 3.4 C, the relative product formation is shown as function of the sulfide concentration. According to the model, the selectivity for SO_4^{2-} of the haloalkaliphilic SOB drops below 10% at a concentration of 2.1mM sulfide. Under process conditions of biological desulfurization, even less SO_4^{2-} will be formed as a result of lower oxygen levels.

3.4.4 Model validation

To cross validate the proposed model structure with its estimated parameters, experimental data, obtained from bench scale gas-lift reactor experiments, were used.
The results of these experiments are shown in Figure 3.5. In this figure, the effect of the sulfide concentration on the formation of SO_4^{2-} is shown. Every data point represents the selectivity for SO_4^{2-} of the bench scale reactor over a period of at least 3 hours of stable reactor performance, i.e. stable ORP levels. The selectivity for SO_4^{2-} formation was very low (0 - 0.0016) at sulfide concentrations above 0.25 mM, while at sulfide concentrations below 25 mM, SO_4^{2-} formation increases with decreasing sulfide concentrations. It is hypothesized in this paper that a decrease of biological SO_4^{2-} formation is a result of the inhibition of CcO (see Eq. 3.11) and as a result, more S^0 is formed. Based upon these findings, it seems essential for the process to operate at sulfide levels above 0.25 mM to obtain a high selectivity for formation of S^0 as the end-product of sulfide oxidation.

The measured oxygen concentration under sulfur forming conditions was always found to

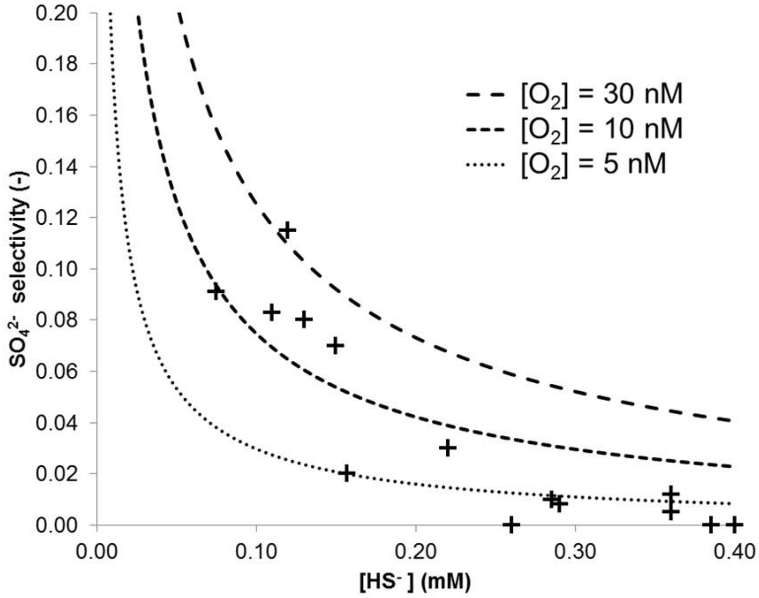

Figuur 3.5: Experimental results of bench experiments (+) with the model outputs (-) at oxygen concentration of 5, 10 and 30 nM

be below 0.1 μM (data not shown). A lower oxygen concentration is expected at higher sulfide concentrations. The identified model structure was used to predict the process selectivity at oxygen concentrations of 5, 10 and 30nM. These results are also shown in Figure 3.5. The experimental results and the model outputs are in good agreement.

At sulfide concentrations lower than 0.15 mM, the model gives an accurate fit for oxygen concentrations of 10 - 30 nM. At higher sulfide concentrations, it appears that an oxygen concentration of 5 nM gives a better model fit. The relative selectivity for SO_4^{2-} appears to be more sensitive for changes in the oxygen concentration at higher sulfide concentrations (>0.15 mM) than at lower sulfide concentrations (<0.15 mM).

3.4.5 Effect of disturbances

The selectivity of the biodesulfurization process has been studied at stable reactor conditions (i.e. reactor operated at constant ORP levels, sulfide and oxygen loading rates) [3, 5, 10]. In a full-scale reactor, however, conditions may vary over the height of the reactor due to non-ideal mixing conditions, leading to concentration gradients. This may play an important role, especially around the sulfide injection points. An (approximate) CFD modeling approach be able to further describe the micro-mixing, spatial heterogeneity and the resulting effects on the selectivity, but this is out of the scope of the paper. Moreover, the sulfide levels in the gas and gas flow may be fluctuating, resulting in fluctuating sulfide loads. It is very likely that these dynamics will affect the process selectivity.

To study the effects of fluctuations of the sulfide load in a bench scale reactor, the supply of both sulfide and oxygen was interrupted three times during reactor operations for a period of 8 minutes. The results are shown in Figure 3.6 A-C. In Figure 3.6 A both the oxygen and the sulfide supply are shown. The first period without sulfide and oxygen supply occurred between t=1.0 up to t=9.0 min, the second period between t=14 and t=22 min and the third period between t=27 and t=35 min. Before, between and after these interruptions, oxygen and sulfide were supplied to the reactor at a molar ratio (O_2/H_2S) of 0.5 mol mol^{-1}.

During the interruptions, the sulfide concentration in the reactor and the oxygen concentration in the gas phase (O_2(g)) were decreasing, as can be seen in Figure 3.6 B. This is an indication that sulfide is oxidized. On the other hand, when sulfide and oxygen were supplied to the reactor, both sulfide levels and oxygen levels were increasing, i.e. more sulfide is supplied than oxidized. This corresponds with previous research where the reactor could not operate at O_2/H_2S supply ratios below 0.6 mol mol^{-1} [3, 10].

The sulfide consumption rate ($cons_{HS^-}$) of the fed-batch reactor, that includes biological and chemical oxidation, is calculated from the following mass balance, and shown in Figure 3.6 C,

$$cons_{HS^-} = supply_{H_2S} - \frac{d[HS^-]}{dt} \tag{3.23}$$

where $supply_{H_2S}$ is the sulfide supply and $\frac{d[HS^-]}{dt}$ the accumulation of sulfide in the bioreactor (mmol L^{-1} s^{-1}). Notice from Figure 3.6 C that the sulfide consumption rate increases significantly when the sulfide supply is switched on. As the substrate levels of the reactor do not show these abrupt changes (Figure 3.6 B), it can be concluded that these effects are due to injection of substrate. As oxygen mass transfer is more limiting than sulfide transfer, probably a locally increased sulfide concentration governs the increased activity. When considering Eq. 3.16 where K_{FQ}=1.8 mM (Table 3.1), it can be concluded that an increase of sulfide concentration from 0.4 mM (Figure 3.6) to 1.8 mM will lead to at least a four-time increase of the activity of FQ. In case of the results shown, the average total sulfide consumption rate with sulfide supply ($5.6 \cdot 10^{-4}$ mmol L^{-1} s^{-1}) is 2.5 times higher than without sulfide supply ($2.3 \cdot 10^{-4}$ mmol L^{-1} s^{-1}).

To predict the dynamic reactor performance with disturbances in the supply of sulfide and oxygen, the proposed model with the estimated parameters is implemented in a reactor model (not shown). As K_{FQox} could not be identified on basis of the respiration test, is is chosen equally to K_{CcO}. The effect of local high sulfide concentrations is compensated via a hypothetical local increase of the sulfide levels. In case of sulfide supply, the sulfide concentration used to calculated the biological and chemical reaction rates is multiplied by a factor 2.5 as mentioned above. The results of the simulation are shown in Figure 3.6 B and D. Figure B shows the model predictions for both sulfide and oxygen levels in the reactor in comparison with the online measured reactor data. The model appears to fit the data satisfactorily. Deviations between the model and the online measurements can be explained by the dynamics of the sensor and delay in biomass (de)activation [32].

Figure 3.6 D shows the predicted process selectivity. The selectivity of the process can not be significantly determined on the time scale of 50 minutes, because of the demanding product analysis. The predicted, abrupt changes in process selectivity seem to be unrealistic, as in practice more gradual shifts are expected in biological product formation. Notice from Figure 3.6 D the relative high process selectivity for $S_2O_3^{2-}$. On basis of previous research, a selectivity of around 13 mol% is expected at pH 9.4 [5], but the model predicts up to 32 mol% selectivity. An explanation for this difference is that the bioreactor is operating at the limits of biological oxidation capacity (O_2/H_2S supply ratio of 0.5 mol/mol). Despite the trend of a decrease of sulfide levels (up to t=35 min) an increase in S^0 selectivity is predicted. These results from the cross-validated model emphasize that in order to optimize large scale applications, both sulfide and oxygen levels determine the selectivity of the process. Furthermore, the model can be used in model-based control studies, as it is able to predict the dynamics in the desulfurization process.

3.4.6 Physiologically based modeling in N-cycle

The model presented in this paper describes in a simple and effective way bacterial end-product formation. The modeling approach has the potential to describe other biological processes governed by O_2 limiting conditions, such as nitrification in the nitrogen cycle. Ammonium-oxidizing bacteria (AOB) oxidize ammonium at low dissolved oxygen concentrations. Via intermediates, NO_2^- is formed. Moreover, a similarity with the desulfurization process is that both cytochromes and quinones are electron acceptors in the pathway of the full oxidation to NO_2^- [33].

A major issue in waste water treatment (WWT) is nitrous oxide (N_2O) emission. Even though N_2O is not present as an intermediate in the main catabolic pathway of nitrification, AOB are known to produce N_2O [34]. Existing model approaches, such as the ASM1 model, are based on a combination of Monod terms. Unfortunately, these are black-box models that do not provide insight in the underlying physical-chemical processes. In contrast, the physiologically based modeling approach allows the description of the formation of products such as N_2O and NO_3^-[35]. Hence, the presented model structure could be a good starting point for minimization of the N2O emission in a WWT.

3.5 Conclusions

From the respiration test it appears that two optima in sulfide oxidation rates can be found. From subsequent test work [10] it follows that two sulfide oxidizing enzyme systems are active in HA-SOB. It is known that at higher sulfide concentrations the CcO/FCC enzymatic system is inhibited [22]. At sulfide concentrations above 2.0 mM, the SOB still shows high respiration activity. This sulfide removal activity can be dedicated to the FQ system.

The proposed model, with combined Michaelis-Menten-cytochrome kinetics, is based on a

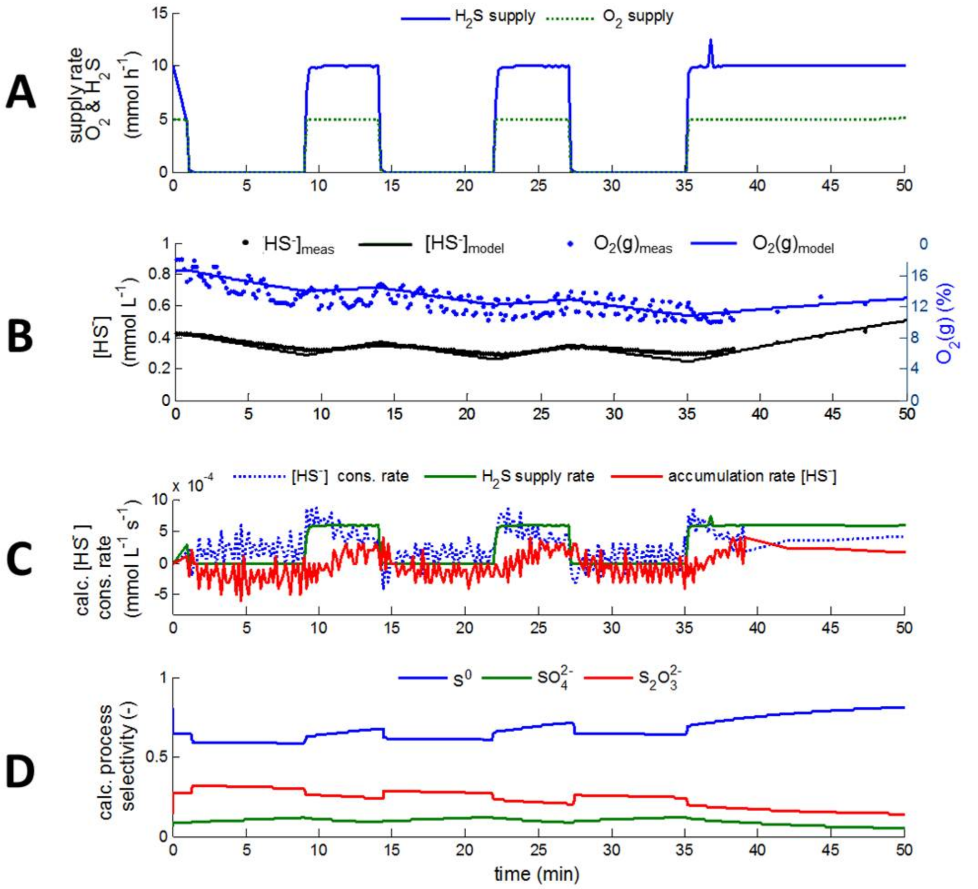

Figuur 3.6: Experimental results of the dynamic bench scale experiments. Three times for 8 minutes, the supply of sulfide and oxygen is interrupted (see figure A). Figure B shows the levels of sulfide in the reactor and oxygen concentration in the gas phase. The online measurements are indicated with (·) and the model prediction with a solid line. The calculated sulfide consumption rate is shown in figure C. In figure D is the model predicted selectivity shown.

’mono-substrate’ removal and ’multi-product’ forming concept. The model structure is successfully validated on data sets from respiration test and real time reactor experiments. The presented model is able to predict about 98 mol% of S^0 formation. A future challenge will be the optimization of the biotechnological process for hydrogen sulfide removal from gas streams, by improving the process design, mixing regime and operation e.g. via advanced substrate injection and the DO control strategy.

Acknowledgements

The authors thank Maarten de Boer for his assistance with the respiration tests.

References

[1] A. J. H. Janssen, R. C. Van Leerdam, P. L. F. Van den Bosch, E. Van Zessen, G. Van Heeringen, and C. J. N. Buisman. Development of a family of large-scale biotechnological processes to desulphurise industrial gases, 2nd international congress on biotechniques for air pollution control, A Coruña, Spain. 2007.

[2] A. J. H. Janssen, R. Ruitenberg, and C. J. N. Buisman. Industrial applications of new sulphur biotechnology. *Water Science and Technology*, 44(8):85–90, 2001.

[3] P. L. F. Van den Bosch, O. C. Van Beusekom, C. J. N. Buisman, and A. J. H. Janssen. Sulfide oxidation at halo-alkaline conditions in a fed-batch bioreactor. *Biotechnology and Bioengineering*, 97(5):1053–1063, 2007.

[4] A. J. H. Janssen, P. N. L. Lens, A. J. M. Stams, C. M. Plugge, D. Y. Sorokin, G. Muyzer, H. Dijkman, E. Van Zessen, P. Luimes, and C. J. N. Buisman. Application of bacteria involved in the biological sulfur cycle for paper mill effluent purification. *Science of the Total Environment*, 407(4):1333–1343, 2009.

[5] P. L. F. Van den Bosch, D. Y. Sorokin, C. J. N. Buisman, and A. J. H. Janssen. The effect of pH on thiosulfate formation in a biotechnological process for the removal of hydrogen sulfide from gas streams. *Environmental Science and Technology*, 42(7):2637–2642, 2008.

[6] J. P. Changeux and S. J. Edelstein. Allosteric mechanisms of signal transduction. *Science*, 308(5727):1424–1428, 2005.

[7] D. Y. Sorokin and J. G. Kuenen. Haloalkaliphilic sulfur-oxidizing bacteria in soda lakes. *FEMS Microbiol. Rev.*, 29(4):685–702, 2005.

[8] D. Y. Sorokin, H. Banciu, M. Van Loosdrecht, and J. G. Kuenen. Growth physiology and competitive interaction of obligately chemolithoautotrophic, haloalkaliphilic, sulfur-oxidizing bacteria from soda lakes. *Extremophiles*, 7:195–203, 2003.

[9] W. E. Kleinjan, A. De Keizer, and A. J. H. Janssen. Kinetics of the chemical oxidation of polysulfide anions in aqueous solution. *Water Research*, 39(17):4096–4100, 2005.

[10] J. B. M. Klok, P. L. F. Van Den Bosch, A. J. M. Stams, C. J. N. Buisman, K. J. Keesman, and A. J. H. Janssen. Pathways of sulfide oxidation by haloalkaliphilic bacteria in limited-oxygen gas lift bioreactors. *Environmental Science and Technology*, 46(14), 2012.

[11] D. P. Kelly. Thermodynamic aspects of energy conservation by chemolithotrophic sulfur bacteria in relation to the sulfur oxidation pathways. *Archives of Microbiology*, 171(4):219–229, 1999.

[12] D. Y. Sorokin, G. A. H. de Jong, L. A. Robertson, and G. J. Kuenen. Purifcation and characterization of sufide dehydrogenase from alkaliphilic chemolithoautotrophic sulfur-oxidizing bacteria. *FEBS letters*, 427(1), 1998.

[13] G. Muyzer, D. Y. Sorokin, K. Mavromatis, A. Lapidus, A. Clum, N. Ivanova, A. Pati, P. d'Haeseleer, T. Woyke, and N. C. Kyrpides. Complete genome sequence of "thioalkalivibrio sulfidophilus"hl-ebgr7. *Standards in Genomic Sciences*, 4:23–35, 2011.

[14] V. A. Bamford, S. Bruno, T. Rasmussen, C. Appia-Ayme, M. R. Cheesman, B. C. Berks, and A. M. Hemmings. Structural basis for the oxidation of thiosulfate by a sulfur cycle enzyme. *EMBO Journal*, 21(21):5599–5610, 2002.

[15] H. Sakurai, T. Ogawa, M. Shiga, and K. Inoue. Inorganic sulfur oxidizing system in green sulfur bacteria. *Photosynthesis Research*, 104(2):163–176, 2010.

[16] J. A. Brito, F. L. Sousa, M. Stelter, T. M. Bandeiras, C. Vonrhein, M. Teixeira, M. M. Pereira, and M. Archer. Structural and functional insights into sulfide:quinone oxidoreductase. *Biochemistry*, 48(24):5613–5622, 2009.

[17] D. Y. Sorokin, G. J. Kuenen, and G. Muyzer. The microbial sulfur cycle at extremely haloalkaline conditions of soda lakes. *Frontiers in Microbiology*, 2(44), 2011.

[18] U. Kappler and S. Bailey. Molecular basis of intramolecular electron transfer in sulfite-oxidizing enzymes is revealed by high resolution structure of a heterodimeric complex of the catalytic molybdopterin subunit and a c-type cytochrome subunit. *J. Biol. Chem.*, 280(26):24999–25007, 2005.

[19] C. Griesbeck, G. Hauska, and M. Schutz. Biological sulfide oxidation: Sulfide-quinone reductase (sqr), the primary reaction. *Recent Research Developments in Microbiology*, 4:179–203, 2000.

[20] P. Mitchell and J. Moyle. Chemiosmotic hypothesis of oxidative phosphorylation. *Nature*, 213(5072):137–139, 1967.

[21] I. Belevich and M. I. Verkhovsky. Molecular mechanism of proton translocation by cytochrome c oxidase. *Antioxidants and Redox Signaling*, 10(1):1–29, 2008.

[22] J. P. Collman, S. Ghosh, A. Dey, and R. A. Decréau. Using a functional enzyme model to understand the chemistry behind hydrogen sulfide induced hibernation. *Proceedings of the National Acadamy of Sciences of the United States of America*, 106(52):22090–22095, 2009.

[23] D. Y. Sorokin, P. L. F. Van Den Bosch, B. Abbas, A. J. H. Janssen, and G. Muyzer. Microbiological analysis of the population of extremely haloalkaliphilic sulfur-oxidizing bacteria dominating in lab-scale sulfide-removing bioreactors. *Appl. Microbiol. Biotechnol.*, 80(6):965–975, 2008.

[24] J. M. Visser, L. A. Robertson, H. W. Van Verseveld, and J. G. Kuenen. Sulfur production by obligately chemolithoautotrophic thiobacillus species. *Applied and Environmental Microbiology*, 63(6):2300–2305, 1997.

[25] W. E. Kleinjan, A. De Keizer, and A. J. H. Janssen. Equilibrium of the reaction between dissolved sodium sulfide and biologically produced sulfur. *Colloids and Surfaces B: Biointerfaces*, 43(3-4):228–237, 2005.

[26] K. J. Keesman. State and parameter estimation in biotechnical batch reactors. *Control Engineering Practice*, 10(2):219 – 225, 2002.

[27] D. J. O'Brien and F. B. Birkner. Kinetics of oxygenation of reduced sulfur species in aqueous solution. *Environmental Science and Technology*, 11(12):1114–1120, 1977.

[28] M. de Graaff, J. B. M. Klok, M. F. M. Bijmans, G. Muyzer, and A. J. H. Janssen. Application of a 2-step process for the biological treatment of sulfidic spent caustics. *Water Research*, 46(3):723 – 730, 2012.

[29] A. Abusam, K. J. Keesman, G. Van Straten, H. Spanjers, and K. Meinema. Parameter estimation procedure for complex non-linear systems: Calibration of ASM No.1 for N-removal in a full-scale oxidation ditch. *Water Science and Technology*, 43(7):357–365, 2001.

[30] G. Sin, P. Odman, N. Petersen, A. E. Lantz, and K. V. Gernaey. Matrix notation for efficient development of first-principles models within PAT applications: Integrated modeling of antibiotic production with Streptomyces coelicolor. *Biotechnology and Bioengineering*, 101(1):153–171, 2008.

[31] A. Holmberg and J. Ranta. Procedures for parameter and state estimation of microbial growth process models. *Automatica*, 18(2):181–193, 1982.

[32] P. A. Vanrolleghem, G. Sin, and K. V. Gernaey. Transient response of aerobic and anoxic activated sludge activities to sudden substrate concentration changes. *Biotechnology and Bioengineering*, 86(3):277–290, 2004.

[33] D. J. Arp and L. Y. Stein. Metabolism of inorganic N compounds by ammonia-oxidizing bacteria. *Critical Reviews in Biochemistry and Molecular Biology*, 38(6):471–495, 2003.

[34] M. J. Kampschreur, H. Temmink, R. Kleerebezem, M. S. M. Jetten, and M. C. M. van Loosdrecht. Nitrous oxide emission during wastewater treatment. *Water Res.*, 43(17):4093–4103, 2009.

[35] Pascal Wunderlin, Joachim Mohn, Adriano Joss, Lukas Emmenegger, and Hansruedi Siegrist. Mechanisms of N2O production in biological wastewater treatment under nitrifying and denitrifying conditions. *Water Res.*, 46(4):1027 – 1037, 2012.

Chapter 4

Temperature effects on the biological desulfurization process

Abstract Short term (3 days) temperature effects between 14 and 60°C were performed to investigate the effect on the biological oxidation rate of dissolved sulfide at haloalkaline process conditions. At temperatures below 15°C, the biological activity is not sufficient to oxidize 2.12 mmol L^{-1} h^{-1} H_2S at a molar O_2/H_2S consumption of 0.70 mol/mol. At temperatures higher than 48°C, biological activity is irreversibly affected. Our results also show that for a robust biodesulfurization process, the operating temperature is between 15-40°C.

4.1 Introduction

Large scale desulfurization of sour gas streams is done by application of the Amine/Claus and Lo-Cat technologies [1]. As an alternative to these technologies, biodesulfurization of hydrocarbon gasses with sulfide loads between 0.01-100 tons per day is an attractive option [2]. For this process, haloalkaline conditions are applied, as at these conditions more hydrogen sulfide (H_2S) is absorbed than at neutral pH conditions [3]. Hence, for the biological oxidation of sulfide haloalkaliphilic sulfide oxidizing bacteria (HA-SOB) are the proper catalyst. Such bacteria are found in alkaline and saline lakes, generally found in arid and semi-arid regions. Well known salt lakes are located in Egypt (Wadi Naturn lakes), North America (Mono lake, Soap lake) and Central Asia (Kulunda steppe lakes) [4, 5]. During the annual climate cycle in these so called 'soda lakes', large variations in temperature, pH, salinity, oxygen and sulfide levels occur [6]. Additionally, in winter steep temperature and concentration gradients are found due to stratification [5]. As a consequence, HA-SOB adapt to large variations in their habitat which is beneficial for the biological desulfurization process as in these processes temperatures can be operated all varying climatic zones.

In general, bacterial growth rates vary with changing process conditions. Temperature variations play a role in the biodesulfurization process, e.g. temperature of the treated sour gas and the occurrence of exothermic reactions. At low temperature, a temperature rise leads to an increase in metabolic activity and growth, hence the catalytic conversion rates increase [7]. A general expression that couples the effect of temperature to the catalytic reaction rates k (mmol L^{-1} s^{-1}) is given by the Arrhenius equation:

$$k(T) = A(T_r)e^{\frac{-E_A}{RT}} \tag{4.1}$$

where $A(T_r)$ is a maximum specific rate (mmol L^{-1} s^{-1}) at reference temperature T_r (K), E_A the activation energy (J mol^{-1}), R the universal gas constant (8.13 J mol^{-1} K^{-1}) and T the temperature (K). However, bacteria have, likewise to pH and salinity, a temperature optimum for growth and activity. Beyond the temperature optimum, denaturation of enzymes, transport carriers and other proteins occur [8]. In addition, the lipid bilayers of the bacterial membranes may become disrupted by temperature extremes [9]. When lowering the temperature, i.e. below a minimum temperature, enzyme activities will become too low to ensure a stable process performance. However, the composition of the cell will not necessarily be affected by low temperatures [10]. Because of these opposing temperature influences, microbial growth exhibits a characteristic temperature dependency with strict optimum temperatures [11].

The effects of salinity [12, 13], pH [13, 14] and oxygen/sulfide consumption ratio [15, 16] (and see **Chapter 2**) on HA-SOB in bioreactors have been studied. However, to the best of our knowledge, temperature effects on the overall reactor performance were not yet fully explored. In the overall biological desulfurization process, both chemical and biological reactions occur. The unwanted chemical formation of thiosulfate ($S_2O_3^{2-}$), proceeds via oxidation of both sulfide and polysulfide ($S_x{}^{2-}$) and is stimulated by an increase in temperature [17, 18]. In addition, solubility and thus availability of oxygen decreases at higher temperatures and will thus affect both chemical and biological oxidation of sulfur compounds. The biological respiration rate and hence the formation of the metabolic end-products S^0 and SO_4^{2-}, is also affected by temperature.

The goal of this study is to assess short-term temperature effects on the biological sulfide oxidation rate and the associated selectivity for product formation. In bench scale bioreactor experiments (4.7 L), the temperature operating window of the process was assessed. Additionally, biological respiration tests (20 ml) were performed to study the biomass activity over a temperature range.

4.2 Materials and methods

4.2.1 Bench scale tests

Fed-batch reactor experiments were conducted in duplicate in two identical gas-lift bioreactors with a wet volume of 4.7 L each. Analytical procedures and side equipment were identical to previous research [15]. Throughout all experiments, supply of H_2S and O_2 was kept constant at 10 and 7 mmol h^{-1} respectively. Previous research has shown that at these supply rates robust process conditions have been ensured and all H_2S is oxidized, thereby forming mainly i.e. 80 mol% S^0 [15]. However, at the start-up phase, the O_2 supply rate was set at 15 mmol h^{-1} to stimulate the growth of biomass. Before measuring the selectivity of the process after a change in temperature of the reactor medium, a two day acclimatization period was applied. Per temperature setting the selectivity of the process was monitored over a period of at least 2.5 days. When ORP levels drop below -420 mV (Ag/AgCl), biological inhibition will occur due to accumulation of sulfide [19]. As a result of a lack in biological oxidation capacity, no stable reactor performance could be achieved (see **Chapter 2**). In these events, the sulfide supply was interrupted as too much sulfide would accumulate, leading to a deterioration of the bioreactor performance.

4.2.2 Biomass respiration tests

Respiration tests were performed in a thermostated 20 mL glass chamber mounted on a magnetic stirrer and closed off with a dissolved oxygen (DO) sensor (PSt3, PreSens Precision Sensing GmbH, Regensburg, Germany). While the solution was saturated with oxygen by sparging air for at least 5 minutes, cell suspension was added to a final concentration of 5 mg N L^{-1}. Experiments commenced by injection of 20 µL of sulfide substrate stock solutions via a sealable opening. The decrease in DO concentration was measured with a sampling time of 5 seconds and the initial slope was used as a measure of the oxidation rate. Biomass oxidation rates were determined at least in triplicate for each temperature setting, at different incubation times (ranging from 5 to 30 minutes). In addition, control tests were performed with buffer solution only (abiotic control). Oxygen consumption rates were obtained at a sulfide concentration of 0.2 mM.

4.2.3 Medium

The mineral medium consisted of a mixture of a bicarbonate (pH 8.3, 19 L) and a carbonate (pH 12.3, 1 L) solution. Both solutions contained 0.66 mol L^{-1} Na^+ and 1.34 mol L^{-1} K^+. Furthermore, the medium contained 1.0 g L^{-1} K_2HPO_4, 0.6 g L^{-1} urea, 6.0 g L^{-1} NaCl and 0.20 g L^{-1} $MgCl_2 \cdot 6\ H_2O$ (all in demineralized water). Trace elements solution was prepared and added as described by Pfennig and Lippert [20]. After addition of all compounds, the pH of the medium was set 8.6.

Sodium sulfide stock solution for the respiration tests was freshly prepared by dissolution of $Na_2S{\cdot}9H_2O$ crystals in water that was de-aerated by flushing with nitrogen gas. The sulfide concentrations of the stock solutions were experimentally validated. For the respiration tests, bicarbonate buffer without nutrients were used to avoid any unwanted side effects of minerals.

4.2.4 Inoculum

The reactors were inoculated with biomass taken from a sulfide-oxidizing gas lift bioreactor [14]. The original inoculum consisted of a mixture of sediments from hypersaline soda lakes in Mongolia, southwestern Siberia and Kenya. An overview of the physiology of the SOB present in the inoculum is given elsewhere [12, 21].

4.3 Results and discussion

Both bioreactors were inoculated with an initial biomass concentration of around 14 mg N L^{-1} and operated at 35°C. During the start-up phase, mainly SO_4^{2-} and some $S_2O_3^{2-}$ were formed. When biomass concentrations of at least 30 mg N L^{-1} were reached, the temperature experiments were initiated. In the first set of tests, the temperature was increased from 35°C to 48°C. Hereafter, the same procedure was repeated from 30°C down to 14°C. The results of the temperature experiments are shown in Figure 4.1. The results at 30°C were similar to those found in previous studies at a pH 8.5, i.e. 83 mol% of the supplied sulfide is oxidized to S^0 (**Chapter 2**). Furthermore, SO_4^{2-} is formed (25 mol%). As the total is 107 mol%, it can be concluded that product formation occurs via both biological oxidation of supplied sulfide and residual $S_2O_3^{2-}$ that was already present in the system and was formed during the start-up phase. Biological oxidation rates appear to exceed the chemical formation rates thereby assuming that $S_2O_3^{2-}$ is only abiotically formed [16] within this interval. This is reflected in a negative (-7.9 mol%) formation rate. Especially between 25-35°C, $S_2O_3^{2-}$ appears to be a substrate for the HA-SOB.

An optimum temperature for biological activity is found between 25-35°C. First, an optimum in the selectivity for SO_4^{2-} formation is found, which is an indication of increased biological

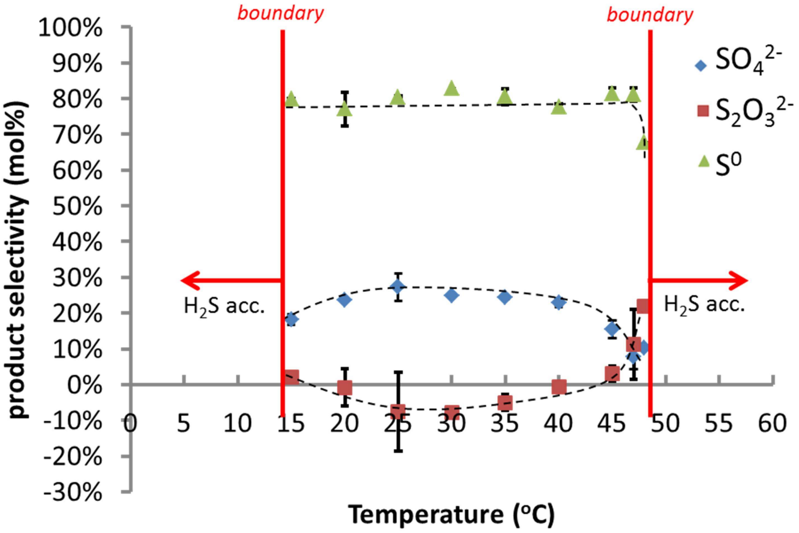

Figuur 4.1: Measured product selectivity in a fed-batch bioreactor at different temperatures with haloalkaliphilic biomass at pH 8.5 and at molar O_2/H_2S supply ratio of 0.7. The indicated points are the average of measurements in duplicate, the corresponding error bars indicate the measurement range. The dotted lines are polynomials fitted to the measured data.

activity. Furthermore, while throughout all experiments $S_2O_3^{2-}$ was detectable in solution, biological oxidation of $S_2O_3^{2-}$ was not affected by an absence of $S_2O_3^{2-}$. Hence, a decrease in selective SO_4^{2-} formation at both higher and lower temperatures is not affected by the substrate levels of S^0 and $S_2O_3^{2-}$. Presumably a decrease in biological activity causes an increase in sulfide levels and consequently an increase in the chemical oxidation rate leading to a higher $S_2O_3^{2-}$ concentration.

Over the entire temperature range (15-45°C), a stable reactor performance was obtained where 80 mol% of the sulfide was converted to S^0. However, at 14°C, ORP levels dropped below -420 mV, which is indicative for a rapid accumulation of H_2S in the solution [19]. Several attempts to obtain a stable reactor operation (e.g. via additional oxygen injection) failed and thus below 15°C the biological desulfurization process is hampered by sufficient microbial activity at the prevailing loading rate. Bioreactor temperatures below 15°C are rare in the desulfurization process, as the oxidation process yields heat. In addition, most gas streams are humid and warm, and pumping energy contributes to heat formation. However, in the natural habitat of the HA-SOB, winter temperatures drop far below 15°C, especially at the Kulunda steppe lakes. It was observed that biomass remains its viability after storage for more than 9 month at 4°C. Hence, it is unlikely that the HA-SOB are irreversibly affected by temperatures below 14°C.

At temperatures higher than 45°C, severe $S_2O_3^{2-}$ accumulation was observed (see Figure 4.1). Compared to biological conversion processes, chemical oxidation rates become predominant at higher temperatures, which is in agreement with Arrhenius' law. At 47°C, almost 6 mol% of sulfide is oxidized to $S_2O_3^{2-}$. Simultaneously, SO_4^{2-} formation drops to 15 mol%. These findings indicate that the biological activity is reduced, as SO_4^{2-} is only formed when the respiration chain of HA-SOB is fully active (**Chapter 3**). Increasing the temperature from 47°C to 48°C resulted in a rapid accumulation of H_2S in one of the two reactors, which is indicative for low microbiological activity. The second reactor remained stable for 7 days, but the selectivity for $S_2O_3^{2-}$ formation was 22 mol% $S_2O_3^{2-}$, indicating that biological activity is significantly reduced compared to the performance of the reactor at 47°C.

After 7 days of stable reactor performance of the second reactor, the temperature was increased from 48°C to 49°C which resulted in a rapid decrease of the ORP levels, which suggests biological deactivation. After 2 hours of incubation at 49°C, the temperature was set back to 45°C. Several attempts to retain activity (extra aeration) failed. Most likely, the biomass was irreversibly inactivated. In the natural habitats of mesophilic HA-SOB, temperatures of 49°C are rare. Hence, from these results, it can be concluded that the biological desulfurization process should be operated well below the maximum temperature of 47°C.

To assess the specific oxygen removal activity of the HA-SOB, additional batch respiration tests were performed. The experiments were performed at a relative low sulfide concentration of 0.2 mM. Previous research had shown that HA-SOB depict the largest respiration activity at this sulfide level (**Chapter 3**). In Figure 4.2, a plot of the calculated chemical oxidation rates for a range of temperatures are presented. The data show a typical Arrhenius' behavior, see Eq. 4.1. The dotted line, shown in the figure, is a model fit, based on the Arrhenius law, with E_A = 50.0 kJ mol^{-1}, A = 3.49 mol L^{-1} s^{-1} and T_r=35°C. Millero et al. (1989) reported

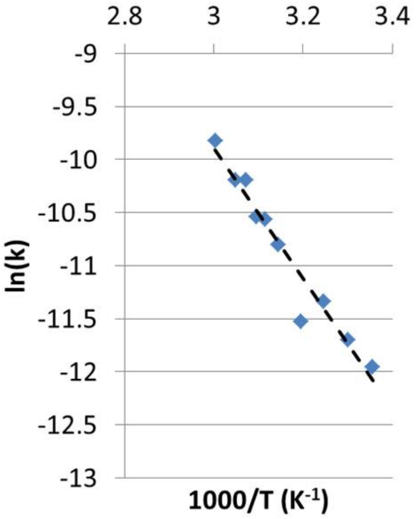

Figuur 4.2: Arrhenius plot of the chemical oxidation rate, measured in the respiration setup

for the activation energy of sulfide oxidation in seawater that E_A = 51 kJ mol^{-1} [22], while Kleinjan et al. (2005) reported 37.6 kJ mol^{-1} [17]. However, in both studies the salt levels were significantly lower than 2M. The chemical oxidation rate, using the Arrhenius model fit at 35°C ($k = 1.18 \cdot 10^{-5}$ mmol L^{-1}), is comparable to rates obtained previously at comparable conditions (i.e. $k = 1.23 \cdot 10^{-5}$ mmol L^{-1} where pH = 8.5 and 2M carbonate buffer, see **Chapter 3**). As the solubility of oxygen in water decreases with increasing temperatures, the fitted model (see Figure 4.2) provides an estimate for k at both different temperatures and varying oxygen saturation conditions.

The Arrhenius plot in Figure 4.2 is used to correct for the chemical sulfide conversions during the biological assays. The resulting biological oxygen respiration rates are shown in Figure 4.3. The average values are indicated with a diamond, and the corresponding range is indicated with error bars. Despite the fact that at higher temperatures less oxygen is dissolved (e.g. at 60°C about 30% less oxygen is dissolved compared to 35°C), it is plausible to assume that this does not affect the maximum oxidation rates of HA-SOB, as the affinity constant of oxygen is in the order of 0.005 mM (<3.3% dissolved oxygen at 35°C, see **Chapter 3**). From 25 up to 45°C, a gradual increase in activity can be seen. When considering the Arrhenius equation (Eq. 4.1), an exponential increase in activity is expected with temperature increase provided that no thermal inhibition occurs. For temperatures up to 45°C, this trend is found (see dotted line representing and exponential increase). However, the measurements deviate from this curve at temperatures higher than 45°C. Furthermore, at these higher temperatures, a large standard deviation in activities is found.

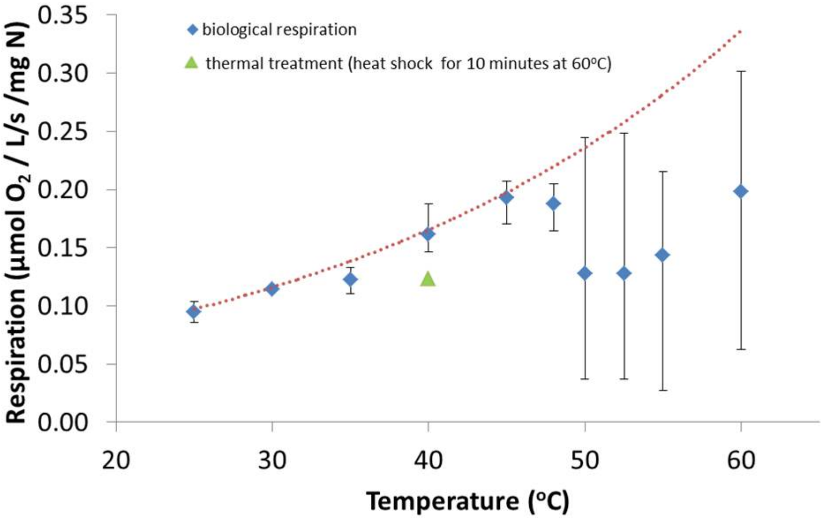

Figuur 4.3: Biological oxidation curve of HA-SOB at different temperatures. The average measurements are indicated with a dot, the measurement range is per indicated by the error bars

The decline in activity can be attributed to thermal inactivation of biomass. A relationship to describe this phenomenon is given by

$$\log S(t) = -b(T)t^{n(T)} \tag{4.2}$$

where $S(t)$ is the momentary survival ratio, and $b(T)$ and $n(T)$ are temperature dependent coefficients [23]. Hence, inactivation of bacteria is time and temperature dependent. For the temperatures 52.5, 55 and 60°C the incubation dependent respiration activity is shown in Figure 4.4. From this figure, it can be seen that the longer the bacteria are exposed to higher temperatures, the more inactivation occurs [24]. While the inactivation model is described by a power law Eq. (4.2), an exponential model is fitted to the data (see Appendix C for details). These measurements are single data points and therefore the curves are only indicative.

To test the impact of heat shocks, an experiment in which biomass was incubated for 10 minutes at 60°C was performed. Subsequently, respiration activity was measured at 40°C. The result is shown in Figure 4.3. After 10 minutes of incubation, almost 24% of activity is lost, i.e. 2.4% of activity per minute. The inactivation process proceeds rather slowly, as other mesophilic bacteria show faster inactivation rates at 60°C. For instance, *Salmonella* species show 90% inactivation within one minute at 60°C [25], *Escherichia coli* species within 1.5 minute [26]. Activated sludge, containing a mixture of bacteria, shows about 60% of activity loss when exposed for 10 minutes at 55°C [27]. However, all these bacteria origin from different habitats with respect to salt concentrations and pH regimes.

Based on the results presented in Figures 4.1 and 4.2, temperatures above 45°C are undesi-

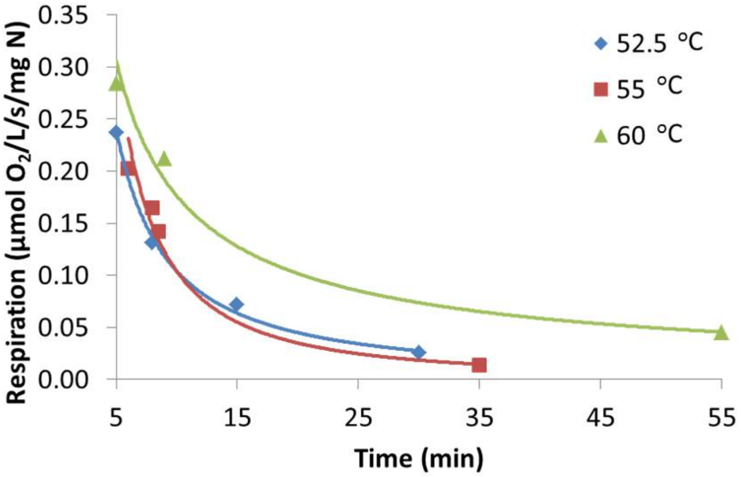

Figuur 4.4: Incubation time dependent respiration of HA-SOB. The data shown are single measurements Hence, the curves are indicative only

rable in full-scale reactors. However, HA-SOB can be exposed to higher temperatures in the absorber section where temperatures can be higher in case hot gasses are treated. As contact time, on the average, is around 3 minutes, about 7% of activity will be lost at 60°C. Furthermore, the heat of reaction, pumping energy and solar radiation are factors which increase bulk temperatures of the system. Hence, cooling is a prerequisite for robust reactor performance at temperatures above 45°C.

4.4 Conclusions

Based on both bench scale reactor tests and batch biomass respiration tests, it can be concluded that the HA-SOB of the biomass used are mesophilic bacteria with T_{min}=15, T_{opt}=25-35 and T_{max}=47°C. At temperatures below 15°C, the biological activity is reversibly inhibited. Furthermore, it is tempting to speculate that an optimum in the biological activity (compared to chemical oxidation rates) can be found between 25-35 °C, as in this temperature range, $S_2O_3^{2-}$ formation was minimal. At higher temperatures, i.e. temperatures above 48°C, biomass respiration tests show that HA-SOB will be irreversibly inactivated. Hence, for a robust biodesulfurization process, the recommended temperature operating window ranges from 15-45°C.

4.5 Acknowledgements

The authors thank Alfons J. M. Stams for stimulating discussions.

References

[1] J. E. Naber, J. A. Wesselingh, and W. Groenendaal. Sulfur developments: new shell process treats claus off gas. *Chemical Engineering Progress*, 69(12):29–34, 1973.

[2] A. J. H. Janssen, R. Ruitenberg, and C. J. N. Buisman. Industrial applications of new sulphur biotechnology. *Water Science and Technology*, 44(8):85–90, 2001.

[3] A. J. H. Janssen, P. N. L. Lens, A. J. M. Stams, C. M. Plugge, D. Y. Sorokin, G. Muyzer, H. Dijkman, E. Van Zessen, P. Luimes, and C. J. N. Buisman. Application of bacteria involved in the biological sulfur cycle for paper mill effluent purification. *Science of the Total Environment*, 407(4):1333–1343, 2009.

[4] G. Schweinfurth and L. Lewin. Beiträge zur Topographie und Geochemie des Ägyptischen Natron-Thals. *Zeitschrift für die Gesamte Erdkunde*, 33:1Ű25, 1898.

[5] A. Wieland and M. Kühl. Short-term temperature effects on oxygen and sulfide cycling in a hypersaline cyanobacterial mat (Solar Lake, Egypt). 2000.

[6] D. Y. Sorokin, G. J. Kuenen, and G. Muyzer. The microbial sulfur cycle at extremely haloalkaline conditions of soda lakes. *Frontiers in Microbiology*, 2(44), 2011.

[7] R. M. Daniel, R. V. Dunn, J. L. Finney, and J. C. Smith. The role of dynamics in enzyme activity. *Annual Review of Biophysics and Biomolecular Structure*, 32:69–92, 2003.

[8] G.N. Somero. Proteins and temperature. *Annual Review of Physiology*, 57:43–68, 1995.

[9] T. J. Denich, L. A. Beaudette, H. Lee, and J. T. Trevors. Effect of selected environmental and physico-chemical factors on bacterial cytoplasmic membranes. *Journal of Microbiological Methods*, 52(2):149–182, 2003.

[10] J. Willey, L. Sherwood, and C. Woolverton. *Prescott's Microbiology*. McGraw-Hill, 2001.

[11] J. B. Van Lier, J. Rintala, J. L. Sanz Martin, and G. Lettinga. Effect of short-term temperature increase on the performance of a mesophilic UASB reactor. *Water Science and Technology*, 22(9):183–190, 1990.

[12] D. Y. Sorokin and J. G. Kuenen. Haloalkaliphilic sulfur-oxidizing bacteria in soda lakes. *FEMS Microbiol. Rev.*, 29(4):685–702, 2005.

[13] D. Y. Sorokin, H. Banciu, L. A. Robertson, J. G. Kuenen, M. S. Muntyan, and G. Muyzer. The prokaryotes - prokaryotic physiology and biochemisry. 2013.

[14] D. Y. Sorokin, P. L. F. Van Den Bosch, B. Abbas, A. J. H. Janssen, and G. Muyzer. Microbiological analysis of the population of extremely haloalkaliphilic sulfur-oxidizing bacteria dominating in lab-scale sulfide-removing bioreactors. *Appl. Microbiol. Biotechnol.*, 80(6):965–975, 2008.

[15] P. L. F. Van den Bosch, O. C. Van Beusekom, C. J. N. Buisman, and A. J. H. Janssen. Sulfide oxidation at halo-alkaline conditions in a fed-batch bioreactor. *Biotechnology and Bioengineering*, 97(5):1053–1063, 2007.

[16] P. L. F. Van den Bosch, D. Y. Sorokin, C. J. N. Buisman, and A. J. H. Janssen. The effect of pH on thiosulfate formation in a biotechnological process for the removal of hydrogen sulfide from gas streams. *Environmental Science and Technology*, 42(7):2637–2642, 2008.

[17] W. E. Kleinjan, A. De Keizer, and A. J. H. Janssen. Kinetics of the chemical oxidation of polysulfide anions in aqueous solution. *Water Research*, 39(17):4096–4100, 2005.

[18] W. E. Kleinjan, A. De Keizer, and A. J. H. Janssen. Kinetics of the reaction between dissolved sodium sulfide and biologically produced sulfur. *Industrial and Engineering Chemsitry Research*, 44:309–317, 2005.

[19] A. J. H. Janssen, S. Meijer, J. Bontsema, and G. Lettinga. Application of the redox potential for controling a sulfide oxidizing bioreactor. *Biotechnol. Bioeng.*, 60(2):147–155, 1998.

[20] N. Pfennig and K.D. Lippert. Über das vitamin B12-bedürfenis phototropher schwefelbakterien. *Archives of Microbiology*, 55(3):245–256, 1966.

[21] D. Y. Sorokin, H. Banciu, M. Van Loosdrecht, and J. G. Kuenen. Growth physiology and competitive interaction of obligately chemolithoautotrophic, haloalkaliphilic, sulfur-oxidizing bacteria from soda lakes. *Extremophiles*, 7:195–203, 2003.

[22] F.J. Millero, A. LeFerriere, M. Fernandez, S. Hubinger, and J.P. Hershey. Oxidation of H_2S with H_2O_2 in natural waters. *Environmental Science and Technology*, 23(2):209–213, 1989.

[23] M. G. Corradini and M. Peleg. Dynamic model of heat inactivation kinetics for bacterial adaptation. *Applied and environmental microbiology*, 75(8):2590–2597, 2009.

[24] A. H. Geeraerd, C. H. Herremans, and J. F. Van Impe. Structural model requirements to describe microbial inactivation during a mild heat treatment. *International Journal of Food Microbiology*, 59(3):185–209, 2000.

[25] V. K. Junenja, B. S. Eblen, and G. M. Ransom. Thermal inactivation of *s*almonalle spp. in chicken broth, beef, pork, turkey, and chicken: Determination of D- and Z-values. *Journal of Food Microbiology and Safety*, 66(1):146–152, 2001.

[26] F. Toldta. *Safety of Meat and Processed Meat*. Springer Science New York, 2009.

[27] Zs. Csikor, P. Mihaltz, A. Hanifa, R. Kovacs, and M. F. Dahab. Identification of factors contributing to degradation in autothermal thermophilic sludge digestion. *Water Science and Technology*, 46(10):131–138, 2002.

Part II

Development of a dynamic model to describe sulfide oxidizing bioreactors

Chapter 5

Input and parameter sensitivity analysis of a physiologically based sulfide oxidation model

Abstract A physiologically based model describing the kinetics of biological sulfide oxidation in reactor systems has been presented in a previous research. In this paper, we study the sensitivity of substrate concentrations with respect to input variables and kinetic parameter that are used in this model. A local sensitivity analysis, based on the evaluation of dynamic sensitivity functions for different sulfide concentration levels, leads to a sensitivity surface. This sensitivity surface reveals that not all parameters in the above mentioned model can be estimated accurately via conventional respiration tests and that the parameter sensitivities, in both magnitudes and sign, could depend on the sulfide concentration level. In addition to this, using a response surface methodology, approximate meta-models of a biodesulfurization reactor are derived from the physiologically based model. An important finding is that the meta-models show that two critical parameters for designing full-scale reactor system, i.e. the oxygen transfer rate and volumetric sulfide loading rate, interact non-linearly. Therefore, a linear scale up of the reactor does not automatically result in a linear increase or decrease of the reactor performance. The study provides a systematic procedure, based on sensitivity and response surfaces, to evaluate both input and parameter sensitivities in multi-input multi-state models, like the physiologically based sulfide oxidation model.

5.1 Introduction

The presence of toxic and corrosive hydrogen sulfide (H_2S) in hydrocarbon gasses demands an effective removal process. Large scale H_2S removal commonly proceeds by physicochemical processes, such as the amine-Claus process. These processes typically operate at high temperatures and pressures and are therefore expensive. Microbiological treatment processes, on the contrary, are operated at ambient temperatures and pressures and are thus cheaper [1]. For certain applications, microbiological treatment of sulfide containing gasses is considered as a good alternative to physicochemical processes [2].

The biological desulfurization process is characterized by a variety of chemical and biological reactions [3]. The abiotic oxidation of sulfide (HS^-) and polysulfide (S_x^{2-}) to thiosulfate ($S_2O_3^{2-}$) occurs via various routes and depends on the prevailing process conditions, such as pH, sulfide and dissolved oxygen concentration [4]. The biological oxidation of sulfide is predominated by chemotrophic sulfur oxidizing bacteria (SOB), which obtain energy from the oxidation of sulfide to elemental sulfur (S^0) and to sulfate (SO_4^{2-}) [1]. In the abundancy of oxygen (O_2), sulfate is the end-product [5], whilst at oxygen limiting conditions, S^0 will be the main product formed [3, 2, 6].

The major overall reaction equations are given by [5, 3, 2, 4]

$$H_2S(g) \rightleftarrows H_2S(aq) \quad \text{(chem)} \tag{5.1}$$

$$H_2S(aq) + OH^- \rightleftarrows HS^- + H_2O \quad \text{(chem)} \tag{5.2}$$

$$HS^- + \frac{1}{2}\,O_2 \rightarrow S^0 + OH^- \quad \text{(bio)} \tag{5.3}$$

$$HS^- + O_2 \rightarrow \frac{1}{2}\,S_2O_3^{2-} + \frac{1}{2}\,H_2O \quad \text{(chem)} \tag{5.4}$$

$$HS^- + 1\frac{1}{2}\,O_2 + H_2O + NAD^+ \rightarrow SO_4^{2-} + NADH + 2\,H^+ \quad \text{(bio)} \tag{5.5}$$

$$HS^- + 2\,O_2 \rightarrow SO_4^{2-} + H^+ \quad \text{(bio)} \tag{5.6}$$

$$HS^- + (x-1)\;S^0 \rightleftarrows S_x^{2-} + H^+ \quad \text{(chem)} \tag{5.7}$$

$$S_x^{2-} + 1\frac{1}{2}\,O_2 \rightarrow S_2O_3^{2-} + (x-2)\;S^0 \quad \text{(chem)} \tag{5.8}$$

where chemical reaction equations are indicated with (chem) and biological reaction equations with (bio).

The process for biotechnological removal is operated in such a way that primarily S^0 is formed (⩾90%) [3, 2]. In addition, SO_4^{2-} and $S_2O_3^{2-}$ are formed. These products are unwanted as (1) they are not reusable like S^0, (2) the addition of caustic is required to compensate for the protons formed and (3) the formed side products are removed via a bleed stream for which make-up water is needed. Maximization of the S^0 formation is essential to allow an economic operation at large scale (i.e. loads of more than 10 tons H_2S per day). Given the complexity of the system, an integrated mathematical model, describing both the kinetics and hydrodynamics, is required. Such a model can also serve to control the process. The reliability of the used model greatly depends on the accuracy of the parameter. Hence, the subject of parameter estimation will be addressed.

The kinetics of the chemical oxidation of sulfide and S_x^{2-} have been described extensively [7, 8, 4, 9], whilst the prevailing biological kinetics are traditionally described by the Monod-Haldane model [10]. A draw-back of the empirical Monod-Haldane model is that the description of the formation of S^0 and SO_4^{2-} requires at least 12 heavily cross correlated parameters [11]. Furthermore, the accuracy of the model is questionable when applied over a large range of substrate concentrations. Recently, a physiologically based kinetic model to describe bacterial sulfide oxidation has been proposed. This model, based upon the respiratory system of haloalkaliphilic sulfur oxidizing bacteria (HA-SOB), was calibrated and validated for a range of substrate levels and reactor setups [12].

A biological desulfurization reactor is a typical example of a complex non-linear system, as several chemical and biological reactions with corresponding non-linear kinetics occur (see Eqs. 5.1-5.8). Sensitivity analysis can be an important tool to understand the dynamic behavior of such a model and to investigate the effect of parameters and inputs on the states and outputs [13, 14, 15]. Via a local or global sensitivity analysis, governing system parameters and inputs that drive the process can be identified. A simplification of the model can be obtained by fixing the non-sensitive parameters at their nominal value. Subsequently, only dominating parameters are estimated from experimental data sets. In addition to this, the so called Response-Surface-Methodology (RSM) facilitates a further exploration of the sensitivity of the responses with respect to parameters and inputs. The obtained results used to facilitate controller design and derivation of polynomial meta-models for describing the biological desulfurization reactor system.

Via the meta-models, dominating parameters and/or input variables are directly related to process responses. The input and parameter sensitivity analysis is an essential step to discriminate between sensitive and insensitive parameters and/or input variables, to understand the model behavior, and to develop an optimal process design of the biological desulfurization process.

The main objective of this paper is to obtain insight in the governing conversion processes via a parameter sensitivity analysis of the recently proposed physiologically based kinetic model for bacterial sulfide oxidation [12]. In this study, an advanced analytical sensitivity approach is suggested. This approach is based upon the evaluation of dynamic sensitivity functions for different sulfide concentration levels, leading to a sensitivity surface. The sensitivity surface is described by a large set of differential equations. The approach combines individual local sensitivities to obtain lumped sensitivities of the multiple-state multiple-input model. The effect of two important design parameters of the biological desulfurization process in the reactor system has been studied using a RSM-based input sensitivity analysis, viz. the volumetric oxygen transfer coefficient (k_LA) and volumetric sulfide loading rate ($load_{H_2S}$), with respect to the S^0 selectivity.

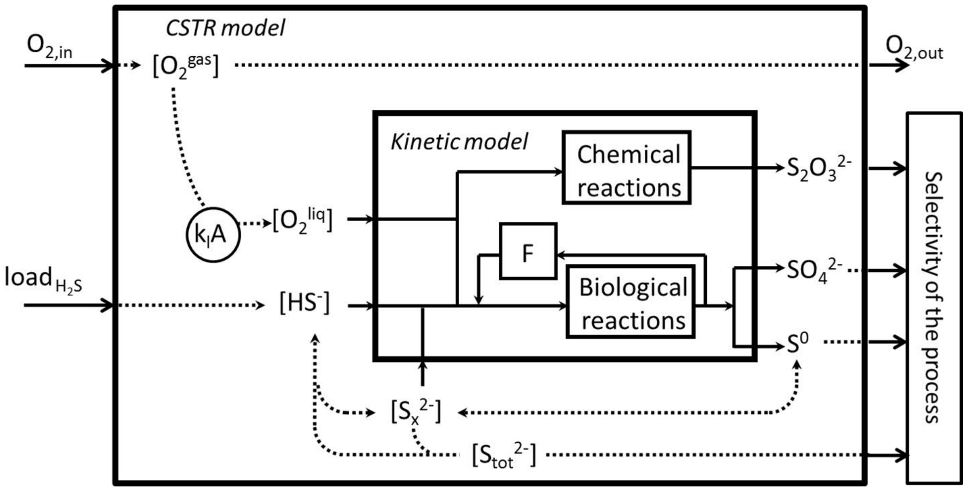

Figuur 5.1: Layout of the model structure. The selectivity of the process is determined by both chemical and biological reactions. The biological reaction kinetics are influenced by the physiological state of the bacteria (reduction degree of cytochrome pool, F). As both chemical and biological reaction kinetics are primarily determined by the concentrations of sulfide and oxygen in the reactor, both k_LA and $load_{H_2S}$ are dominating model inputs.

5.2 Kinetic models for sulfide oxidation

The formed end-product depend on both chemical and biological reaction kinetics (see Figure 5.1). The kinetics of the chemical oxidation of sulfide and polysulfide (see Eqs. 5.4, 5.7 and 5.8) are generally described by the rate equation law, as suggested by O'Brien et al. [7],

$$\frac{d[O_2]}{dt} = -k_{S_2O_3^{2-}}[HS^-]^{\delta_1}[O_2]^{\delta_2} \tag{5.9}$$

The chemical kinetic parameters at haloalkaline conditions have been estimated in previous studies and are shown in Table 5.1 [4, 12]. Recently, the biological kinetics have been described by a physiologically based model [12]. These kinetics are based on the main respiratory enzymes in the electron chain of the bacteria and, as a result, all corresponding parameters do have a physiological background.

Two sulfide oxidizing enzymes of HA-SOB are flavocytochrome c oxidoreductase (FCC) [16, 17] and a variant of FCC that transfers electrons to quinones (FQ) [2]. Both enzymes oxidize sulfide to S^0. Further oxidation of S^0 depends on the reduction degree of the cytochrome pool (*F*), which determines implicitly the product formation of the bacteria [12, 18]. Reduced cytochrome c is oxidized by the enzyme cytochrome c oxidase (CcO). This enzyme is one of the key enzymes in the respiration chain, as it is inhibited by high sulfide concentrations. Low sulfide levels lead to the formation of SO_4^{2-}, whereas high sulfide levels lead to the inhibition of CcO and consequently S^0 is formed.

Tabel 5.1: estimated parameters

parameter	unit	nominal value
$k_{S_2O_3^{2-}}$	mM s^{-1}	$2.91{\cdot}10^{-4}$
$\delta_{HS^-,1}$	-	1.02
$\delta_{HS^-,2}$	-	0.8
$k_{S_x^{2-},S_2O_3^{2-}}$	mM s^{-1}	$2.91{\cdot}10^{-4}$
$\delta_{S_x^{2-},1}$	-	1.02
$\delta_{S_x^{2-},2}$	-	1.02
$q_{FCC,max}$	mmol mg N^{-1} s^{-1}	$1.35{\cdot}10^{-4}$
$q_{CcO,max}$	mmol mg N^{-1} s^{-1}	$6.71{\cdot}10^{-4}$
$q_{FQ,max}$	mmol mg N^{-1} s^{-1}	$1.23{\cdot}10^{-4}$
$q_{FQox,max}$	mmol mg N^{-1} s^{-1}	$2.15{\cdot}10^{-4}$
K_{FCC}	mM	$5.0{\cdot}10^{-2}$
K_{CcO}	mM	$2.3{\cdot}10^{-3}$
K_i	mM	$6.18{\cdot}10^{-2}$
K_{FQ}	mM	1.8
K_{FQox}	mM	-*

* not identifiable

In our previous paper, it was proposed that the enzyme kinetics involved in the biological sulfide oxidation can be described by the following rate equations [12].

$$q_{FCC} = q_{FCC,max}\,(1 - F)\,\frac{[HS^-]}{K_{FCC} + [HS^-]} \tag{5.10}$$

$$q_{CcO} = q_{CcO,max} F \frac{[O_2]}{K_{CcO} + [O_2]}\,\frac{K_i}{K_i + [HS^-]} \tag{5.11}$$

$$q_{FQ} = \frac{q_{FQ,max}[HS^-]}{\frac{q_{FQ,max}}{q_{FQox,max}}\left(\frac{[O_2]+K_{FQox}}{[O_2]}\right)[HS^-] + [HS^-] + K_{FQ}} \tag{5.12}$$

where $q_\bullet$ is the oxidation rate (mmol s^{-1} mg N^{-1}), $q_{\bullet,max}$ the maximal oxidation rate (mmol s^{-1} mg N^{-1}) and $K_\bullet$ the substrate affinity constant (mmol L^{-1}) of the enzymes. The substrate affinity constant K_{FQox} is associated with the oxidation of quinones and K_i with the inhibition of CcO. It is assumed that F changes almost instantaneously upon changing the sulfide and oxygen levels. Hence, F is considered to be in quasi steady-state.

The enzymatic rates q_{FCC} and q_{FQ} are used to describe the overall oxidation rate of sulfide by the bacteria (q_{tot}), according to:

$$q_{tot} = q_{FCC} + q_{FQ} \tag{5.13}$$

q_{CcO} is not directly related to the oxidation rate of sulfide, as it describes the reduction rate of oxygen. To allow steady-state operation, the reduction rate of oxygen should balance the oxidation rate of FCC and FQ complexes. When, at intermediate sulfide levels, both biological products S^0 and SO_4^{2-} are formed, the product formation function (P) of the bacteria can be described by the linear equation [12]:

$$P_{SO_4^{2-}}(F) = \eta_1 \cdot F + \eta_2, \quad 0 \geq \P_{SO_4^{2-}} \geq 1 \tag{5.14}$$

with $\eta_1 = -2.86$ and $\eta_2 = 2.86$. These parameters are derived from the work of Visser et al. [18]. It shall be noted that the system used by Visser et al. was operated at neutrophilic conditions with *Thiobacillus* species. Hence, the estimated value for η_1 and η_2 can be different for HA-SOB. This does however not impact on the proposed methodology. Via $P_{SO_4^{2-}}$, the biological formation rates of both S^0 and SO_4^{2-} can be defined as:

$$q_{SO_4^{2-}} = P_{SO_4^{2-}}(F) q_{tot} \tag{5.15}$$

$$q_{S^0} = q_{tot} - q_{SO_4^{2-}} \tag{5.16}$$

with q_{tot} given by (13). At oxygen saturation and at low sulfide levels, all sulfide is converted to SO_4^{2-}. Hence, $P_{SO_4^{2-}} = 0$ for $F = 1$, and $P_{SO_4^{2-}}$=1 when $F \leq 0.65$. For more details on the physiologically based kinetic model, we refer to Klok et al. (2012) [12]. As the biomass growth rate is relatively low compared to the conversion rates of sulfide, it is assumed to be constant and therefor not taken into account in this research.

5.3 Materials and methods

5.3.1 Input and parameter sensitivity

Sensitivity analysis was carried out on a physiologically based model for biological sulfide oxidation. This model was calibrated and validated against respiration tests of biomass and on pilot-scale experiments (4.7 L) [12]. In these respiration tests, oxygen consumption of HA-SOB was measured at initial dissolved oxygen levels of approximately 100% for different sulfide concentrations. During the tests, the oxygen concentration decreases in time, which is a measure for the respiration activity.

In general terms, the model structure of the physiologically based model can be represented by the dynamical equations of the form

$$\frac{d}{dt}x(t) = f(x(t); \theta), \; x(0) = x_0 \tag{5.17}$$

where $x(t)$ is the n-dimensional state vector, f a non-linear vector function of dimension n, and θ the p-dimensional parameter vector that may include constant inputs. In what follows, we assume that all states are observed so that $y(t) = x(t)$, with $y(t)$ the output of the system at time t. In parametric models, the output sensitivity with respect to a specific parameter, θ_j, i.e. $\partial y(t)/\partial\theta_j$, determines whether the parameter θ_j can be estimated from input/output data. The necessary conditions for this are: $\frac{\partial y(t)}{\partial\theta_j} \neq 0$ and $\frac{\partial y(t)}{\partial\theta_j} \neq \sum_{i\neq j} \lambda_i \frac{\partial y(t)}{\partial\theta_i}$ on a time interval $[t_1, t_2]$ with $t_2 > t_1$ and λ_i a positive or negative real number. Local, first-order sensitivity functions, $S_j(t) := \frac{\partial y(t)}{\partial\theta_j}$, can be derived from Eq. 5.17, assuming time invariant θ_j, leading to

$$\frac{d}{dt}S_j(t) = \frac{\partial f}{\partial x}S_j(t) + \frac{\partial f}{\partial\theta_j}, S_j(0) = 0 \tag{5.18}$$

where S_j is the n-dimensional output sensitivity vector with respect to parameter θ_j, $\frac{\partial f}{\partial x}$ the n x n Jacobi-matrix and $\frac{\partial f}{\partial\theta}$, the n-dimensional direct sensitivity term (see Appendix A for the derivation of individual sensitivity coefficients). As the desulfurization reactor system contains n states, p parameters and N sulfide levels, for $j = 1, .., p$ and $k = 1, .., N$, an overall normalized sensitivity term ($S^{on}_{j,k}$) can be defined as,

$$S^{on}_{j,k}(t) := \sum_{i=1}^{n} \frac{\mid S_{i,j,k}(t) \mid}{max_k \mid S_{i,j,k}(t) \mid} \tag{5.19}$$

Where $S^{on}_{j,k}(t)$ is the local sensitivity of all states x with respect to parameter θ_j and at sulfide concentration level k, $\mid S_{i,j,k}(t) \mid$ is the absolute sensitivity of state x_i with respect to parameter θ_j and at sulfide concentration level k. Furthermore, $max_k \mid S_{i,j,k}(t) \mid$ is the maximal absolute sensitivity of state x_i with respect to parameter θ_j over all sulfide concentration levels. Thus, Eq. 5.19 can be used as an expression of the overall normalized sensitivity of the process of biological sulfide oxidation with respect to the model parameters and constant model inputs.

5.3.2 Response surface methodology

In addition to a local sensitivity analysis with sensitivity functions ($S_j(t)$), global sensitivity analysis based on RSM [14, 19], have been proposed as well. In what follows, in particular input sensitivities, for model reduction in a region of interest will be explored. As both chemical and biological reaction kinetics are primarily determined by the concentration of sulfide and oxygen, two important inputs of the process are k_LA and $load_{H_2S}$ (see also Figure 5.1). The oxygen flux is generally defined as

$$N_O = k_LA\left(\frac{[O_2]_{gas}}{m} - [O_2]\right) \tag{5.20}$$

where (N_O) is the oxygen flux (mol L^{-1} s^{-1}), $[O_2]_{gas}$ and $[O_2]$ the oxygen concentration in respectively the gas and liquid phase (mol L^{-1}) and m the partition coefficient (-). Hence, in addition to k_LA, the overall oxygen transfer rate depends on the driving force $\Delta[O]_2$. In practice, k_LA and $\Delta[O_2]$ are the result of reactor design and operating conditions. As the oxygen concentrations in both the gas and liquid phase is fixed by process design and operating conditions (i.e. redox $\leq$ -400 mV [5], such that $\frac{[O_2]_{gas}}{m} \gg [O_2]$ and thus $N_O = k_LA\ [O_2]$, k_LA can be varied by for example bubble distributions. As such, we consider k_LA as an input for the design of the process.

The values of the process inputs have been systematically varied to determine the effects on the selectivity for S^0 formation. Subsequently, a simple quadratic equation is fitted to the resulting selectivity for S^0 formation:

$$y = \alpha_0 + \alpha_1 \cdot x_1 + \alpha_2 \cdot x_2 + \alpha_{11} \cdot x_1^2 + \alpha_{22} \cdot x_2^2 + \alpha_{12} \cdot x_1 \cdot x_2 \tag{5.21}$$

where y is the selectivity for S^0, x_1 the oxygen transfer rate, x_2 the sulfide loading rate and α_0 ,.., α_{12} the coefficients that need to be determined from the numerical experimental data. The coefficients α_1,.., α_{12} are the (partial) sensitivity coefficients of y with respect to x_1 (main factor),.., $x_1 \cdot x_2$ (interaction). The model is finally used to predict the performance of a pilot-scale continuously stirred reactor (CSTR) using a model with (bio)kinetics described by Eq. 5.9-5.17. In matrix notation, the so-called meta-model (Eq. 5.21) as an approximation of the full dynamic model, can be written as

$$y = \alpha_0 + Ax + x^T Bx \tag{5.22}$$

where $x=[x_1\ x_2]^T$, $A=[\alpha_1\ \alpha_2]$ and $B = \begin{bmatrix} \alpha_{11} & \frac{\alpha_{12}}{2} \\ \frac{\alpha_{12}}{2} & \alpha_{22} \end{bmatrix}$. This type of input sensitivity analysis gives more information on the selectivity for S^0 of the overall process. Especially the matrix B will can further analyzed, using an eigenvalue decomposition analysis, for interaction effects between the inputs.

5.4 Numerical results and discussion

5.4.1 Parameter sensitivity

Results of the main effects of local, dynamic parameter sensitivities are shown in Figure 5.2 and Figure 5.3. In Figure 5.2 the normalized (individual) sensitivity ($S_{i,j,k} \cdot \frac{\bar{\theta}}{\bar{x}_i}$, where the overbar denotes nominal values) of a single state (sulfide concentration HS^-) to a single parameter (affinity constant K_{FCC} of the sulfide oxidizing system FCC) is plotted against time over a range of sulfide concentrations. At low sulfide levels and at 100% dissolved oxygen levels, a high sensitivity of HS^- with respect to K_{FCC} is observed. Hence, this confirms that under these conditions HA-SOB oxidizes sulfide mainly via the FCC enzyme. At increasing sulfide levels, a decrease in the sensitivity of K_{FCC} for sulfide is seen. From Table 5.1, K_{FCC}=0.05 mM and thus it is expected that at sulfide levels above 0.25 mM, the sensitivity of K_{FCC} will not change significantly. The results in Figure 5.2 confirm this reasoning. At

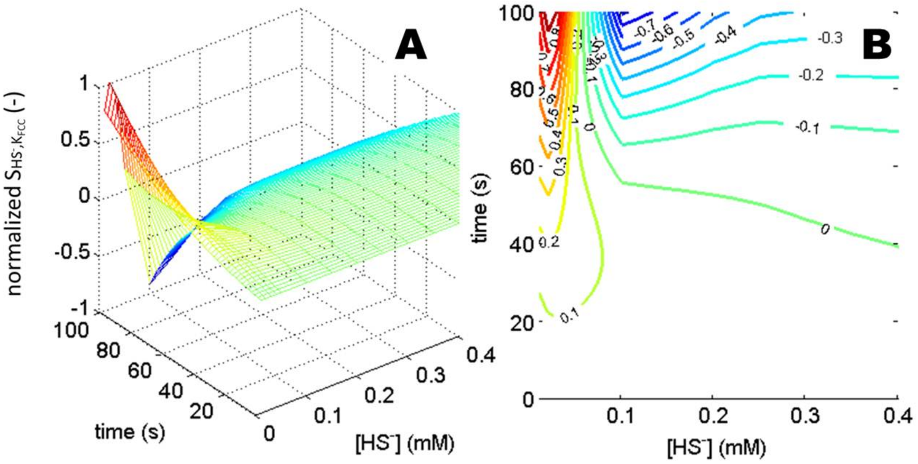

Figuur 5.2: The normalized $S_{HS^-,K_{FCC}}$ of a single state (sulfide concentration) to a single parameter (affinity constant K_{FCC} of the sulfide oxidizing system FCC) for a range of sulfide concentrations and 100% dissolved oxygen. Figure A shows the 3D course of the normalized sensitivity in time and figure B shows a contour plot. At low sulfide levels (i.e. below 0.05 mM) an increase of the parameter value of K_{FCC} will lead to a decrease of the biological sulfide oxidation rate. On the other hand, at higher sulfide levels (i.e. above 0.05 mM) an increase of the parameter value will lead to an increase of the biological sulfide oxidation rate and above 0.25 mM sensitiviy independent of HS^-.

sulfide levels above 0.25 mM, the sensitivity is independent of the sulfide concentration: the normalized sensitivity decreases in time. At sulfide levels below 0.05 mM, the sensitivity for sulfide concentration to K_{FCC} shows a different pattern than at higher sulfide levels. The sensitivity increases in time while at higher concentrations the sensitivity decreases with time. In practice, this means that a decrease of K_{FCC}, i.e. higher affinity for sulfide, at low sulfide levels will lead to an increase of the sulfide oxidation rate and thus to a decrease of the sulfide concentration. Surprisingly, at higher sulfide levels an increase in K_{FCC} will also lead to an increase in sulfide oxidation rates and subsequent decrease of sulfide concentrations. From these results, it can be concluded that K_{FCC} can be estimated best from respiration tests at low sulfide concentrations, i.e. at approximately the end of a test. As such, K_{FCC} has been calibrated correctly in previous research [12].

The calculated overall normalized sensitivities ($S^{on}_{j,k}$, see Eq. 5.19) are shown in Figure 5.3 A and B for all parameters in Eqs. 5.9 - 5.12 at time t=10 sec for both saturated oxygen concentrations (100% DO, figure A) and limited oxygen concentrations (5% DO, figure B). Although substrate levels are close to initial concentrations in this time frame, large differences are found for the calculated overall normalized sensitivities.

The calculations were performed up to sulfide concentrations of 5 mM. However, at sulfide concentrations above 1 mM, no additional information is found. Notice from this figure

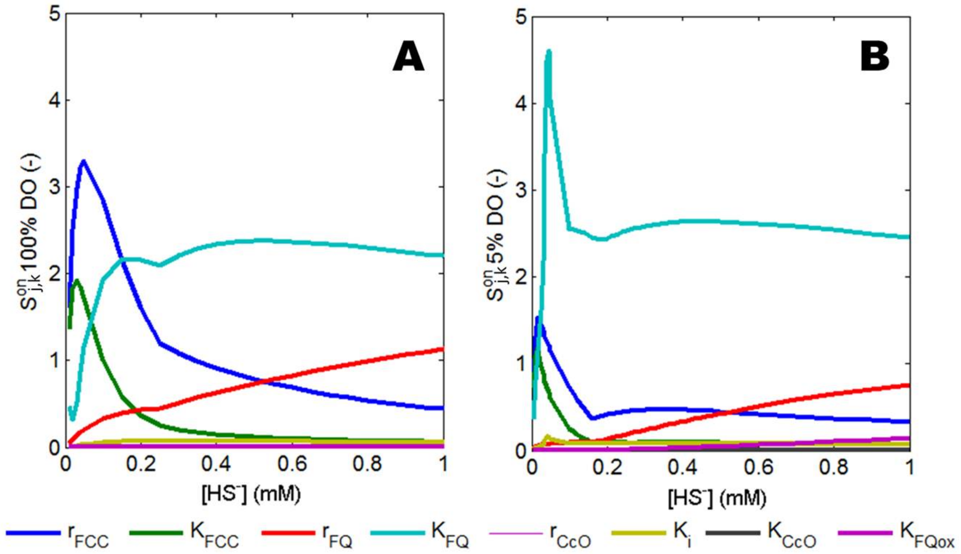

Figuur 5.3: The calculated overall normalized sensitivity ($S^{on}_{j,k}$) at 100% dissolved oxygen (A) and 5% dissolved oxygen (B). In A four parameters (i.e. $q_{FCC,max}$, K_{FCC}, $q_{FQ,max}$ and K_{FQ}) appear to be sensitive towards sulfide, while in B mainly K_{FQ} appears to be a sulfide sensitive parameter. Thus at decreasing levels of dissolved oxygen, K_{FQ} becomes a governing parameter.

that only 4 parameters are sensitive for variations in sulfide concentrations in the respiration test, i.e. $q_{FCC,max}$, K_{FCC}, $q_{FQ,max}$ and K_{FQ}. All other parameters, $q_{CcO,max}$, K_{CcO}, K_i and K_{FQox} do not show a significant sensitivity towards changes in the sulfide concentration.

Because the respiration of HA-SOB takes place at approximately 100% dissolved oxygen concentrations (Figure 5.3 A), it is obvious that parameters related to oxygen limiting conditions will not appear to be sensitive in these tests (i.e. saturated oxygen conditions). Notice the discontinuity of the sensitivities at [HS$^-$]=0.25 for all S_j^{on}. At this sulfide concentration, a shift in biological product formation occurs from strictly SO_4^{2-} formation to combined S^0 and SO_4^{2-} formation.

The parameters for the FCC enzyme, i.e. $q_{FCC,max}$ and K_{FCC} show a high sensitivity at lower sulfide concentrations (below 0.25 mM). This enzyme is mainly active at relative low sulfide levels [2]. Hence, changes to these parameters will have a major effect on the sulfide oxidation at low sulfide concentrations.

The parameters for the FQ enzyme. i.e. $q_{FQ,max}$ and K_{FQ} show a high sensitivity over the whole range of sulfide concentrations. As such, changes to these parameters and corresponding oxidation rate (q_{FQ}) will have an effect on the sulfide oxidation rate at all sulfide levels.

Figure 5.3 B shows $S_{j,k}^{on}$ at 5% dissolved oxygen. Compared to the systems at 100% dissolved oxygen, it can be concluded that the parameters describing the FCC enzyme are less sensitive. In addition, K_{FQ} shows a higher overall normalized sensitivity. The same parameters which are insensitive at 5% are insensitive at 100% dissolved oxygen. Hence, these parameters can not be accurately estimated via respiration tests. As the biological desulfurization process under S^0 forming conditions occurs at oxygen levels below 0.1 µM (=0.07% dissolved oxygen) [12], the non-sensitive parameters at 100% and 5% dissolved oxygen, i.e. q_{CcO}, K_{CcO}, K_i and K_{FQox}, could be sensitive at oxygen depleting conditions. Consequently, for an accurate estimation of these parameters a different experimental design is required than the one used in previous research.

5.4.2 Input sensitivity

In addition to the parameter sensitivity study, the approximate effect of fixed control inputs on model output, e.g. selectivity for S^0 of the overall process, can be explored via an input sensitivity study. Two important control inputs determining the process selectivity are k_LA and $load_{H_2S}$ (see Figure 5.1). In Figure 5.4 steady state results, using the parameter values from Table 5.1, are shown for an ideally mixed CSTR. In the figure, clearly an optimum of S^0 selectivity can be observed, up to approximately 98 mol% S^0 formation. Starting from the optimum for S^0 selectivity, higher sulfide loading rates result in an increase in chemical $S_2O_3^{2-}$ formation and lower sulfide loading rates will lead to an increase in biological SO_4^{2-} formation. At small k_LA values, not all sulfide is oxidized, especially at large sulfide loading rates (≥ 1.0 mmol L^{-1} s^{-1}). Notice in particular the sharp transition between 100 mol% SO_4^{2-}

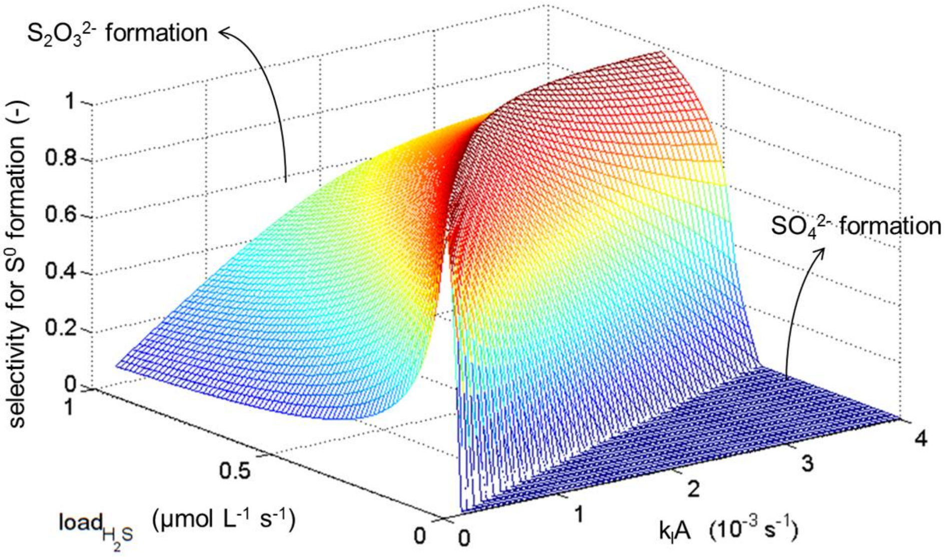

Figuur 5.4: The calculated influence of k_LA and $load_{H_2S}$ on the formation of S^0 in a ideally mixed CSTR bioreactor. When considering the optimum for S^0 selectivity, higher sulfide loading rates result in an increase in chemical $S_2O_3^{2-}$ formation and lower sulfide loading rates will lead to an increase in biological SO_4^{2-} formation.

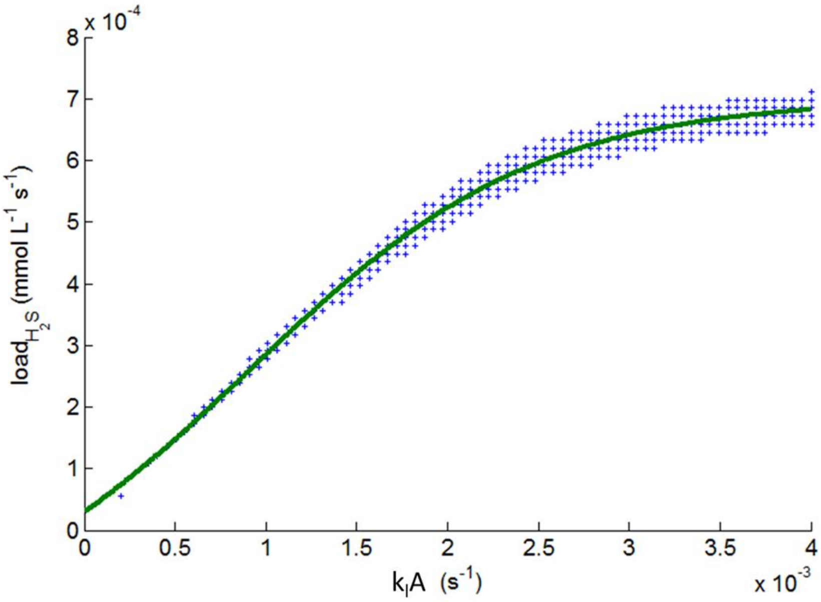

Figuur 5.5: A derived functional relationship for an optimal design for S^0 formation. The +'s are model calculations where selectivity for $S^0 \geq$ 95mol%. The relationship holds for $k_L A \geq 5.0 \cdot 10^{-4}$ s^{-1}.

formation, and thus S^0 selectivity equal to zero, and combined S^0 and SO_4^{2-} formation. The steep slope results from the imposed model structure for product formation (see Eq. 5.14). The transition to chemical $S_2O_3^{2-}$ formation is smoother, especially at larger $k_L A$.

While an increase in $load_{H_2S}$ always affects the selectivity for S^0, an increase of $k_L A$ mainly effects the model output at a relative small $k_L A$ (up to $1.5 \cdot 10^{-3}$ s^{-1}). At larger $k_L A$, an increase seems hardly to effect to optimum for S^0 formation. In practice, this means that at larger volumetric sulfide loading rates, the sensitivity of S^0 formation towards $k_L A$ decreases.

From the model evaluations, such as in Figure 5.4, a functional relationship can be derived for an optimal S^0 ($\geq$ 95 mol%). For our specific case, we derive the following fixed control law (see also Figure 5.5):

$$load_{H_2S} = p_1 + \frac{p_2}{p_3 + e^{(p_4\ k_L A)}} \tag{5.23}$$

for optimal S^0 formation and where p_1=1.8·10^{-4} (mmol s^{-1}), p_2=2.8·10^{-4} (mmol s^{-1}), p_3=0.32 (-) and p_4=-1.3·10^3 (s). It shall be noted that these calculations are performed for an ideally mixed system without external disturbances. Large scale reactors are however often characterized by substrate gradients and dead zones. Additionally, loading rates are not constant. We hypothesize that at large scale conditions a functional relationship like Eq. 5.23 still holds since the underlying reaction kinetics are assumed to be scale independent.

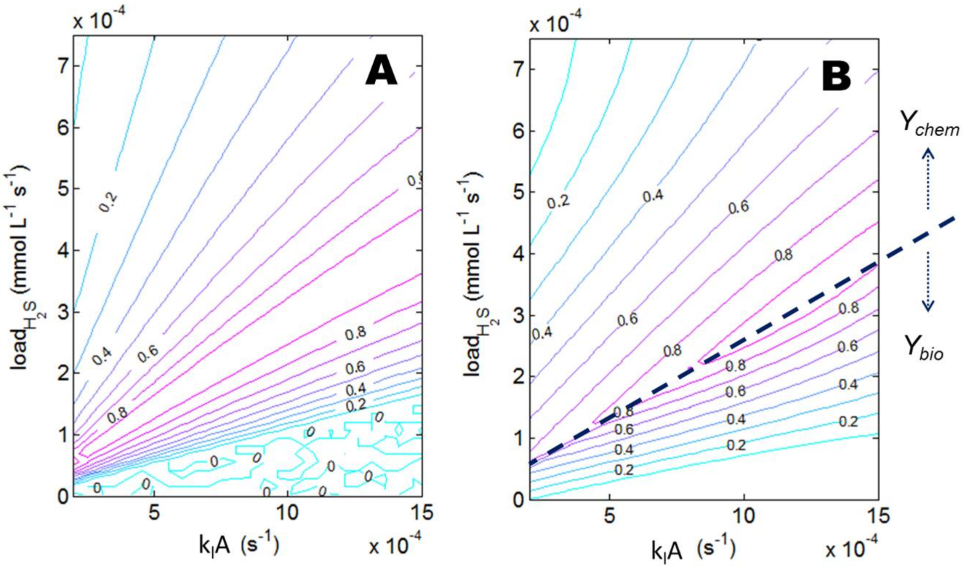

Figuur 5.6: A comparison between model evaluations of the CSTR (A) and the fitted meta models (B). Figure B is a combination of two meta models. The first model describes the competition of biological S^0 and SO_4^{2-} formation (Y_{bio}). The second model describes the competition between biological S^0 formation and chemical $S_2O_3^{2-}$ formation (Y_{chem}).

To study the main and higher-order effects of parameters and/or inputs on model responses, the response surface methodology is a valuable tool. In our case, we only evaluated the effect of fixed inputs on the S^0 formation, since the parameter interactions were calculated from an eigenvalue decomposition of the covariance matrix of the parameter estimates [12]. Two meta-models (see Eq. 5.21), as approximation of the full physiologically based model, were fitted to the response surface data of Figure 5.4. The first model approximates the relationship between S^0 and k_LA, $load_{H_2S}$ under the competition between biological S^0 and SO_4^{2-} formation (Y_{bio}) and the second model approximates this relationship in the region where the competition between biological S^0 formation and chemical $S_2O_3^{2-}$ formation (Y_{chem}) takes place. The models were fitted to data presented in Figure 5.4 with $k_LA \leq 1.5{\cdot}10^{-3}$ s^{-1}) and where S^0 selectivity $\geq$ 50 mol% (see also Figure 5.6 A). The matrices found (see Eq. 5.22) are shown in appendix B and the meta-model responses are shown in Figure 5.6 B.

In this figure, it can be seen that the sensitivity of S^0 formation with respect to the inputs will vary per input level. For example, at k_LA $1 \cdot 10^{-3}$ s^{-1} and $load_{H_2S}$ = 0.5 mmol L^{-1} s^{-1}, both inputs are not sensitive. However, at $load_{H_2S}$ = 1.0 mmol L^{-1} s^{-1}, the sensitivities for both input parameters are high. The selectivity for S^0 mainly depends on $load_{H_2S}$.

When considering the terms Ax and x^TBx for both meta-models (see Eq. 5.22), both terms are in the same order of magnitude. Therefore, it can be concluded that the second-order term plays a significant role in the selectivity for S^0 and as such, the scaling of the system will not be linear.

An eigenvalue decomposition of the matrix B gives insight into the sensitivity of S^0 formation with respect to combinations of control inputs [14]. As such, Eq. 5.22 provides a static relationship between output and inputs that can be used in controller design studies, see Eq. 5.23 as an example. In our case with two inputs, the input sensitivity can be evaluated graphically (see Figure 5.6). The smaller the distance between the contour lines, the large the input sensitivity. In meta-models with more that two factors (i.e. more inputs/parameters), determination of eigenvalues and eigenvectors is a simple manner to obtain insight in parameter interactions [20].

5.4.3 Applications of sensitivity methods

In general, sensitivity analysis aims to obtain information on relevant components that determine model behavior. In this paper, the suggested local, overall normalized parameter sensitivity method delivered insights in the biological conversion kinetics. The RSM-based input sensitivity method provided a meta-model for interactions between control inputs and optimal design of the process. In addition, these methods can also be applied to calibrate models and design experiments. As such, these are useful tools for process optimization.

This work focused specifically on the biological desulfurization process. This process optimum entails unwanted processes, such as chemical oxidation and biological by-product formation. Tuning the substrate levels of both sulfide and oxygen is essential to optimize the formation of S^0.

The suggested modeling approach has the potential to describe other biological processes governed by O_2 limiting conditions, such as nitrification in the nitrogen cycle. Even though N_2O is not present as an intermediate in the main catabolic pathway of nitrification, AOB are known to produce the unwanted N_2O next to NO_3^- [21]. Existing model approaches, such as the ASM1 model, are still based on a combination of Monod terms and contain a number of closely related parameters [22]. Via the suggested methods in this paper, a minimization of the N_2O emission can be visualized.

5.5 Conclusions

This study demonstrates that for a wide range of sulfide levels (0.05-5 mM), not all parameters in the kinetic equations for the biological desulfurization process can be estimated accurately via conventional respiration tests, i.e. at oxygen saturation, and additional tests under oxygen limiting conditions are required.

Via the proposed local, overall normalized sensitivity method, the earlier proposed physiologically based model is systematically explored with respect to parameters, input and model structure. In addition, the overall (normalized) sensitivities are explored over a range of initial sulfide concentrations, instead of one set of conditions, and lead to a sensitivity surface. It appears that K_{FCC} affects the activity of the biomass in two extremes at different substrate levels. At low sulfide levels an increase in K_{FCC} leads to a decrease of the overall sulfide oxidation rate, while at high sulfide levels, it leads to an increase of the overall sulfide oxidation rate. The overall normalized sensitivity method appears to be a useful tool to investigate multi-input multi-state processes, such as the presented biodesulfurization process.

It has been demonstrated that up-scaling of the biological desulfurization process from small lab system to full scale industrial systems will show non-linear effects due to large influences of the second-order quadratic terms in the approximate meta-models. From the CSTR model responses it can be concluded that the oxygen transfer rate (k_LA) of the reactor system is mainly determining the selectivity of the process at limiting oxygen transfer conditions. At relative large k_LA, the process selectivity is only determined by the sulfide load ($load_{H_2S}$). For optimal S^0 formation a fixed control law between k_LA and $load_{H_2S}$ has been found. This control law will facilitate the design of a dynamic control strategy. These results emphasize that both accurate models and input/parameter sensitivity analysis are essential to understand and optimize large scale reactor biological desulfurization.

References

[1] A. J. H. Janssen, P. N. L. Lens, A. J. M. Stams, C. M. Plugge, D. Y. Sorokin, G. Muyzer, H. Dijkman, E. Van Zessen, P. Luimes, and C. J. N. Buisman. Application of bacteria involved in the biological sulfur cycle for paper mill effluent purification. *Science of the Total Environment*, 407(4):1333–1343, 2009.

[2] J. B. M. Klok, P. L. F. Van Den Bosch, A. J. M. Stams, C. J. N. Buisman, K. J. Keesman, and A. J. H. Janssen. Pathways of sulfide oxidation by haloalkaliphilic bacteria in limited-oxygen gas lift bioreactors. *Environmental Science and Technology*, 46(14), 2012.

[3] P. L. F. Van den Bosch, O. C. Van Beusekom, C. J. N. Buisman, and A. J. H. Janssen. Sulfide oxidation at halo-alkaline conditions in a fed-batch bioreactor. *Biotechnology and Bioengineering*, 97(5):1053–1063, 2007.

[4] W. E. Kleinjan, A. De Keizer, and A. J. H. Janssen. Kinetics of the chemical oxidation of polysulfide anions in aqueous solution. *Water Research*, 39(17):4096–4100, 2005.

[5] A. J. H. Janssen, R. Sleyster, C. van der Kaa, J. Bontsema, , and G. Lettinga. Biological sulphide oxidation in a fed-batch reactor. *Biotechnol. Bioeng.*, 47(3):327–333, 1995.

[6] S. Alcántara, A. Velasco, A. Muñoz, J. Cid, S. Revah, and E. Razo-Flores. Hydrogen sulfide oxidation by a microbial consortium in a recirculation reactor system: Sulfur formation under oxygen limitation and removal of phenols. *Environmental Science and Technology*, 38(3):918–923, 2004.

[7] D. J. O'Brien and F. B. Birkner. Kinetics of oxygenation of reduced sulfur species in aqueous solution. *Environmental Science and Technology*, 11(12):1114–1120, 1977.

[8] C. J. N. Buisman, P. IJspeert, A. Hof, A. J. H. Janssen, R. Ten Hagen, and G. Lettinga. Kinetic parameters of a mixed culture oxidizing sulfide and sulfur with oxygen. *Biotechnology and Bioengineering*, 38(8):813–820, 1990.

[9] W. E. Kleinjan, A. De Keizer, and A. J. H. Janssen. Equilibrium of the reaction between dissolved sodium sulfide and biologically produced sulfur. *Colloids and Surfaces B: Biointerfaces*, 43(3-4):228–237, 2005.

[10] J. F. Andrews. A mathematical model for the continuous culture of microorganisms utilizing inhibitory substance. *Biotechnology and Bioengineering*, 10:707–723, 1968.

[11] A. Holmberg and J. Ranta. Procedures for parameter and state estimation of microbial growth process models. *Automatica*, 18(2):181–193, 1982.

[12] J. B. M. Klok, M. M. de Graaff, P. L. F. van den Bosch, N. C. Boelee, K. J. Keesman, and A. J. H. Janssen. A physiologically based kinetic model for bacterial sulfide oxidation. *Water Research*, 47(2):483–492, 2013.

[13] R. Tomavic. *Sensitivity analysis of dynamic systems*. McGraw-Hill Book Co Inc New York, 1963.

[14] A. Abusam, K. J. Keesman, G. Van Straten, H. Spanjers, and K. Meinema. Parameter estimation procedure for complex non-linear systems: Calibration of ASM No.1 for N-removal in a full-scale oxidation ditch. *Water Science and Technology*, 43(7):357–365, 2001.

[15] S. Tarantola and A. Saltelli. Samo 2001 Methodological advances and innovative applications of sensitivity analysis. *Reliability Engineering and System Safety*, 79(2):121–122, 2003.

[16] G. Muyzer, D. Y. Sorokin, K. Mavromatis, A. Lapidus, A. Clum, N. Ivanova, A. Pati, P. d'Haeseleer, T. Woyke, and N. C. Kyrpides. Complete genome sequence of "thioalkalivibrio sulfidophilus"hl-ebgr7. *Standards in Genomic Sciences*, 4:23–35, 2011.

[17] D. Y. Sorokin, P. L. F. Van Den Bosch, B. Abbas, A. J. H. Janssen, and G. Muyzer. Microbiological analysis of the population of extremely haloalkaliphilic sulfur-oxidizing bacteria dominating in lab-scale sulfide-removing bioreactors. *Appl. Microbiol. Biotechnol.*, 80(6):965–975, 2008.

[18] J. M. Visser, G .C. Stefess, L. A. Robertson, and J. G. Kuenen. Thiobacillus sp. W5, the dominant autotroph oxidizing sulfide to sulfur in a reactor for aerobic treatment of sulfidic wastes. *Antonie van Leeuwenhoek, International Journal of General and Molecular Microbiology*, 72(2):127–134, 1997.

[19] A. Saltelli, M. Ratto, T. Andres, F. Campolongo, J. Cariboni, D. Gatelli, M. Saisana, and S. Tarantola. *Global Sensitivity Analysis The Primer*. John Wiley & Sons, 2008.

[20] K. J. Keesman. *System Identification an Introduction*. Springer Verlag London, 2011.

[21] M. J. Kampschreur, H. Temmink, R. Kleerebezem, M. S. M. Jetten, and M. C. M. van Loosdrecht. Nitrous oxide emission during wastewater treatment. *Water Res.*, 43(17):4093–4103, 2009.

[22] Pascal Wunderlin, Joachim Mohn, Adriano Joss, Lukas Emmenegger, and Hansruedi Siegrist. Mechanisms of N2O production in biological wastewater treatment under nitrifying and denitrifying conditions. *Water Res.*, 46(4):1027 – 1037, 2012.

Chapter 6

Modelling of full-scale haloalkaline biodesulfurization systems

Abstract

In the biotechnological full-scale process of gas desulfurization under haloalkaline conditions, commonly used online measurements to control bioreactor performance are the oxidation reduction potential (ORP), pH and conductivity. The ORP measurements are used to control oxygen supply to the bioreactor and is governed by the dissolved sulfide concentration. The pH and conductivity are measured to maintain stable haloalkaline conditions. In this study, a full scale model is described and validated for dynamic operating data. The results are promising, as on the basis of online measured ORP, sour gas and air compressor flow, the dynamic behavior of the system could be explained. Furthermore, selectivity for formation of S^0 was estimated around 92 mol%, which in practice varies between 90-94%. Hence, the model can be used as a tool to design model-based control strategies which will lead to better overall process performance, i.e. maximize sulfur production and minimize chemical consumption rates.

6.1 Nomenclature

parameter	description and unit
A	surface area (m^2)
C_O*	gas solubility (mmol L^{-1})
E_h^0	standard redox potential (mV)
E_h	redox potential (mV)
F	reduction degree cytochrome pool bacteria (-)
k	chemical generic rate constant ($mmol^{\alpha+\beta-1}$ $L^{1-\alpha-\beta}$ s^{-1})
k_LA	oxygen transfer coefficient (s^{-1})
K	substrate affinity/inhibition constant (mmol L^{-1})
n	partition coefficient (-)
N_O	oxygen transfer rate (mmol L^{-1} s^{-1})
r	biological rate constant (mmol L^{-1} s^{-1})
q	biological oxidation rate (mmol s^{-1} mg N^{-1})
q_{max}	maximum biological oxidation rate (mmol s^{-1} mg N^{-1})
Q	gas flow (m^3 s^{-1})
t	time (s)
u	control input air flow (m^3 s^{-1})
v^{liq}	liquid velocity (m s^{-1})
v_{sup}	superficial gas velocity (m s^{-1})
Greek letters	**description and unit**
α & β	empirical coefficients chemical kinetics
γ	activity chemical compound (-)
ϵ	gas hold-up (-)
κ	empirical coefficients apparent viscosity
ψ	apparent viscosity (Pa s)
τ	time constant (s)
ξ	empirical coefficients ORP
subscript	**description and unit**
air	air
FCC	flavocytochrome c oxidase
FQ	flavoquinone oxidase
FQox	quinone dehydrogenase
biogas	biogas
i	inhibition
riser	riser
downer	downer
bub	gas bubbles

6.2 Introduction

Biogas, synthesis and natural gas streams often require treatment because of the presence of gaseous sulfur compounds like hydrogen sulfide, disulfides and thiols. Commonly applied desulfurization processes rely on physicochemical technologies. About 25 years ago, a new biotechnological gas treatment process was developed as an alternative to these conventionally applied technologies [12]. This biotechnological process offers a number of advantages, such as (i) applicable operating at a wide range of feed gas pressures, (ii) no production of sulfide-containing waste streams, (iii) no formation of concentrated H_2S gas streams, (iv) no requirement of chelating agents, (v) low chemical consumption and (vi) formation of reusable biosulfur. However, the biotechnological process does require the addition of caustic to neutralize any formed H_2SO_4, which is typically less than 6-10 mol% of the hydrogensulfide feed, and make-up water to discharge the formed H_2SO_4. In order to enable cost effective large scale biotechnological applications, e.g. of H_2S loads up to 100 tons per day it is of paramount importance to minimize the caustic requirements by maximizing the production of elemental sulfur (S^0). The objective of this study is to reach a selectivity for S^0 formation of at least 98 mol%.

In the haloalkaline biotechnological gas desulfurization process, hydrogen sulfide is absorbed in a carbonate rich solution and subsequently fed to a micro-aerophilic bioreactor. The dissolved sulfide (HS^-) is oxidized by a mixed population of chemolithoautotrophic haloalkaliphilic sulfide oxidizing bacteria (HA-SOB) to elemental sulfur (S^0), whilst a relatively small part (i.e. less than 10 mol%) is oxidized to sulfate (SO_4^{2-}). The governing pathways can be derived from are described in **Chapter 2**:

$$HS^- + \frac{1}{2}O_2 \rightarrow S^0 + OH^- \tag{6.1}$$

$$HS^- + 1\frac{1}{2}O_2 + H_2O + NAD^+ \rightarrow SO_4^{2-} + NADH + 2H^+ \tag{6.2}$$

The formed NADH can be oxidized via 2 routes, via O_2 as electron acceptor or via CO_2 fixation:

$$NADH + \frac{1}{2}O_2 \rightarrow NAD^+ + \frac{1}{2}H_2O \tag{6.3}$$

$$k\text{NADH} + CO_2 \rightarrow CH_{(k-2j)}O_{(2-j)} + jH_2O \tag{6.4}$$

At oxygen limiting conditions, the governing route will be Eq. 6.4. As a consequence, 25% less oxygen is consumed for the formation of one mole of SO_4^{2-} compared to oxidation with oxygen as the sole electron acceptor (Eq. 6.3).

In addition to these biological oxidation reactions, a fraction of the dissolved sulfide (HS^-), including polysulfide (S_x^{2-}), is abiotically oxidized to thiosulfate ($S_2O_3^{2-}$), according to

[15, 25]

$$HS^- + O_2 \rightarrow \frac{1}{2}S_2O_3^{2-} + \frac{1}{2}H_2O \tag{6.5}$$

$$S_x^{2-} + 1\frac{1}{2}O_2 \rightarrow S_2O_3^{2-} + (x-2)\,S^0 \tag{6.6}$$

At elevated redox conditions, i.e. typically above -200 mV (Ag/AgCl reference electrode at 35°C), HA-SOB will produce SO_4^{2-} as an end-product as this route yields the largest change in Gibbs free energy [14]. However, from an application point of view, the formation of S^0 is preferred, as biological sulfur can be used as a raw material, e.g. as soil fertilizer and fungicide. Moreover, both $S_2O_3^{2-}$ and SO_4^{2-} formation will lead to an increase in operating cost, because caustic and make-up water are needed to maintain pH and salinity, respectively.

Several studies show that biological S^0 formation is enhanced at relative low oxidation reduction potential (ORP, i.e. ORP < -350 mV) and oxygen levels [5, 14, 26]. Chemical sulfide oxidation (see in Eqs. 6.5 and 6.6) is enhanced at increasing dissolved sulfide concentrations [21], while biological sulfide oxidation is inhibited at relatively high concentrations (**Chapter 3**). Both biological and chemical sulfide oxidation rates (see in Eqs. 6.5 and 6.6) are enhanced at increasing oxygen concentrations [26]. Also the degree of liquid mixing in the bioreactor content will impact on the overall process performance. A high degree of mixing is required to prevent the occurrence of concentration gradients that will otherwise lead to elevated levels of chemical oxidation. In industrial biological biodesulfurization plants, mixing of the reactor fluid is mainly achieved by air injection. Depending on the size of the bioreactor different reactor systems are in operation, such as bubble columns and gaslift loop reactors. The air supply rate should be controlled by the O_2 demand of the system. Because of this dual function, a relationship exists between hydrodynamics and product formation. When fluid mixing velocities are too low, unwanted sulfide and oxygen gradients will appear along the height of the reactor column which will negatively impact on overall the selectivity for sulfur formation.

In order to optimize the S^0 formation, more insight is needed in the relation between the prevailing biological and chemical reaction kinetics and the hydraulic mixing regime in the bioreactor. Mathematical models are needed to provide these insights in a quantitative manner. In a recent study, we propose a physiologically based kinetic model, describing the formation of the various end-products formed in the biodesulfurization process. The proposed model was successfully validated against independent data obtained from biological respiration tests and bench-scale gas-lift reactor experiments (**Chapter 3**). While in practice the selectivity for S^0 ranges between 90-94 mol% H_2S, our model predicts a maximum selectivity for S^0 formation of about 98 mol% H_2S. The selectivity of 98 mol% would make the biotechnological process better suitable for large scale desulfurization (**Chapter 5**) as both caustic and make-up water consumption will be reduced drastically.

In addition to optimize process designs, mathematical models are also required to accurately monitor and control critical process variables such as air injection and biological activity.

An advanced process control strategy is highly dependent on the successful online measurement of key state variables, e.g. the concentrations of S^0, SO_4^{2-}, $S_2O_3^{2-}$ and O_2 to directly compensate for any disturbances in the dynamic process. Unfortunately, but no robust cost effective online S^0-sensor exists. Furthermore, product formation cannot be accurately monitored off-line within an acceptable time frame of e.g. a few minutes. In addition to product formation sensors, commercially available O_2 sensors for industrial applications are not suitable due to their too high detection limit or relative large resolution, as dissolved oxygen levels in well operating plant are presumably below 100 nM (**Chapter 3**). Therefore, the currently implemented control strategy for oxygen supply is based on the online measurements of the redox potential (ORP). This strategy was developed at our university and is commonly implemented in all full scale bioreactor systems [13]. The ORP is a measure for the solution's tendency to donate or accept electrons in equilibrium and is thermodynamically described by Nernst's equation:

$$E_H = E_H^0 + \frac{2.303RT}{nF} \log\left(\frac{\prod_i ox^{n_i}}{\prod_j red^{n_j}}\right) \tag{6.7}$$

for the half reaction: $n_i\ ox_i + n\ e \rightarrow n_j\ red_j$, with E_H the redox potential (mV) and E_H^0 the standard redox potential (mV). It should be noted that the measured value of E_H is a result of a mixture of all dissolved components that donate or accept electrons. Janssen et al. (1998) showed that in case of oxygen-limiting conditions ORP can be used as the controlled variable thereby using a classical PI-control strategy [13]. It was concluded that mainly sulfide ions determine the dynamic response of the ORP-sensors, as oxygen ions have a lower current exchange density at the redox electrode. At equilibrium conditions a linear relationship between $\log(S)^{2-}$ and E_h was found. However, the response rate is determined by the specific electrode surface. Hence, a too low electrode surface prevents a fast response.

Van den Bosch et al. (2007) have shown that also at haloalkaliphilic conditions the selectivity of the biodesulfurization process, at stable reactor conditions, can be related to the ORP [26]. Generally, the full scale process is operated at ORP values around -350 mV (Ag/AgCl). In laboratory experiments, it was shown that at ORP values below -400 mV, selectivity of SO_4^{2-} formation drops below 2 mol%. However, large variations in the selectivity for SO_4^{2-} formation was found, ranging from 15 to 35 mol% at higher ORP levels (i.e. above -350 mV).

As online ORP values are used for control of the aeration rate, it is essential to properly understand the relationship between ORP and the sulfide and oxygen concentration. So far, the role of oxygen with respect to ORP has not been incorporated in the mathematical model. In (**Chapter 3**), we propose the following equation for ORP in terms of oxygen and sulfide, based on the Nernst equation:

$$ORP = \xi_1 + \xi_2 \log(\gamma_{O_2}) + \xi_3 \log(\gamma_{HS^-}) \tag{6.8}$$

Where γ describes the activity coefficient of a dissolved compound. In previous research, it has been shown that ORP is more sensitive to HS^- than to O_2 [13].

The objective of this chapter is to develop and validate a mathematical model to describe a full scale biotechnological desulfurization processes. Based upon our current knowledge from experimental work, a dynamic simulation model has been developed. The flow rates and mass transfer coefficients are described by expressions that have been derived from literature and full-scale experiments. Subsequently, our model is validated using real-time sensor data, that has been obtained from the full-scale biogas desulfurization plant at "Industiewater Eerbeek B.V."[12].

6.3 Development of a simulation model to describe a full-scale biodesulfurization reactor

In this section, the development of a simulation model is described that is based on a combination of biological and abiotic kinetics for sulfide oxidation, oxygen transfer models and fluid mixing models. The reaction kinetics have been described and validated elsewhere (see [15] and **Chapter 3** of this thesis). The oxygen transfer equation to describe prevailing reactor conditions (i.e. at high salt levels) are based on literature data.

Air-lift loop bioreactors form a distinct group of bioreactors in which fluid mixing is achieved by air sparging [2]. Typically, air-lift loop reactors are applied in large full scale applications because of their good mixing properties, the absence of any rotating devices and relatively their small footprint. Generally, air-lift loop reactors consist of two distinct zones, i.e. a riser and a downcomer [27]. Both sections are inter connected [1]. Detailed models are available to described the relationship between the gas hold up (ϵ), gas/liquid velocities (v) and oxygen transfer (k_LA) [20, 11, 4].

In this study, the liquid flows in the riser and downer sections are described by the combination of two plug flow models [24]. Both the riser and downcomer section are divided into a series of ideally mixed segments, whereby mixing between the segments is described by mass exchange between the various segments (see Figure 6.1 A & B). In each of the segments, a gas phase and a liquid phase are present. Biological and chemical oxidation reactions occur in the liquid phase of each of these segments and are driven by sulfide and oxygen levels.

6.3.1 Description of biological and abiotic kinetics

Kinetic equations to model the chemical reaction rates in the presented model were described in previous studies [21, 17, 15] and in **Chapter 3 & 4**. Generally, the rate equations can be expressed as follows:

$$r_{\bullet} = k_{\bullet}[HS^{-}]^{\alpha}[O_2]^{\beta} \tag{6.9}$$

where the sulfide concentration may be replaced by polysulfide or a combination of sulfide and polysulfide. In this equation, $r_{\bullet}$ presents a generic rate constant (mmol L^{-1} s^{-1}), $k_{\bullet}$ the chemical reaction coefficient (mmol$^{1-\alpha-\beta}$ L$^{\alpha+\beta-1}$ s^{-1}) and α,β are empirical coefficients (-). The constants in Eq. 6.9 are estimated from batch experiments, see [16], **Chapter 3** and **4**.

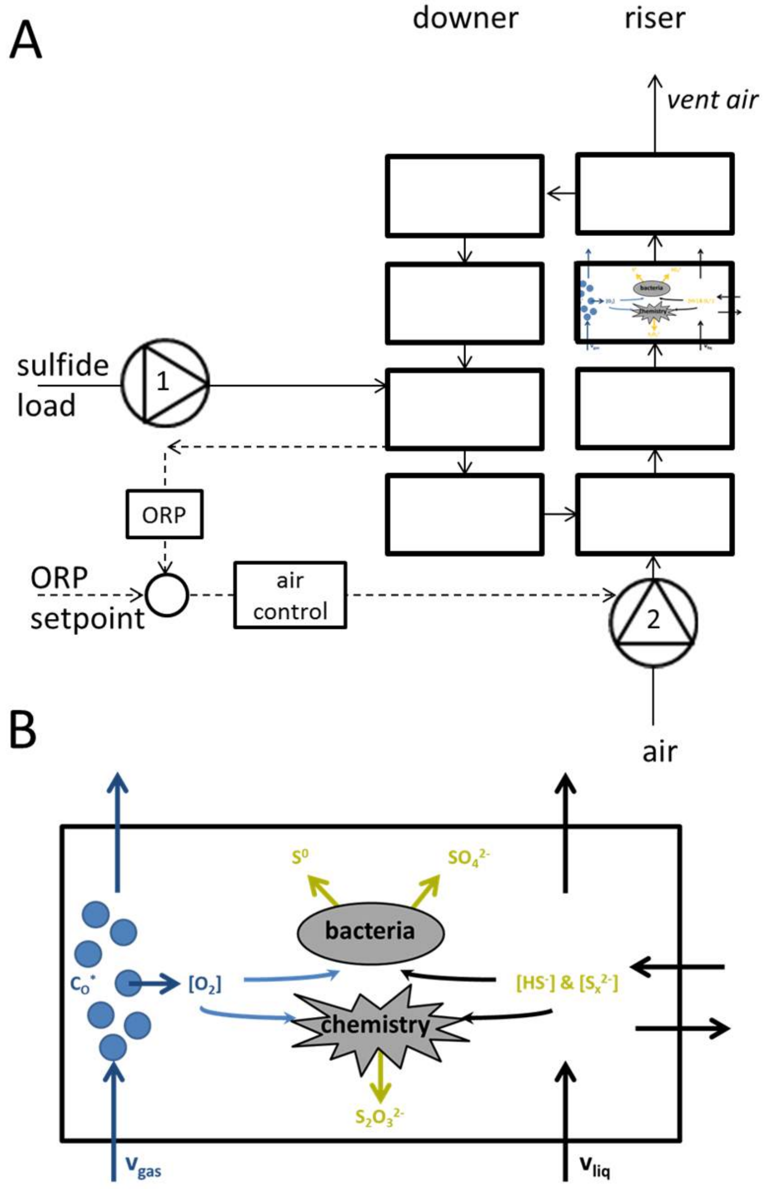
A
downer
riser
vent air
sulfide load
1
ORP
ORP setpoint
air control
2
air
B
S^0
SO_4^{2-}
bacteria
C_O^*
$[O_2]$
$[HS^-]$ & $[S_x^{2-}]$
chemistry
$S_2O_3^{2-}$
v_{gas}
v_{liq}

Figuur 6.1: A: schematic overview of the full-scale process, where 1 and 2 are actuators to control the sulfide load and the air flow, respectively. The dotted line represents an information flow. For the sake of simplicity, only eight segments are shown in this scheme. In this study, 20 segments are applied. B: a simplified picture to illustrate the reactions and mass transfer in a single reactor segment.

The biological reactions to describe sulfide oxidation by HA-SOB have been proposed in **Chapter 3**. The physiologically based kinetic model describes product formation rates of both S^0 and SO_4^{2-}, based upon bacterial respiration enzyme systems. The model has been validated at different volumetric scales, i.e. from 5 ml to 5 L and at various static and dynamic experimental conditions. It has been assumed that the systems studied were always ideally mixed. The general specific rate expressions for the two active sulfide enzyme systems in HA-SOB (FCC and FQ) and oxygen reduction enzyme (CcO) are given by:

$$q_{FCC} = q_{FCC,max}(1-F)\frac{[HS^-]}{K_{FCC}+[HS^-]} \tag{6.10}$$

$$q_{CcO} = q_{CCO,max}F\frac{[O_2]}{K_{CcO}+[O_2]}\frac{K_i}{K_i+[HS^-]} \tag{6.11}$$

$$q_{FQ} = \frac{q_{FQ,max}[HS^-]}{\frac{q_{FQ,max}}{q_{FQox,max}}\left(\frac{[O_2]+K_{FQox}}{[O_2]}\right)[HS^-]+[HS^-]+K_{FQ}} \tag{6.12}$$

where $q_\bullet$ is the specific oxidation rate (mmol s^{-1} mg N^{-1}), $q_{\bullet,max}$ the maximum specific oxidation rate (mmol s^{-1} mg N^{-1}), $K_\bullet$ the substrate affinity/inhibition constant (mmol L^{-1}) of the enzymes (indicated with •), F the reduction degree of the bacterial cytochrome pool (-). Based upon the work by Visser et al. [28], it is assumed that F changes instantaneously according to changes in the sulfide and oxygen levels (**Chapter 3**). Consequently, it follows that F is in quasi-steady state at all times, with values between 0 and 1. Moreover, the selectivity for S^0 and SO_4^{2-} formation is directly related to the value of F. As product formation depends on the electron transfer capacity (i.e. oxidation state of the cytochromes), a higher value of F will lead to more S^0 formation and less SO_4^{2-} production. For more details, we refer to **Chapter 3**.

6.3.2 Oxygen and fluid mass transfer

The availability of dissolved oxygen determines the system's oxidation capacity. Hence, it is important to maximize the gas to liquid oxygen transfer capacity. The oxygen transfer rate depends on the mass transfer coefficient and the difference in concentration between the gas and liquid phase, and is defined as [10]:

$$N_O = k_LA\left(\frac{C_O*}{m}-[O_2]\right) \tag{6.13}$$

where N_O is the oxygen transfer rate (mmol L^{-1} s^{-1}), k_LA the oxygen transfer coefficient (s^{-1}), C_O* the gas solubility (mmol L^{-1}) and m the liquid/gas partition coefficient for oxygen (-) [8]. C_O* is determined by the partial oxygen pressure in the gas phase and may therefore vary over a series of plug flow segments. Furthermore, k_LA depends on the total surface area of the gas bubbles, gas velocities and shear forces. k_LA can be calculated according to the following equation [7]:

$$k_LA = 123v_{sup}^{0.524}\psi^{-0.255}A_{bub} \tag{6.14}$$

where v_{sup} is the superficial gas velocity (m s^{-1}), ψ the apparent viscosity (Pa s) and A_{bub} the surface area of all gas bubbles (m^2) in the riser and downcomer. ψ is of the form [9]:

$$\psi = \kappa_1 v_{sup}^{\kappa_2} \tag{6.15}$$

with κ_1 and κ_2 empirical coefficients. It has been assumed that all injected air dissipates the reactor via the vent air stream, hence v_{sup} is directly related to the amount of air that is injected into the system. In practice, only 3-5 mol% oxygen is consumed (Paques B.V., personal communication). Additionally, any carbon dioxide that is dissolved in the absorber will be removed in the reactor via the injected air. Hence, in practice v_{sup} will be slightly different.

In addition to the equation for k_LA (Eq. 6.14), empirical models for gas hold-up (ϵ_{riser}) and liquid velocity (v_{riser}^{liq}) in the riser have been defined [9].

$$\epsilon_{riser} = 0.465v_{sup}^{0.65}\left(1 + \frac{A_{downer}}{A_{riser}}\right)^{1.06}\psi^{-0.103} \tag{6.16}$$

$$v_{riser}^{liq} = 0.23v_{sup}^{0.322}\left(\frac{A_{downer}}{A_{riser}}\right)^{0.97}\psi^{-0.103} \tag{6.17}$$

Furthermore, as ϵ_{riser} is known (see Eq. 6.16), ϵ_{downer} is calculated according to [3]:

$$\epsilon_{downer} = 0.79\epsilon_{riser} - 0.057 \tag{6.18}$$

Liquid velocities in the downer can be calculated from Eqs. 6.16-6.18, as both liquid volume and flows are known. Consequently, the overall flow profiles in riser and downer are known.

6.3.3 Industriewater Eerbeek B.V.

The simulation model was calibrated using results obtained from a Thiopaq reactor located at Industriewater Eerbeek B.V.. This installation is in operation since 1993 and treats a biogas stream from an anaerobic UASB reactor (typical gas flows ranges between 300 and 500 Nm^3 h^{-1}) containing hydrogen sulfide levels ranging from 0.8-1.2% (on average 1%). Hydrogen sulfide levels are reduced to values below 60 ppm. An overview of the overall process scheme is given by Janssen et al. (2009) [12]. In Figure 6.1 A a schematic overview of the modeled process is shown. Rich solvent enters the reactor system via pump 1. The sour biogas flow is measured online using a gas flow-meter at the outlet of the anaerobic reactor. As the hydrogen sulfide content in the sour gas and in the liquid feed stream is more or less constant, the sulfide loading rate to the bioreactor can be calculated online based on gas flow rates. The time delay between the flow measurement sour gas and actual injection in the bioreactor as a result of liquid residence time in pipes and absorber, needs to be determined.

The air injection point is located in the bottom section of the riser. The air flow (Q_{air} in m^3 s^{-1}) is online monitored and controlled via a PI controller using the ORP as the controlled variable. Obviously, changes in air injection rates will lead to changes in the gas hold-up, k_LA, flow patterns and consequently the dissolved oxygen concentration. As the flow dynamics in Eqs. 6.16-6.18 are defined by static equations, the following first-order response function is proposed to describe the dynamic response between the air flow and the computed air flow from the *PI* controller ($u(t)$).

$$Q_{air}(t) = \left(1 + e^{-\frac{t}{\tau}}\right) u(t) \tag{6.19}$$

The time constant τ, was chosen to be τ=20 sec. Furthermore, any sensor dynamics are neglected. An overview of additional specific process parameters are shown in Table 6.1.

Tabel 6.1: Description of specific parameters of the Thiopaq reactor model in "Eerbeek"

design parameter	value (unit)
Number of segments	20
Volume reactor	34.3 (m^3)
A_{riser}	2.7 (m^2)
A_{downer}	2.2 (m^2)
average bubble diameter	(6 mm)
pH	8.5
κ_1	0.0141
κ_2	0.0410
operation variables	**unit**
Liquid flow	m s^{-1}
Q_{biogas}	m^3 s^{-1}
Q_{air}	m^3 s^{-1}
total sulfide	mM

6.4 Materials and Methods

6.4.1 Respiration tests

ORP calibration tests were performed in a thermostated 20 mL glass chamber mounted on a magnetic stirrer and closed off with a dissolved oxygen (DO) sensor (PSt3 / PSt6, PreSens Precision Sensing GmbH, Regensburg, Germany) and an ORP sensor (ProSense, Ag/AgCl reference electrode). A small opening allowed for the injection of a sodium sulfide stock solution (0.1 mol/L). Before sulfide addition, the buffer solution in the reaction chamber and sensors were flushed with nitrogen gas to remove any dissolved oxygen. Experiments commenced by injection of 10 - 100 µL of sulfide stock solutions. After injection, a mixed gas consisting of nitrogen and air, leading to a 1.5% concentration of dissolved oxygen was bubbled via a needle in the solution. During aeration, the dissolved oxygen concentration slightly increased and liquid samples were taken. As chemical oxidation rates are relatively low at oxygen concentrations below 1µmol/L, it has been assumed that sulfide levels were constant during 15 minutes of testing (e.g. less than 1% of sulfide is oxidized in 15 minutes when $[HS^{-1}] = 0.5$ mM and $[O_2] = 0.015$ mM according to the kinetics (see **Chapter 3**).

6.4.2 Chemicals used

A carbonate buffer solution was prepared by mixing sodium and potassium (1:2) bicarbonate (pH 8.3) and carbonate (pH 12.3) buffer solutions, reaching a final pH of 8.5. Sodium sulfide stock solutions were freshly prepared by dissolution of $Na_2S{\cdot}9H_2O$ crystals in de-aerated water by flushing with nitrogen gas. The sulfide concentrations of the stock solutions were experimentally validated using Hach Lange tests (LCK653).

6.5 Results and Discussion

6.5.1 ORP models

The results from the lab scale experiments to test the effects of oxygen and sulfide on the ORP are shown in Figure 6.2. The following sulfide concentrations were tested: 0.0 ,0.01, 0.05, 0.1, 0.2, 0.3, 0.4, and 0.5 mM. The ORP depends on both the oxygen and sulfide concentrations, as can be seen from the measuring results. Trends are in accordance with literature data: increasing sulfide levels will lead to decreasing ORP values [13] whilst an increase in oxygen levels will lead to an increase in ORP values [22].

From Figure 6.2 it also follows that at oxygen concentrations below 0.0010 mM (i.e. when sulfide is available in excess) and at sulfide concentration above 0.05 mM, the measured ORP can be predicted using a linear regression method (see Eq. 6.8). Thus, for constant sulfide concentrations and for oxygen levels smaller than 0.001 mM, ORP is linearly dependent on $\log[O_2]$, as a linear relationship can be seen on a logarithmic scale. However, for higher oxygen levels, a non-linear relationship between ORP and $\log \gamma_{O_2}$ is found. The unknown coefficient ξ_1, ξ_2 and ξ_3 in Eq. 6.8 have been estimated via a least-squares estimation routine, for oxygen concentrations up to 0.001 mM. When the activity coefficients for both sulfide and oxygen are assumed to be equal to one, ξ_1, ξ_2 and ξ_3 were estimated at: -332.9 mV , 25.3 mV and -60.36 mV, respectively. Model predictions for $[HS^-]=0$ mM are not shown as this is beyond the validity range of the model since log(0) does not exist. However, the operation window for the full-scale process (i.e. ORP < -350 mV, oxygen concentrations < 0.001 mM) appears to be covered well by the proposed linear regression. The area where the calibrated model is valid is indicated in the dashed box in Figure 6.2.

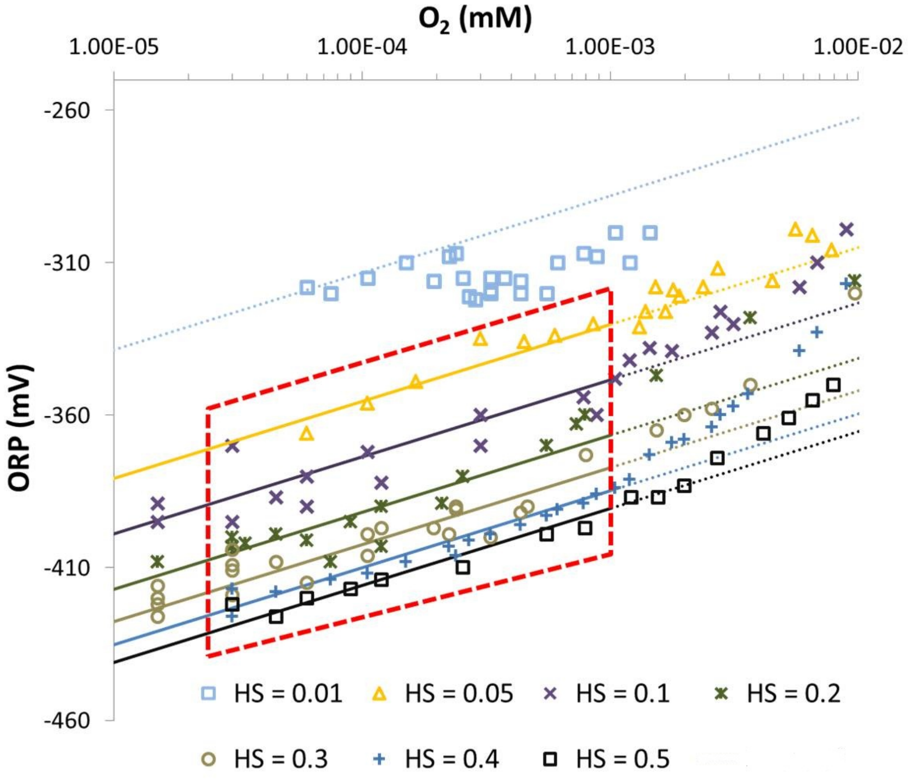

Figuur 6.2: ORP dependency for oxygen and sulfide (semi-logarithmic scale). The symbols represent measured data points, the solid lines represent the model fit, according to Eq. 6.8

6.5.2 Full-scale model

The proposed model as described in Eqs. 6.1-6.19 has been implemented in a Matlab Simulink routine, whereafter simulations were performed to calculate the dynamic ORP behavior of the full-scale biodesulfurization reactor at 'Industriewater Eerbeek'. The model consists of two input values, Q_{air} (control input) and Q_{biogas} (disturbance input), and ORP as an output variable. As initial states are unknown for all the individual segments and states, an initial guess is chosen. As such, the first 6 minutes of the model simulations will not be shown.

The simulation results of a 1 hour operating period are shown in Figure 6.3. The time delay that has been chosen to mimic the time between the actual flow measurement of the sour gas stream and the injection of the sulfide rich solution in the bioreactor (liquid residence time) is 185 seconds. Initially, this number was set 20 seconds. However, increasing this time delay to 185 seconds resulted a better fit between model and measurement. A larger liquid residence time would shift the ORP model more to the left in Figure 6.3 A whilst a lower liquid residence time shifts the ORP model to the right.

In Figure 6.3A both measured and predicted ORP values are shown during the first 0.3h, a significant difference exists between the predicted and measured ORP. From t = 0.3 h onwards, model outputs and measurements show similar behavior, both in magnitude as in dynamics, except for the period between t = 0.6 h up to t = 0.7 h. Hence it can be concluded that calculated values are governed by the chosen initial values. The reason for this discrepancy is yet unknown. Possibly by assuming modeling inconsistencies (due to assumptions) or to (temporary) sensor inaccuracy. For instance, for the modeling of the hydrodynamics 20 compartments for liquid circulation in internal loop-reactor airlift reactor systems was chosen. Another assumption is the biological diversity present in the process. Next to HA-SOB, more bacteria have been found in the biodesulfurization systems at haloalkaline conditions, e.g. heterotrophic and sulfate reducing bacteria [23]. Hence, the ORP behavior of the system will be affected as well. Furthermore, as ORP measurements in this 'period remain constant, sensor inaccuracies could also cause differences between model predictions and online measurements.

The predictions of the product formation over the period t = 0.3 up to t = 1.1 h are for S^0, $S_2O_3^{2-}$ and SO_4^{2-} formation 92.3 mol%, 2.5 mol% and 5.2 mol%, respectively. However, due to large hydraulic retention times and inaccuracy of off-line measurements, it is not possible to accurately determine the process selectivity over such a short time interval. The estimated selectivity for S^0 formation is between 90 and 95 mol%, which is in the range of the predicted value. Hence, without further fitting any other process parameters (except for the estimated liquid residence time of 185 seconds in the sump of the absorber and pipes), these results indicate that the model is able to predict the biological desulfurization process under actual conditions.

In Figure 6.3B, predicted variations in substrate levels of both dissolved oxygen and sulfide are shown. The same trends in dynamics are found: that is when sulfide concentrations increase, oxygen concentrations increase and vice versa. This is a logic consequence of the implemented control strategy. A general method to test the correlation between model results is by calculating the cross correlation coefficients. The closer the normalized cross correlation coefficient to 1, the more correlated the signals are. At lag zero (sulfide and oxygen levels at

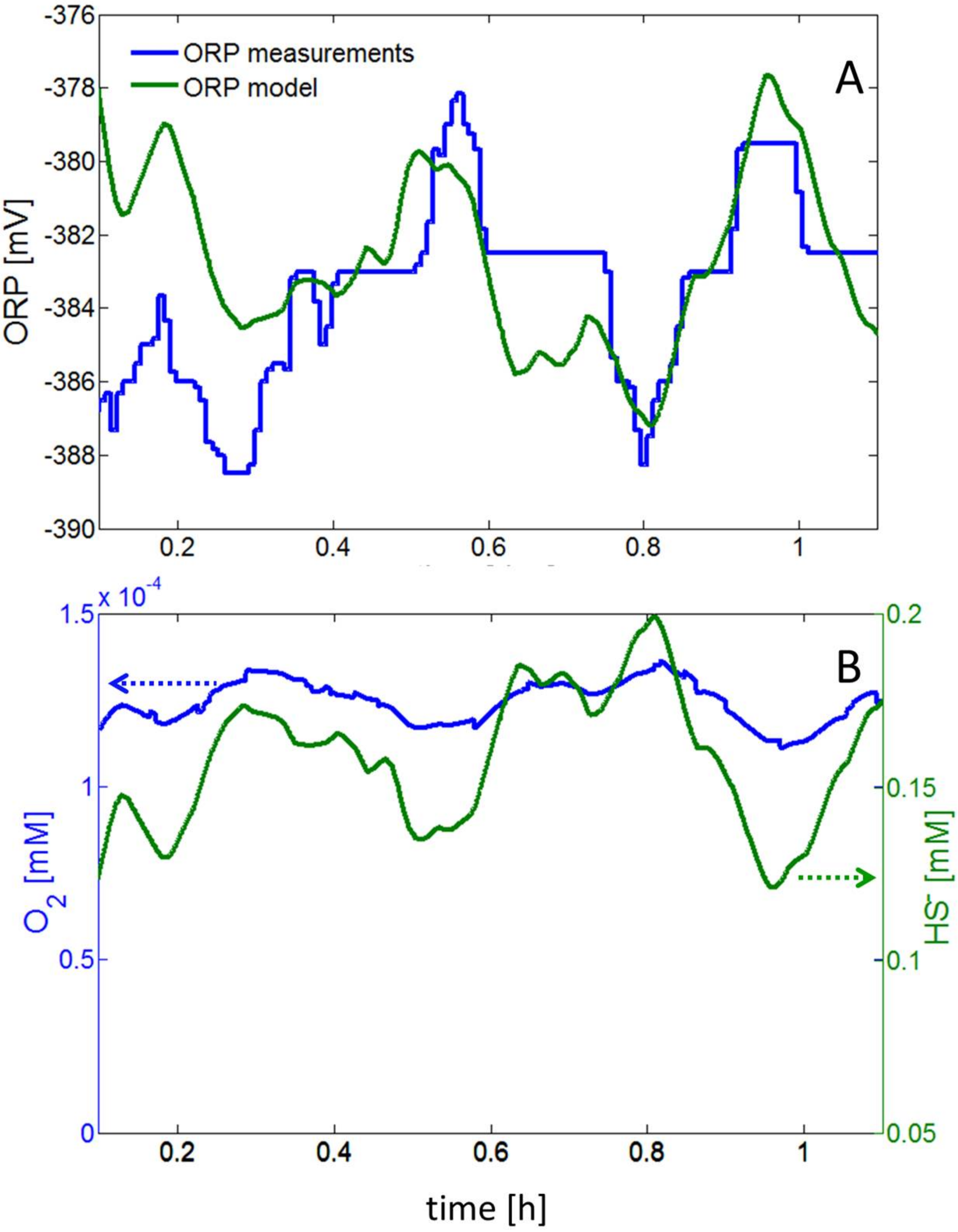

Figuur 6.3: Model results using dynamic data of a full-scale biodesulfurization reactor, showing measured as well as estimated ORP (A) and estimated substrate levels of oxygen (blue) and sulfide (green) (B). The experimental data are typical for a stable performance of full-scale biodesulfurization reactor of 'Industrie water Eerbeek'. The sour-gas stream contains hydrogen sulfide levels ranging from 0.8-1.2% (on average 1%). Hydrogen sulfide levels are reduced to values below 60 ppm.

the same time t) the normalized cross correlation coefficient is equal to 0.80. This supports our observation that the dynamic trends between oxygen and sulfide are largely correlated. However, the relative variations in concentrations are different. The absolute variations in sulfide levels are larger (between 0.12 and 0.20 mM) than in oxygen levels (between 11 nM and 14 nM). Hence, for almost constant oxygen levels, the ORP predictions can be simplified to:

$$E_H = \tilde{\xi}_1 + \xi_3 \log(\gamma_{HS^-}) \tag{6.20}$$

where the oxygen dependency is lumped into the parameter $\tilde{\xi}_1$, with $\tilde{\xi}_1 = \xi_1 + \xi_2 \log(\gamma_{O_2})$. This model for ORP and dissolved sulfide is in-line with Janssen et al. 1998 [13].

It is assumed from that a mixing point of view the mixing behavior in the full-scale reactor at "Industriewater Eerbeek B.V."can be modeled by an air-lift loop reactor. In the reactor, internals are installed to stimulate mixing regime with a riser and downer section. In practice, however, possibly a combination of both an air-lift loop reactor and a bubble column would be a more appropriate description of the flow regime in a full-scale plant. Hence, future work should include CFD modeling and experimental validation to obtain detailed insight in the hydrodynamics of a full scale plant.

6.5.3 Concluding remarks

In the full-scale processes, the common online measurements concerning bioreactor performance are ORP, pH and conductivity. The ORP measurements are used to control the selectivity of the process and is an indirect measure for selectivity for S^0 formation. As an alternative to the existing controlled strategy for oxygen supply, the presented model can be used in dynamic optimization schemes to calculate the optimal air-oxygen supply. These type of schemes can be found in so-called receding horizon optimal or model predictive controllers [18, 6] and that have been applied at waste water treatment plants [19]. These advanced process control methods allow both optimization of the current as future plant performance. Previous research showed that selectivity up to 98% of S^0 formation can be reached (**Chapter 5**). Hence, a large gap exists between current and optimal performance. Especially for large scale, e.g. processes up to 100 tons of sulfide per day, improvement of the selectivity of the process will lead to large reduction of operational costs due to a decrease in caustic addition.

References

[1] J. A. Asenjo and J. C. Merchuk. *Bioreactor system design*. CRC Press, 1995.

[2] W. A. M. Bakker, P. E. M. Overdevest, H. H. Beeftink, J. Tramper, and C. D. De Gooijer. Serial air-lift bioreactors for the approximation of aerated plug flow. *Trends in Biotechnology*, 15(7):264–269, 1997.

[3] R. A. Bello, C. W. Robinson, and M. Moo-Young. Liquid circulation and mixing characteristics of airlift contactors. *Canadian Journal of Chemical Engineering*, 62:573–577, 1985.

[4] M. Boon and J. J. Heijnen. Gas-liquid mass transfer phenomena in bio-oxidation experiments of sulphide minerals: A critical review of literature data. *Hydrometallurgy*, 48(2):187 – 204, 1998.

[5] C. J. N. Buisman, R. Post, P. IJspeert, B. G. Geraats, and G. Lettinga. Biotechnological process for sulphide removal with sulphur reclamation. *Acta Biotechnology*, 9(3):255–267, 1989.

[6] A. E. Byrson (Jr.). *Dyncamic Optimization*. Addison Wesley, 1999.

[7] M. Y. Chisty, B. Halard, and M. Moo-Young. Liquid circulation in airlift reactors. *Chemical engeneering sciences*, 43(3):451–457, 1988.

[8] F. Garcia-Ochoa and E. Gomez. Bioreactor scale-up and oxygen transfer rate in microbial processes: An overview. *Biotechnology Advances*, 27(2):153 – 176, 2009.

[9] M. Gavrilescu and R. Z. Tudose. Study of the liquid circulation velocity in external-loop airlift bioreactors. *Bioprocess Engineering*, 14(1):33–39, 1995.

[10] D. W. Green and R. H. Perry. *Perry's Chemical Engineers' Handbook*. McGraw-Hill, 2008.

[11] J. J. Heijnen, J. Hols, R. G. J. M. van der Lans, H.L.J.M. van Leeuwen, A. Mulder, and R. Weltevrede. A simple hydrodynamic model for the liquid circulation velocity in a full-scale two- and three-phase internal airlift reactor operating in the gas recirculation regime. *Chemical Engineering Science*, 52(15):2527 – 2540, 1997.

[12] A. J. H. Janssen, P. N. L. Lens, A. J. M. Stams, C. M. Plugge, D. Y. Sorokin, G. Muyzer, H. Dijkman, E. Van Zessen, P. Luimes, and C. J. N. Buisman. Application of bacteria involved in the biological sulfur cycle for paper mill effluent purification. *Science of the Total Environment*, 407(4):1333–1343, 2009.

[13] A. J. H. Janssen, S. Meijer, J. Bontsema, and G. Lettinga. Application of the redox potential for controling a sulfide oxidizing bioreactor. *Biotechnol. Bioeng.*, 60(2):147–155, 1998.

[14] A. J. H. Janssen, R. Sleyster, C. van der Kaa, J. Bontsema, , and G. Lettinga. Biological sulphide oxidation in a fed-batch reactor. *Biotechnol. Bioeng.*, 47(3):327–333, 1995.

[15] W. E. Kleinjan, A. De Keizer, and A. J. H. Janssen. Kinetics of the chemical oxidation of polysulfide anions in aqueous solution. *Water Research*, 39(17):4093–4100, 2005.

[16] W. E. Kleinjan, A. De Keizer, and A. J. H. Janssen. Kinetics of the chemical oxidation of polysulfide anions in aqueous solution. *Water Research*, 39(17):4096–4100, 2005.

[17] W. E. Kleinjan, A. De Keizer, and A. J. H. Janssen. Kinetics of the reaction between dissolved sodium sulfide and biologically produced sulfur. *Industrial and Engineering Chemsitry Research*, 44:309–317, 2005.

[18] F. L. Lewis and V. L. Syrmos. *Optimal Control*. Wiley-Interscience, 1995.

[19] L. J. S. Lukasse and K. J. Keesman. *Water Research*, (33):2651–2659, 1999.

[20] J. C. Merchuk, N. Ladwa, A. Cameron, M. Bulmer, and A. Pickett. Concentric-tube airlift reactors: Effects of geometrical design on performance. *AIChE Journal*, 40(7):1105–1117, 1994.

[21] D. J. O'Brien and F. B. Birkner. Kinetics of oxygenation of reduced sulfur species in aqueous solution. *Environmental Science and Technology*, 11(12):1114–1120, 1977.

[22] O. N. Oktyabrskii and G. V. Smirnova. Redox potential changes in bacterial cultures under stress conditions. *Microbiology*, 81(2):131–142, 2012.

[23] D. Y. Sorokin, P. L. F. Van Den Bosch, B. Abbas, A. J. H. Janssen, and G. Muyzer. Microbiological analysis of the population of extremely haloalkaliphilic sulfur-oxidizing bacteria dominating in lab-scale sulfide-removing bioreactors. *Appl. Microbiol. Biotechnol.*, 80(6):965–975, 2008.

[24] W. A. J. van Benthum, J. H. A. van den Hoogen, R. G. J. M. van der Lans, M. C. M. van Loosdrecht, and J. J. Heijnen. The biofilm airlift suspension extension reactor. part i: Design and two-phase hydrodynamics. *Chemical Engineering Science*, 54(12):1909 – 1924, 1999.

[25] P. L. F. Van den Bosch, D. Y. Sorokin, C. J. N. Buisman, and A. J. H. Janssen. The effect of pH on thiosulfate formation in a biotechnological process for the removal of hydrogen sulfide from gas streams. *Environmental Science and Technology*, 42(7):2637–2642, 2008.

[26] P. L. F. Van den Bosch, O. C. Van Beusekom, C. J. N. Buisman, and A. J. H. Janssen. Sulfide oxidation at halo-alkaline conditions in a fed-batch bioreactor. *Biotechnology and Bioengineering*, 97(5):1053–1063, 2007.

[27] K. van 't Riet and J. Tramper. *Basic Bioreactor design*. Marcel Dekker, 1991.

[28] J. M. Visser, L. A. Robertson, H. W. Van Verseveld, and J. G. Kuenen. Sulfur production by obligately chemolithoautotrophic thiobacillus species. *Applied and Environmental Microbiology*, 63(6):2300–2305, 1997.

Part III

Discussions & Summary

Chapter 7

General discussion

7.1 Introduction

In 1989, Buisman et al. reported that the selectivity for elemental sulfur (S^0) formation in a sulfide-removing bioreactor can reach values as high as 95 mol%, while almost complete hydrogen sulfide removal takes place [5]. That paper was the basis for the development of a family of biotechnological processes for gas biodesulfurization. Together with Delft University of Technology, Paques B.V. and Shell, Wageningen University developed and deployed a range of biological processes that rely on the biological sulfur cycle for the treatment of sulfur-containing anaerobic effluents and gas streams. The research evolved from the screening of neutrophilic sulfide-oxidizing bacteria that can form S^0 under oxygen-limiting conditions [13] to bioreactor implementation [12], biomass analysis [30], analysis of the chemical kinetics of sulfide oxidation [4, 14] and finally the development of the haloalkaline process, which requires less water and energy [20, 29].

Each subsequent research step contributed to the further optimization of the process that is commercialized today. As a result of this line of research, over 200 full-scale biodesulfurization installations have been installed worldwide so far (Figure 7.1 Paques B.V., personal communication).

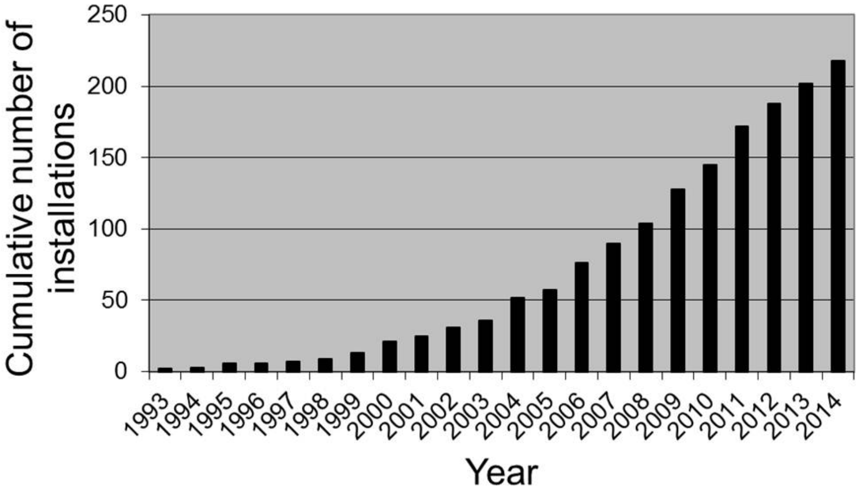

Figuur 7.1: Cumulative number of Thiopaq installations for biological desulfurization of gas (biogas, landfill gas and natural gas)

The first process step comprises the absorption of hydrogen sulfide in a slightly alkaline and carbonate-buffered solution. Subsequently, neutrophilic or haloalkaliphilic (high salt concentrations > 1M and elevated pH values, i.e. > 8.5) sulfur-oxidizing bacteria oxidize dissolved sulfide to elemental sulfur (S^0). Bench-scale experiments have shown that part of the sulfide (typically less than 10 mol%) is oxidized to sulfate (SO_4^{2-}) [29]. Additionally, a fraction of the total dissolved sulfides, including polysulfide (S_x^{2-}), is chemically oxidized to thiosulfate ($S_2O_3^{2-}$) [14, 28]. The key biological and chemical reactions in this process are as follows:

$$HS^- + \frac{1}{2}O_2 \rightarrow S^0 + OH^- \text{ (bio)} \tag{7.1}$$

$$HS^- + 1\frac{1}{2}O_2 + H_2O + NAD^+ \rightarrow SO_4^{2-} + NADH + 2H^+ \text{ (bio)} \tag{7.2}$$

$$HS^- + O_2 \rightarrow \frac{1}{2}S_2O_3^{2-} + \frac{1}{2}H_2O \text{ (chem)} \tag{7.3}$$

$$HS^- + (x-1)S^0 \leftrightarrow S_x^{2-} + H^+ \text{ (chem)} \tag{7.4}$$

$$S_x^{2-} + 1\frac{1}{2}O_2 \rightarrow S_2O_3^{2-} + (x-2)\,S^0 \text{ (chem)} \tag{7.5}$$

The formation of S^0 (Eq. 7.1) is preferred because S^0 can be re-used for agricultural purposes and therefore has commercial value. Moreover, $S_2O_3^{2-}$ and SO_4^{2-} formation increases the caustic consumption and therefore the operating costs. Chemical sulfide oxidation is enhanced at higher sulfide concentrations first of all, because biological oxidation is inhibited under these conditions. Furthermore, the chemical oxidation depends on only one reactant and can be described with first-order reaction kinetics as On the other hand, the formation of SO_4^{2-} is stimulated at higher oxygen levels [29]. Therefore, there are optimum dissolved sulfide and oxygen concentrations at which the selectivity for S^0 formation is maximized.

In general, bioreactor design and process optimization depend on a variety of interrelated considerations, as depicted in Fig. 7.2. In-depth knowledge of reaction kinetics, transport phenomena and mechanical aspects related to the construction of the installation is important for the successful design and operation of the integrated process [6]. In industrial biodesulfurization plants, mixing of the reactor fluid is mainly achieved by injection of air, which also serves to supply oxygen to the system. Because of this dual function, there is a direct yet complex relationship between hydrodynamics and product formation.

The PhD research presented in this thesis builds on the work carried out in our group during the past two decades, aimed at increasing the selectivity for S^0 formation. Initially, this PhD project focused on the kinetics of biological sulfide oxidation. Later on, the temperature effects on the overall biological respiration were studied. Furthermore, as there was a need for a thorough basis for the reaction stoichiometry and kinetics, a biological kinetic model was proposed. The development and evaluation of this biological kinetic model were supported by experiments on the scale of microbiological respiration (4 - 20 mL scale) and on bench scale(4.7 L). The first chapters of this thesis (**Chapters 2 - 4**) described these aspects.

The second part of this thesis (**Chapters 5 & 6**) focuses on the modeling of full-scale systems. Initially, the developed dynamic biological kinetic models were approximated by static meta-models describing a simplified, ideally mixed, full-scale reactor. The meta-models were evaluated with the aid of parameter sensitivity analysis and response surface methodology. Bioreactor systems also were investigated for dynamic conditions, by comparing modeling results with data from a full-scale plant.

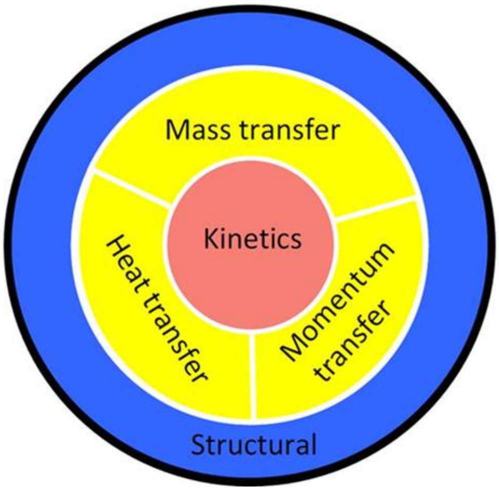

Figuur 7.2: bioreactor design considerations [6]

7.2 Reaction pathways and kinetics

7.2.1 Two enzyme systems

A major finding from the respiration experiments was that presumably two enzyme systems are involved in the oxidation of sulfide (**Chapter 3**). One of these systems is based on electron transfer to cytochrome c, the so-called flavocytochrome c oxidoreductase (FCC). This system has been described in literature [17, 16], and cytochrome-dependent removal of sulfide has been demonstrated [22]. Another well-known enzyme associated with sulfide oxidation is sulfide:quinone oxidoreductase (SQR) [11]. The FCC and SQR enzymes are related, having a common ancestor and a similar catalytic (flavin) domain [24]. Based on the measured decyl-ubiquinone-dependent oxidation of sulfide, activity of SQR in HA-SOB has been suggested [22]. The genomic sequence of several *Thioalkalivibrio* species confirmed the presence of several ubiquinone-dependent enzymes, but genes encoding for SQR have not yet been identified [16, 17]. Therefore, based on an analysis of our experimental reactor data obtained at different scales, we hypothesize that in the absence of SQR, some variants of FCC (hereafter called FQ) may act as SQR, i.e. donate electrons to ubiquinone instead of to cytochrome c, (**Chapters 2 & 3**). There clearly is a need to investigate SQR and quinine-related enzymes in HA-SOB further. Future research should focus on cultivation conditions (e.g. grow sulfide-oxidizing bacteria with sulfide, as Muyzer et al. used solely $S_2O_3^{2-}$ as an electron donor [16, 17]). As no strain has been isolated yet, selective cultivation conditions may be delicate (i.e. low oxygen concentrations and or higher sulfide concentrations).

Another important result described in this thesis relates to the reaction stoichiometry of SO_4^{2-} formation. In bench-scale gas lift reactors, HA-SOB appear able to oxidize sulfide to SO_4^{2-} along several respiration routes (**Chapter 2**). One of the routes, the limited oxygen route

(LOR), features under oxygen-limiting conditions. It is hypothesized that sulfide is oxidized to S^0 with the aid of FQ; the electron acceptor would not be oxygen but NAD^+. As a consequence, up to 25% less oxygen would be consumed for the formation of one mole of SO_4^{2-} relative to oxidation with oxygen as the sole electron acceptor. In this case, NADH would be used for CO_2 fixation. These results contribute to a deeper understanding of the process as at limiting oxygen levels, more SO_4^{2-} is formed than can be expected on the basis of the full oxygen route.

7.3 Models

7.3.1 Physically based kinetic model

The work described in this thesis focuses on the development of a mathematical model to describe biological sulfide oxidation in large-scale reactor systems. Formation of the main end products, S^0 and SO_4^{2-}, indirectly depends on the substrate concentration, as the intermediate reactions are mediated by electron transfer chains. In models, biological product formation (and therefore the microbiological kinetics) depends on the physiological oxidation state of the involved enzyme systems. The physiological state, in turn, depends on the substrate levels. Hence, the overall kinetics are based on biochemical and microbiological principles instead of on hypothesized overall chemical reaction equations leading to the frequently proposed Haldane/Monod kinetics [3, 12, 27, 22, 2, 21, 9, 10].

In this thesis research, the biological as well as the abiotic kinetics of sulfide oxidation were calibrated only once, with the aid of a data set obtained from laboratory respiration experiments (**Chapter 3**). All the model predictions in this thesis are based on the same estimated kinetic parameter set. For all scales (respiration, bench and full scale), this parameter set appeared sufficient to obtain accurate predictions. However, there is a need for multi-scale modeling to understand the enzyme kinetics and transfer processes (e.g. nano scale) better.

7.3.2 Respiration kinetics

The biological respiration tests described in this thesis do not provide all the necessary information required to articulate a complete kinetic model for the biodesulfurization process. The following aspects still need further work:

- The respiration tests are based on both biological and chemical removal of dissolved oxygen under oxygen-saturated conditions. In full-scale plants, however, the oxygen concentrations are much lower. Hence, the experimental conditions are not representative of the field conditions.

- In addition, the calibrated developed kinetic model is mainly based on the oxygen concentration. The substrate sulfide concentrations in the respiration tests are estimates. In short periods (i.e. 1-minute intervals), the currently available tests do not determine the sulfide removal with sufficient accuracy.
- It is still unknown which compound (i.e. oxygen or sulfide) is the limiting factor for the HA-SOB, in both uptake and enzymatic kinetics. For example, Van den Bosch et al. (2009) showed that there is a difference in the substrate sulfide and polysulfide [26]. However, the preferred substrate for both enzymatic systems (FCC / FQ) remains unknown. Furthermore, the mechanism of uptake of the (poly)sulfide and oxygen from the solution by the bacteria still has not been identified.
- Neutrophilic sulfur-oxidizing bacteria are able to store sulfur in their periplasm [7]. Therefore, it is likely that also HA-SOB can store sulfur particles in their periplasm, which will influence the measured respiration in the specific respiration test.
- Another unknown parameter is the actual product formation in the respiration tests. S^0 cannot be measured, and therefore product formation cannot be determined accurately. Furthermore, analytical limitations also make it impossible to measure the formation of sulfate and thiosulfate within a period of minutes.
- Biomass composition can change in time as a result of adaptation to changing process conditions. Different biodesulfurization installations will have different biomass compositions, for example related to differences in feed gas composition or redox levels [22]. It is therefore likely that the ratio between FCC and FQ will also be different. When the expression of FQ is more pronounced, relative to that of the FCC system, this will also influence biological kinetics and reaction selectivity.

All these unknowns will greatly affect the overall kinetics of the system. To facilitate greater microbiological insight and future developments, it is therefore of key importance to come up with more advanced biological respiration tests.

7.3.3 Sensitivities and surface methodology

Parameter sensitivity analysis is an important tool for 1) understanding the relative importance of a cluster of parameters deployed in mathematical models, 2) the dynamic behavior of kinetic models and 3) the effect of parameters and inputs on the states and outputs of the model [19, 25, 1, 23]. A new procedure was used to study the physiology-based model for its sensitivity of substrate concentrations with respect to input variables and kinetic parameters (**Chapter 5**.) This procedure combines individual local sensitivities to obtain lumped sensitivities of the multiple-input multiple-state model. This revealed that the local parameter sensitivities, in both magnitude and sign, are governed by sulfide levels when oxygen levels are elevated. Additionally, it was shown that two parameters that are important at oxygen-limiting conditions, show very limited sensitivity in a conventional respiration test setup. An advanced experimental setup is required to determine accurate estimates in all oxygen ranges.

In addition to the local sensitivity analysis, approximate meta-models of a biodesulfurization reactor were derived with the use of a response surface methodology (RSM). RSM explores the relationship between several control variables and response variables. RSM for example allows us to explore the effect of air injection on process performance, provided that a full-scale model is available. As described before, a direct and complex relationship exists between fluid mixing and reaction selectivity. The selectivity for sulfide oxidation reactions can be visualized by evaluating different air injection flows with RSM. This requires both local and global sensitivity analyses to obtain a complete picture of parameter sensitivity.

7.3.4 Dynamic models in bench and full-scale systems

The results of the cross-validation tests (**Chapter 3**) investigating the effect of the injection of sulfide and oxygen on overall process performance was surprising. A previous study [29] and additional work described in this thesis (**Chapter 2**) did not result in stable reactor performance with more than 90 mol% sulfur formation, although these systems are seen as having an ideally mixed regime. Full-scale reactor systems, on the other hand, can approach up to 94 mol% of S^0 formation (Paques B.V., personal communication). Differences between the two types of system are that in the bench-scale upflow reactor, H_2S and oxygen are injected via the same gas sparger located at the base of the reactor while in a full-scale system, H_2S is first absorbed in a separate absorber and sulfide injection does not occur in the same location as air injection. As a result of the way sulfide and air are injected into the bench-scale reactor compared with full-scale systems, sulfide concentrations are locally high (at least 2.5 times higher), resulting in increased chemical oxidation rates and thus a higher formation rate of $S_2O_3^{2-}$ (**Chapter 3**).

Analysis of the bench-scale reactor model shows that S^0 formation can be as high as 98 mol% of the supplied sulfide (**Chapter 5**). Compared with an average of 90-94 mol% S^0 formation in full-scale plants, formation of 98 mol% S^0 would lead to a 80% reduction in caustic consumption. This reduction is directly related to a reduction in proton formation. Additionally, the bleed stream of the overall process would also be smaller as there would be reduced formation of dissolved sulfur compounds (i.e. SO_4^{2-} and $S_2O_3^{2-}$). However, this optimum of 98 mol% also entails unwanted phenomena, such as chemical oxidation and biological by-product formation. These process perturbations will irrevocably lead to a decrease of S^0 formation.

7.3.5 Full-scale model considerations

The presented full-scale model serves as a stepping stone for the development of more accurate models. It can be improved on several points, which will lead to more insight in the workings of full-scale plants:

- Carbon dioxide (CO_2) plays an important role in the process. First, in the absorption column, H_2S and CO_2 are absorbed simultaneously which acidifies the solvent due to the consumption of hydroxyl ions. Hence, pH gradients play a role in the process. Furthermore, while dissolved HS^- is converted by the bacteria, CO_2 is stripped in the bioreactor. Detailed models for both carbonate buffer systems and CO_2 stripping are required. Second, to maintain the pH at 8.5, additional caustic (NaOH) has to be added when CO_2 is present in the gas; this leads to higher salinities.

- The mixing / fluid models in this thesis are based on rules described in literature. However, there are no good models that describe the mixing and fluid behavior under the high salinity conditions of the halo-alkaline biodesulfurization process. Hence, process-specific experiments need to be designed to develop an accurate fluid model.

- The model studies discussed in **Chapter 3** revealed that the formation of $S_2O_3^{2-}$ mainly occurs around injection points, as the sulfide levels are high there compared with the bulk concentration. A CFD model of the injection points needs to be developed to identify the impact of sulfide injection in full-scale systems.

- The complex chemistry of the interaction between S^0, sulfides and polysulfides is not yet fully understood. For volatile organic sulfur compounds, the (bio) chemistry is even more complex [15, 8, 18].

7.3.6 Research objectives

Initially, the work described in this thesis focused on the kinetics and pathways of the biological processes in biological gas desulfurization (first objective). It built on work described in literature and recently obtained experimental data. The governing pathway of sulfate formation under oxygen-limiting conditions turned out to consume less oxygen than previously described in literature, which therefore was called the limited-oxygen route (LOR). Furthermore, temperature effects and biological respiration of HA-SOB were studied.

Subsequently, these results were used as input for the second research goal, i.e. articulation of a mathematical model describing the processes in a sulfur-producing bioreactor. The proposed model for describing biological sulfide oxidation by HA-SOB was calibrated, validated and studied with a newly developed normalized sensitivity method. This provided several new insights into the biological process.

Using the kinetic models in a simplified full-scale model made it possible to derive approximate meta-models of a biodesulfurization reactor with the aid of response surface methodology (RSM). Using the response surface instead of an imposed control structure such as a classical PI or PID controller also yielded a static (feed forward) control law (third objective). The response surface describes the complex reaction kinetics and mass transfer phenomena.

7.4 Final considerations

From the developed and validated kinetic models and the static optimization rules derived from the developed models, it follows that a selectivity for S^0 formation of 98 mol% from the biological oxidation of sulfide is possible. For large-scale industrial processes, this would mean a significant cost reduction as the current processes produce up to 90-94 mol% S^0. Biodesulfurization processes yielding to 100 tons of sulfur per day would become economically feasible. However, optimal control strategies need to be developed and several microbiological questions still require answering. Continued research can translate these promising model results into industrial practice.

On the basis of these new insights in biological desulfurization, namely regarding different enzymatic activities under haloalkaline conditions, a patent has been filed. For more details: International patent application PCT/EP2015/051872, Title: A process for the biological conversion of bisulphide into elemental sulphur, filed 30 January 2015.

References

[1] A. Abusam, K. J. Keesman, G. Van Straten, H. Spanjers, and K. Meinema. Parameter estimation procedure for complex non-linear systems: Calibration of ASM No.1 for N-removal in a full-scale oxidation ditch. *Water Science and Technology*, 43(7):357–365, 2001.

[2] H. Banciu, D. Y. Sorokin, R. Kleerebezem, G. Muyzer, E. A. Galinski, and J. G. Kuenen. Growth kinetics of haloalkaliphilic, sulfur-oxidizing bacterium *Thioalkalivibrio versutus* strain ALJ 15 in continuous culture. *Extremophiles*, 8(3):185–192, 2004.

[3] C. J. N. Buisman, P. IJspeert, A. Hof, A. J. H. Janssen, R. Ten Hagen, and G. Lettinga. Kinetic parameters of a mixed culture oxidizing sulfide and sulfur with oxygen. *Biotechnology and Bioengineering*, 38(8):813–820, 1990.

[4] C. J. N. Buisman, P. IJspeert, A. J. H. Janssen, and G. Lettinga. Kinetics of chemical and biological sulphide oxidation in aqueous solutions. *Water Research*, 24(5):667–671, 1990.

[5] C. J. N. Buisman, R. Post, P. IJspeert, B. G. Geraats, and G. Lettinga. Biotechnological process for sulphide removal with sulphur reclamation. *Acta Biotechnology*, 9(3):255–267, 1989.

[6] M. Y. Chisty. *Airlift Bioreactors*. Elsevier, London, 1989.

[7] C. Dahl and C. G. Friedrich. *Microbial Sulfur Metabolism*. Springer, 2007.

[8] M. de Graaff. *Biological treatment of sulfidic spent caustics under haloalkaline conditions using soda lake bacteria*. Ph.D. thesis, Wageningen University, Wageningen, The Netherlands, 2012.

[9] A. Gonzalez-Sanchez and S. Revah. The effect of chemical oxidation on the biological sulfide oxidation by an alkaliphilc sulfoxidizing bacterial consortium. *Enzeme and Microbial Technology*, 40:292–298, 2006.

[10] A. Gonzalez-Sanchez, M. Tomas, A. D. Dorado, X. Gamisans, A. Guisasola, J. Lafuente, and D. Gabriel. Development of a kinetic model for elemental sulfur and sulfate formation form the autotrophic sulfide oxidation using respirometric techniques. *Water Science and Technology*, 59:1323–1329, 2009.

[11] C. Griesbeck, G. Hauska, and M. Schutz. Biological sulfide oxidation: Sulfide-quinone reductase (sqr), the primary reaction. *Recent Research Developments in Microbiology*, 4:179–203, 2000.

[12] A. J. H. Janssen, S. C. Ma, P. Lens, and G. Lettinga. Performance of a sulfide-oxidizing expanded-bed reactor supplied with dissolved oxygen. *Biotechnol. Bioeng.*, 53(1):32–40, 1996.

[13] A. J. H. Janssen, R. Sleyster, C. van der Kaa, J. Bontsema, , and G. Lettinga. Biological sulphide oxidation in a fed-batch reactor. *Biotechnol. Bioeng.*, 47(3):327–333, 1995.

[14] W. E. Kleinjan, A. De Keizer, and A. J. H. Janssen. Kinetics of the chemical oxidation of polysulfide anions in aqueous solution. *Water Research*, 39(17):4093–4100, 2005.

[15] R. C. Leerdam. *Anaerobic degradation of methanethiol in a process for Liquid Petroleum Gas (LPG) biodesulfurization*. PhD thesis, Wageningen University, Wageningen, The Netherlands, 2007.

[16] G. Muyzer, D. Y. Sorokin, K. Mavromatis, A. Lapidus, A. Clum, N. Ivanova, A. Pati, P. d'Haeseleer, T. Woyke, and N. C. Kyrpides. Complete genome sequence of "thioalkalivibrio sulfidophilus"hl-ebgr7. *Standards in Genomic Sciences*, 4:23–35, 2011.

[17] G. Muyzer, D. Y. Sorokin, K. Mavromatis, A. Lapidus, B. Foster, H. Sun, N. Ivanova, A. Pati, P. D'haeseleer, T. Woyke, and N. C. Kyrpides. Complete genome sequence of thioalkalivibrio sp. k90mix. *Standards in Genomic Sciences*, 5, 2011.

[18] P. Roman, M. F. M. Bijmans, and A. J. H. Janssen. Quantification of individual polysulfides in lab-scale and full-scale desulfurisation bioreactors. *Environmental Chemistry*, 11:702–708, 2014.

[19] A. Saltelli, M. Ratto, T. Andres, F. Campolongo, J. Cariboni, D. Gatelli, M. Saisana, and S. Tarantola. *Global Sensitivity Analysis The Primer*. John Wiley & Sons, 2008.

[20] D. Y. Sorokin, G. J. Kuenen, and G. Muyzer. The microbial sulfur cycle at extremely haloalkaline conditions of soda lakes. *Frontiers in Microbiology*, 2(44), 2011.

[21] D. Y. Sorokin, T. P. Tourova, A. M. Lysenko, L. L. Mitushina, and J. G. Kuenen. Thioalkalivirbio thiocyanoxidans sp. nov. and Thioalkalivibrio paradoxus sp. nov., novel alkaliphilic, obligately autotrophic, sulfur-oxidizing bacteria capable of growth on thiocyanate, from soda lakes. *International Journal of Systematic and Evolutionary Microbiology*, 52:657–664, 2002.

[22] D. Y. Sorokin, P. L. F. Van Den Bosch, B. Abbas, A. J. H. Janssen, and G. Muyzer. Microbiological analysis of the population of extremely haloalkaliphilic sulfur-oxidizing bacteria dominating in lab-scale sulfide-removing bioreactors. *Appl. Microbiol. Biotechnol.*, 80(6):965–975, 2008.

[23] S. Tarantola and A. Saltelli. Samo 2001 Methodological advances and innovative applications of sensitivity analysis. *Reliability Engineering and System Safety*, 79(2):121–122, 2003.

[24] U. Theissen, M. Hoffmeister, M. Grieshaber, and W. Martin. Single eubacterial origin of eukaryotic sulfide:quinone oxidoreductase, a mitochondrial enzyme conserved from the early evolution of eukaryotes during anoxic and sulfidic times. *Molecular Biology and Evolution*, 20(9):1564–1574, 2003.

[25] R. Tomavic. *Sensitivity analysis of dynamic systems*. McGraw-Hill Book Co Inc New York, 1963.

[26] P. L. F. Van den Bosch, M. de Graaf, M. Fortuny-Picornell, R. C. Leerdam, and A. J. H. Janssen. Inhibition of microbiological sulfide oxidation by methanethiol and dimethyl polysulfides at natron-alkaline conditions. *Environmental biotechnology*, 83:579–587, 2009.

[27] P. L. F. Van den Bosch, M. Fortuny-Picornell, and A. J. H. Janssen. Effects of methanethiol on the biological oxidation of sulfide at natron-alkaline conditions. *Environmental Science and Technology*, 43(2):453–459, 2009.

[28] P. L. F. Van den Bosch, D. Y. Sorokin, C. J. N. Buisman, and A. J. H. Janssen. The effect of pH on thiosulfate formation in a biotechnological process for the removal of hydrogen sulfide from gas streams. *Environmental Science and Technology*, 42(7):2637–2642, 2008.

[29] P. L. F. Van den Bosch, O. C. Van Beusekom, C. J. N. Buisman, and A. J. H. Janssen. Sulfide oxidation at halo-alkaline conditions in a fed-batch bioreactor. *Biotechnology and Bioengineering*, 97(5):1053–1063, 2007.

[30] J. M. Visser, G .C. Stefess, L. A. Robertson, and J. G. Kuenen. Thiobacillus sp. W5, the dominant autotroph oxidizing sulfide to sulfur in a reactor for aerobic treatment of sulfidic wastes. *Antonie van Leeuwenhoek, International Journal of General and Molecular Microbiology*, 72(2):127–134, 1997.

Chapter 8

Summary

Biogas, synthesis and natural gas streams may require treatment to remove toxic and corrosive gaseous sulfur compounds like hydrogen sulfide, disulfides and thiols. Traditionally, physicochemical processing technologies accomplished this gas desulfurization. However, about 25 years ago, a biotechnological gas treatment process was developed as an alternative. It offers a number of advantages, such as high hydrogen sulfide removal efficiency while operating at a wide range of feed gas pressures, absence of sulfide-containing waste streams and of concentrated sulfidic streams, and lack of need for chelating agents. However, the biotechnological process requires the addition of caustic and makeup water to compensate for any unwanted acidic sulfur components. This means that there is also a bleed stream. For cost-effective large-scale application of this new biotechnological process, the current set of design and control rules requires more fine-tuning toward minimizing the addition of caustic and makeup water by maximizing the elemental sulfur (S^0) production at the lowest possible cost.

Initially, the work described in this thesis focused on the reaction stoichiometries of the biological oxidation of dissolved sulfide (**Chapter 2**). Our experimental results show that haloalkaliphilic sulfur-oxidizing bacteria in bench-scale gas lift reactors are able to oxidize sulfide to SO_4^{2-} along several respiration routes. One of the routes features at limiting oxygen levels. We hypothesize that in the latter route, sulfide is oxidized to S^0 with the aid of a variant of flavocytochrome c oxidoreductase (FCC) acting as sulfide:quinone oxidoreductase (SQR). We think that in this case, electrons are donated to ubiquinone instead of to cytochrome c and that the electron acceptor is not oxygen but NAD^+. As a consequence, this route consumes up to 25% less oxygen for the formation of one mole of SO_4^{2-} relative to oxidation with oxygen as the sole electron acceptor. These findings may have consequences for the optimization of S^0 formation as at limiting oxygen levels, more SO_4^{2-} may be formed, which would be undesirable.

Biological respiration tests also indicated at least two local optima in oxygen removal at different sulfide concentrations. From the work in **Chapter 3**, it follows that two sulfide-oxidizing enzyme systems are active in haloalkaliphilic sulfur-oxidizing bacteria, namely

FCC and a variant of FCC that acts like SQR. It is known that at higher sulfide concentrations, the CcO/FCC enzymatic system is inhibited. At sulfide concentrations above 2.0 mM, however, the SOB still showed high respiration activity in our experiments. This sulfide removal activity must therefore be ascribed to some form of SQR.

Chapter 3 proposes a model on the basis of a concept involving multi-substrate removal and multi-product formation. The model structure was successfully validated on the basis of data sets from respiration tests and real-time reactor experiments. The presented model predicts up to 98 mol% of S^0 formation. A future challenge will be to optimize the biotechnological process to achieve that 98 mol% of S^0 formation in practice, by improving the process design, mixing regime and operation, e.g. through advanced substrate injection and dissolved oxygen (DO) control strategies.

This thesis also explores the effect of temperature. **Chapter 4** describes experiments that covered a range of temperatures in fed-batch tests (long-term effects) and respiration tests (short-term effects). The biological activity was reversibly limited at temperatures below 15°C. However, at higher temperatures, i.e. at temperatures above 48°C, stable operation became impossible as HA-SOB are irreversibly inactivated at such high temperatures. Using a temperature operation window of 15 - 45°C will therefore likely be required for robust performance of the biodesulfurization process.

Chapter 5 described how the biological respiration tests carried out in this PhD research were evaluated with the aid of a so-called overall normalized sensitivity method. This evaluation showed that for a wide range of sulfide levels (0.05-5 mM), not all parameters in the kinetic equations for the biological desulfurization process can be estimated accurately by means of conventional respiration tests, i.e. at oxygen saturation. Additional tests under oxygen limiting conditions are required. Furthermore, it appears that some parameters affect the activity of the biomass in two extremes at different substrate levels. In addition, in this chapter it has been shown that non-linear effects will impact significantly on scaling-up of the process from lab-scale to a full filed industrial system.

A linear relationship is generally described by a constant ratio between input and output. However, due to large influences of the quadratic terms in the approximate meta-models, it is evident that the upscale of the biodesulfurization process will show non-linear effects. This can be attributed to the combination of biological kinetic reaction rates and the ratio between oxygen transfer rate and sulfide load of the system. The resulting non-linear effects will play a significant role in the scaling up of the process from lab-scale to a full-scale industrial system in the field. The responses of a continuous stirred tank reactor (CSTR) model led to the conclusion that it is mainly the oxygen transfer rate of the reactor system that determines the selectivity of the process under limiting oxygen transfer conditions.

The physiologically-based kinetic model proposed in Chapter 3 was also incorporated in a full-scale biodesulfurization model that includes the effects of turbulent flow regimes and mass transfer of oxygen (**Chapter 6**). This full-scale biodesulfurization model was subsequently used to calculate the ORP behavior of a Thiopaq installation located at "Industriewater Eerbeek B.V.". The results are promising, as the model was able to explain the dynamic behavior of the system on the basis of inline ORP measurements, sour gas and air compressor flow. Furthermore, selectivity for formation of S^0 was estimated to be around 92 mol%, but varies between 90 and 94 mol% in practice. It is therefore likely that, in addition as tools for better process design, the developed models for ORP, kinetics and full-scale setups can also be used to develop better real-time, model-based control strategies, and will lead to better overall biodesulfurization plant performance.

Hoofdstuk 8

Samenvatting

Stromen van biologisch-, synthetisch- en aardgas vereisen mogelijk een behandeling om de aanwezige giftige en bijtende gasvormige zwavelverbindingen zoals waterstofsulfide, sulfiden en thiolen te verwijderen. Traditioneel worden fysisch-chemische technologieën gebruikt om dit gas te ontzwavelen. Ongeveer 25 jaar geleden werd een alternatief ontwikkeld, gebaseerd op de biotechnologische behandeling van gas. Deze manier biedt een aantal voordelen. Er is een hoge waterstofsulfide verwijderingsefficiëntie terwijl dit proces kan opereren bij een breed gebied van gasdrukken. Hiernaast zijn er geen stromen van sulfide rijk afval en geconcentreerd zwavelzuur. Tot slot maakt dit proces geen gebruik van chelatoren. Het biotechnologische proces vereist wel de toevoeging van natronloog en make-up water om te compenseren voor ongewenst gevormde zwavelverbindingen. Dit betekent dat er ook een spuistroom wordt gevormd. Om de kosteneffectiviteit van een grootschalige toepassing voor dit biotechnologisch proces te waarborgen is er een belangrijke vereiste. Dit is dat er een verbetering wordt doorgevoerd van het huidige ontwerp als mede van de controle regels. Deze verbetering richt zich op het minimaliseren van de toevoeging van natronloog en make-up water door het maximaliseren van de vorming van elementaire zwavel (S^0) bij de laagst mogelijke kosten.

Dit proefschrift start met een beschrijving van het werk dat is gericht op de reactie stoechiometrieën van de biologische oxidatie van opgeloste sulfide (**Hoofdstuk 2**). De experimentele resultaten tonen aan dat haloalkalifiele zwavel-oxiderende bacteriën in de bench-scale gas lift reactoren sulfide kunnen oxideren naar SO_4^{2-} via verschillende routes. Een van de routes vindt plaats wanneer opgeloste zuurstof concentraties worden gelimiteerd. We veronderstellen dat in deze route sulfide wordt geoxideerd tot S0 met behulp van een variant van flavocytochrome c oxidoreductase (FCC), sulfide: quinone oxidoreductase (SQR). We denken dat elektronen worden gedoneerd aan ubiquinone in plaats van cytochroom c en dat de elektronacceptor in plaats van zuurstof, NAD^+ is. Dit heeft tot gevolg dat deze route tot 25% minder zuurstof verbruikt voor de vorming van één mol SO_4^{2-} ten opzichte van oxidatie met zuurstof als enige elektronenacceptor. Deze bevindingen hebben gevolgen voor het optimaliseren van de vorming van S^0 omdat bij beperkte hoeveelheden opgelost zuurstof meer SO_4^{2-} kan worden gevormd, hetgeen ongewenst is.

Uit het werk beschreven in **Hoofdstuk 3** volgt dat twee sulfide-oxiderende enzymsystemen actief zijn in haloalkaliphilic zwavel oxiderende bacteriën, namelijk FCC en een variant van FCC die zich gedraagt als SQR. De uitgevoerde biologische respiratie testen geven als resultaat ten minste twee lokale optima in zuurstofverwijdering bij verschillende sulfide concentraties. Het is bekend dat bij hogere concentraties sulfide, het CCO / FCC enzymatische systeem wordt geremd. Bij sulfide concentraties boven 2,0 mM vertonen de sulfide oxiderende bacterieën (SOB) echter nog steeds een hoge respiratie activiteit. Deze activiteit van verwijdering van sulfide wordt toegeschreven aan een vorm van SQR. Tevens wordt in **Hoofdstuk 3** een model beschreven op basis van een concept van multi-substraat verwijdering en vorming van meerdere producten. De modelstructuur werd succesvol gevalideerd aan de hand van data sets van zowel de biologische respiratie testen als real-time reactor experimenten. Het gepresenteerde model voorspelt tot 98 mol% van S^0 formatie. Een uitdaging voor de toekomst zal zijn om de biologische vorming van S^0 te optimalizeren tot 98 mol% in de praktijk door verbetering van hetprocesontwerp. Hierbij valt te denken aan menging en operatie, bijvoorbeeld door middel van geavanceerde substraat injectie en opgeloste zuurstof (DO) regelstrategieën.

Dit proefschrift geeft ook zicht op het effect van de temperatuur. **Hoofdstuk 4** beschrijft de resultaten van fed-batch experimenten (lange termijn) en respiratie experimenten (effecten op korte termijn). Deze experimenten zijn uitgevoerd onder verschillende operatie temperaturen. De biologische activiteit werd omkeerbaar beperkt bij temperaturen beneden 15°C. Bij hogere temperaturen, dat wil zeggen bij temperaturen boven 48°C, was stabiele operatie in de fed-batch experimenten onmogelijk omdat de SOB onomkeerbaar geïnactiveerd wordt bij dergelijke hoge temperaturen. Het operatie gebied voor een stabiel biodesulfurizatie proces zal daarom liggen tussen de 15 - 45°C.

In **Hoofdstuk 5** wordt beschreven hoe de biologische respiratie testen, die in dit promotieonderzoek zijn uitgevoerd, werden geëvalueerd met behulp van een zogenaamde globale genormaliseerde gevoeligheids methode. Uit deze evaluatie bleek dat bij een grote variatie in sulfide niveaus (0,05-5 mM), niet alle parameters uit de kinetische vergelijkingen voor het biologische ontzwavelingsproces nauwkeurig kunnen worden geschat door middel van de gebruikelijke condities in de respiratie experimenten, dat wil zeggen bij zuurstofverzadiging. Aanvullende experimenten onder zuurstof limitatie zijn daarvoor vereist. Bovendien is gebleken dat bepaalde parameters de activiteit van de biomassa beïnvloeden in twee extremen door verschillende niveaus van het substraat.

Een lineair verband wordt algemeen beschreven door een constante verhouding tussen een ingangs- en een uitgangssignaal. De grote invloed van de kwadratische termen in de ontwikkelde meta-modellen maakt duidelijk dat het ontzwavelingsproces niet-lineaire effecten vertoont. Dit kan worden toegeschreven aan de combinatie van biologische kinetische reactiesnelheden en de verhouding tussen zuurstof overdrachtssnelheid en sulfide belasting van het systeem. De resulterende niet-lineaire effecten spelen een belangrijke rol bij het opschalen van laboratoriumschaal naar een grootschalig industrieel systeem. De model responties van een continu geroerde tank reactor (CSTR) model leidde tot de conclusie dat vooral de zuurstof overdrachtssnelheid van het specifieke reactor systeem bepaalt wat de selectiviteit van het proces wordt onder S^0 vormende condities.

Het in **Hoofdstuk 3** voorgestelde fysiologisch-gebaseerde kinetisch model werd ook toegepast in een full-scale biodesulfurization model. Dit model omvat de effecten van de turbulente stroming regimes en massa-overdracht van zuurstof (**Hoofdstuk 6**). Dit full-scale biodesulfurization model werd vervolgens gebruikt om het ORP gedrag van een THIOPAQ installatie "Industriewater Eerbeek BV"te evalueren. De resultaten zijn veelbelovend, omdat het model het dynamische gedrag van het systeem op basis van de metingen van de ORP, de stroming van het zure gas en de uitsturing van de luchtcompressor kon verklaren. Bovendien werd de selectiviteit voor de vorming van S^0 geschat op ongeveer 92 mol%, waarbij de praktijk varieert tussen de 90 en 94 mol%. Het is daarom waarschijnlijk dat, als instrument voor een betere procesontwerp, de ontwikkelde modellen voor ORP, kinetiek en de full-scale modellen ook gebruikt kunnen worden voor een ontwikkeling van real-time, modelgebaseerde controle strategieën. Dit zal uiteindelijk leiden tot een betere werking van het biotechnologische ontzwavelings proces.

Part IV

Appendices

Appendix A

Non-linear least-squares estimation physiologically based model

The unknown kinetic parameters in the physiologically based model, represented by the vector θ, are estimated using the experimental data of the respiration tests. The parameter vector θ is estimated in a (constrained) least-squares sense, which for the single-output case gives

$$\hat{\theta}_N = arg\ min_{\theta \in\ D} \sum_{k=1}^{N} \varepsilon([HS^-]_k \mid \theta)^2 \tag{A.1}$$

where $\varepsilon(.|\theta) = y(k) - \hat{y}(.;\theta)$ is the output error at time index k with sulfide concentration $[HS^-]_k$, $y(k)$ the measured oxygen respiration at k, $\hat{y}(.;\theta)$ the predicted model output at k given an estimate of θ $(\hat{\theta})$, D is the prior parameter domain and N the number of data points. A measure for the model fit is the error variance σ_ε^2, which is given by

$$\sigma_\varepsilon^2 = \frac{1}{N-p} \sum_{k=1}^{N} \varepsilon([HS^-]_k \mid \theta)^2 \tag{A.2}$$

with p the number of parameters. Local parameter (co)variances around the estimate $\hat{\theta}_N$ are given by the covariance matrix of the estimates (COV), defined by

$$COV\ \hat{\theta}_N = \sigma_\varepsilon^2 (X^T X)^{-1} \tag{A.3}$$

where X is the (N x p)] sensitivity matrix $\frac{\partial \varepsilon(HS_k^- | \theta)}{\partial \theta_j}$ with $k = 1, ..., N$ and $j = 1, ..., p$. Hence, the standard deviation of the estimates std$_{\hat{\theta}_N}$ are found after taking the square root of the diagonal of COV $\hat{\theta}_N$. Dominant directions of the estimates in the parameter space, are found from an eigenvalue decomposition of the covariance matrix, that is

$$V^T COV\ \hat{\theta}_N V = \Lambda \tag{A.4}$$

where V is an orthogonal matrix of eigenvectors and Λ is a diagonal matrix with eigenvalues. A large value of a diagonal element of Λ indicates a relatively large uncertainty in a direction in the parameter space, defined by the corresponding column of V. For details of the eigenvalue decomposition and its interpretation, we refer to Keesman (2011) [1].

References

[1] K. J. Keesman. *System Identification an Introduction*. Springer Verlag London, 2011.

Appendix B

Parameter estimation results physiologically based model

The final estimate of parameter vector θ with corresponding covariance matrix COV are given by

$$\hat{\theta}_N = \begin{pmatrix} \hat{q}_{FCC,max} \\ \hat{q}_{FQ,max} \\ \hat{q}_{CcO,max} \\ \hat{K}_i \end{pmatrix} = \begin{pmatrix} 1.35 \cdot 10^{-4} \\ 1.23 \cdot 10^{-4} \\ 6.71 \cdot 10^{-4} \\ 5.87 \cdot 10^{-2} \end{pmatrix} \tag{B.1}$$

$$COV\hat{\theta}_N = \begin{pmatrix} 3.91 \cdot 10^{-11} & -7.22 \cdot 10^{-12} & -1.02 \cdot 10^{-10} & 1.02 \cdot 10^{-7} \\ -7.25 \cdot 10^{-12} & 3.32 \cdot 10^{-12} & 2.21 \cdot 10^{-11} & -2.32 \cdot 10^{-8} \\ -1.02 \cdot 10^{-9} & 2.11 \cdot 10^{-10} & 2.88 \cdot 10^{-9} & -2.89 \cdot 10^{-6} \\ 1.02 \cdot 10^{-7} & -2.32 \cdot 10^{-8} & -2.89 \cdot 10^{-7} & 2.91 \cdot 10^{-4} \end{pmatrix} \tag{B.2}$$

The standard deviation of the estimates $\mathrm{std}_{\hat{\theta}_N}$ are found after taking the square root of the diagonal of $COV\hat{\theta}_N$ and are given by:

$$std_{\hat{\theta}_N} = \begin{pmatrix} 6.25 \cdot 10^{-6} \\ 1.82 \cdot 10^{-6} \\ 1.70 \cdot 10^{-4} \\ 1.70 \cdot 10^{-2} \end{pmatrix} \tag{B.3}$$

The eigenvalue decomposition of the covariance matrix results in

$$V = \begin{pmatrix} 3.49 \cdot 10^{-4} & -1.12 \cdot 10^{-1} & \mathbf{-9.88 \cdot 10^{-1}} & 1.00 \cdot 10^{-1} \\ -7.93 \cdot 10^{-5} & -7.29 \cdot 10^{-2} & 1.08 \cdot 10^{-1} & \mathbf{9.91 \cdot 10^{-1}} \\ -9.94 \cdot 10^{-3} & \mathbf{9.90 \cdot 10^{-1}} & -1.04 \cdot 10^{-1} & 8.43 \cdot 10^{-2} \\ \mathbf{1.00} & 9.88 \cdot 10^{-3} & -6.79 \cdot 10^{-4} & 8.81 \cdot 10^{-4} \end{pmatrix} \tag{B.4}$$

$$\Lambda = \begin{pmatrix} 2.91 \cdot 10^{-4} & 0 & 0 & 0 \\ 0 & 1.18 \cdot 10^{-10} & 0 & 0 \\ 0 & 0 & 2.28 \cdot 10^{-12} & 0 \\ 0 & 0 & 0 & 8.43 \cdot 10^{-13} \end{pmatrix} \tag{B.5}$$

Appendix C

Thermal inactivation

Considering the proposed inactivation equation [1], i.e.

$$\log S(t) = -b(T)t^{n(T)} \tag{C.1}$$

inactivation can be expressed in terms of the natural logarithm, such that

$$\frac{\log S(t)}{\log e} = \ln S(t) = -b'(T)t^{n(T)} \tag{C.2}$$

with $b'(T) = b(T)\log e$. As $S(t) := X(t)/X_0$, where $X(t)$ is the total amount of active biomass at time t and X_0 is the amount of active biomass at $t = 0$, the following relationship can be derived.

$$X(t) = X_0 e^{-b'(T)t^{n(T)}} \tag{C.3}$$

In case $n(T) = 1$, the following exponential law results:

$$X(t) = X_0 e^{-b'(T)t} \tag{C.4}$$

References

[1] M. G. Corradini and M. Peleg. Dynamic model of heat inactivation kinetics for bacterial adaptation. *Applied and environmental microbiology*, 75(8):2590–2597, 2009.

Appendix D

Sensitivity functions

When the following general non-linear, dynamic system is considered

$$\dot{x} = f(x, u; \theta) \tag{D.1}$$

where $\dot{x} := \frac{dx}{dt}$, a deviation in parameter θ_j will lead to

$$\frac{\partial}{\partial \theta_j} \dot{x} = \frac{\partial}{\partial \theta_j} f(x, u; \theta) = \frac{\partial f}{\partial x} \frac{\partial x}{\partial \theta_j} + \frac{\partial f}{\partial u} \frac{\partial u}{\partial \theta_j} + \frac{\partial f}{\partial \theta} \frac{\partial \theta}{\partial \theta_j} \tag{D.2}$$

with $j = 1 \cdots p$. Consequently, for input u independent of θ_j, the sensitivity functions, x an n-dimensional vector, are given by

$$\frac{\partial}{\partial \theta_j} \begin{bmatrix} \dot{x}_1 \\ \dot{x}_2 \\ \vdots \\ \dot{x}_n \end{bmatrix} := \begin{bmatrix} \dot{S}_{1,j} \\ \dot{S}_{2,j} \\ \vdots \\ \dot{S}_{n,j} \end{bmatrix} = \left[\frac{\partial f}{\partial x}\right]_{n \times n} \begin{bmatrix} S_{1,j} \\ S_{2,j} \\ \vdots \\ S_{n,j} \end{bmatrix} + \begin{bmatrix} \frac{\partial f_1}{\partial \theta_j} \\ \frac{\partial f_2}{\partial \theta_j} \\ \vdots \\ \frac{\partial f_n}{\partial \theta_j} \end{bmatrix} \tag{D.3}$$

with $S_{i,j} = \frac{\partial x_i}{\partial \theta_j}$. In matrix notation, for all sensitivities $\dot{S}_{1,1} \cdots \dot{S}_{n,p}$

$$\begin{bmatrix} \dot{S}_{1,1} & \cdots & \dot{S}_{1,p} \\ \vdots & \ddots & \vdots \\ \dot{S}_{n,1} & \cdots & \dot{S}_{n,p} \end{bmatrix} = \begin{bmatrix} \frac{\partial f_1}{\partial x_1} & \cdots & \frac{\partial f_1}{\partial x_n} \\ \vdots & \ddots & \vdots \\ \frac{\partial f_n}{\partial x_1} & \cdots & \frac{\partial f_n}{\partial x_n} \end{bmatrix} \begin{bmatrix} S_{1,1} & \cdots & S_{1,p} \\ \vdots & \ddots & \vdots \\ S_{n,1} & \cdots & S_{n,p} \end{bmatrix} + \begin{bmatrix} \frac{\partial f_1}{\partial \theta_1} & \cdots & \frac{\partial f_1}{\partial \theta_p} \\ \vdots & \ddots & \vdots \\ \frac{\partial f_n}{\partial \theta_1} & \cdots & \frac{\partial f_j}{\partial \theta_p} \end{bmatrix} \tag{D.4}$$

Notice from Eq. D.4 that the calculation of one single sensitivity function ($S_{i,j}(t)$) would require the simultaneous simulation of all sensitivities.

Appendix E

Meta models

The following vectors and matrices were found for the meta models (Eq. 5.21), describing the competition between biological S^0 and SO_4^{2-} formation (Y_{bio}):

A_{bio} =

$$\begin{pmatrix} -9.8 \cdot 10^2 \\ 2.0 \cdot 10^3 \end{pmatrix}$$

B_{bio} =

$$\begin{pmatrix} 4.2 \cdot 10^5 & -4.0 \cdot 10^5 \\ -4.0 \cdot 10^5 & -5.4 \cdot 10^4 \end{pmatrix}$$

And, describing the competition between biological S^0 formation and chemical $S_2O_3^{2-}$ formation (Y_{chem})

A_{chem} =

$$\begin{pmatrix} 1.0 \cdot 10^3 \\ -6.1 \cdot 10^2 \end{pmatrix}$$

B_{chem} =

$$\begin{pmatrix} 1.1 \cdot 10^5 & -4.9 \cdot 10^4 \\ -4.9 \cdot 10^4 & 9.4 \cdot 10^4 \end{pmatrix}$$

List of publications

M. de Graaff, J.B.M. Klok, M.F.M. Bijmans, G. Muyzer, and A.J.H. Janssen. Application of a 2-step process for the biological treatment of sulfidic spent caustics. *Water Research*, 46(3):723-730, 2012.

J.B.M. Klok, P.L.F. van Den Bosch, A.J.M. Stams, C.J.N. Buisman, K.J. Keesman, and A.J.H. Janssen. Pathways of sulfide oxidation by haloalkaliphilic bacteria in limited-oxygen gas lift bioreactors. *Environmental Science and Technology*, 45(14):7581-7586, 2012.

J.B.M. Klok, M.M. de Graaff, P.L.F. van den Bosch, N.C. Boelee, K.J. Keesman, and A.J.H. Janssen. A physiologically based kinetic model for bacterial sulfide oxidation. *Water Research*, 45(2):483-492, 2013.

Dankwoord

Het lijkt alweer lang geleden dat het allemaal begon. De Ir-titel was nog niet officieel binnen en ik zat al weer achter een computer op de universiteit. In de vier jaar die ik aan het onderzoek heb besteed, zoals beschreven in deze thesis, ben ik een klein rad geweest van een groot team. Daarom wil ook mijn oprechte dank uitspreken voor de volgende mensen zonder wie dit onderzoek nooit tot een goed einde zou zijn gekomen.

Als allereerst wil ik graag Albert Janssen, mijn promotor, bedanken. Het was voor mij al snel duidelijk dat ik, met jouw wetenschappelijk lading, een hele goede 'kapitein' op het onderzoek had. Dat je niet standaard aanwezig was op de vakgroep, belette het onderzoek niet. Er waren veel momenten waarop de koers van het onderzoek uitvoerig besproken werd. Je hebt me altijd bij de les gehouden door scherpe maar haalbare doelen te stellen. Daarnaast had ik ook nog eens de luxe dat mijn schrijf-/lab-/modelwerk snel en accuraat door jouw werd bekeken en met grote snelheid van waardevolle feedback werd voorzien. Je was altijd bereikbaar. Voor dit alles heb ik heel veel waardering.

Ook Karel Keesman, mijn co-promoter, ben ik erg dankbaar. Eigenlijk ben ik van de leerschool *Keesman*. Omdat ik al jouw vakken heb gevolgd, een afstudeervak en stage onder jouw begeleiding heb gedaan, en nu dus ook mijn promotie bij jou heb afgerond. Dankzij jou ben ik niet vast komen te zitten in het onderzoek, jij zag altijd openingen. Volgens mij hebben we nog nooit een kort gesprek gevoerd, dat was volgens mij niet mogelijk met alle ideeën die over en weer gingen. Het was een bijzonder fijne samenwerking.

Dankzij mijn voorganger bij milieutechnologie, Pim van den Bosch, heb ik een vliegende start kunnen maken. Je hebt me in contact gebracht met het ontzwavelingsproces in het lab Daarnaast ben je mijn gids geweest in de eerste maanden van het project op de vakgroep. Ook mijn partner in crime, Marco de Graaff, ben ik erg dankbaar. Nadat we elkaar hebben gevonden kreeg het onderzoek een boost door interpretatie van de respiratie curves die werden gevonden. Ik kan me niet indenken hoe ik het onderzoek zonder jou heb kunnen doen.

Een belangrijk aspect van het onderzoek lag in de praktische toepassing. Ik ben daarom ook bevoorrecht geweest dat we in een groot zwavel team werkten met specialisten die veel input aan dit project hebben geleverd: Gijs van Heeringen, Jiri van Straelen, Erik van Zessen, Jan-Henk van Dijk, Fons Stams, Martijn Bijmans, Gerard Muyzer, Caroline Plugge, Dimitri Sorokin, Pawel Roman en Joao Sousa. Pawel en Joao in het bijzonder bedankt voor het aanleveren van het materiaal voor de laatste testen die ik heb kunnen doen.

Graag zou ook de personen willen bedanken die actief hebben mee gedacht met mijn onderzoek: Cees Buisman (het was bijzonder om ook jouw resultaten tegen het licht te houden), Bert Hamelers (cytochromen zijn interessante moleculen), Maarten Biesheuvel (wat zijn modellen toch mooi), Kees van Asselt (sensoren zijn toch niet zomaar plug en play), Rene van Veldhuis (Industrie water Eerbeek) en Kees van den Ban (Paques, voor de gesprekken over en data van de moeder van alle Thiopaq reactoren), Rachel van Ooteghem (Latex en Matlab tips) en Gerard van Willegenburg ('White box' modeleren is te gek). Dank Vinnie de Wilde, Bert Willemsen, Hillion Wegh, Ilse Gerritse, Katja Grolle, Ardy Beurskens, Hans Beijleveld en Jan Kubiak voor jullie onmisbare hulp in het lab. En natuurlijk dank aan de mensen van het secretariaat: Liesbeth Kesaulya, Anita van de Weerd, Marja Portengen, Romana Zigova en Gea Witsiers. Ook een speciale dank voor mijn BHV-collega's Mieke van Eerten en Miriam van Eekert, wat waren die herhalingslessen toch zonniger met jullie aanwezigheid.

Ook zijn er veel collega's die mijn periode bij de beide vakgroepen tot een mooie periode hebben gemaakt. Met name Paula, Claudia, Kanjana, Simon, Kirsten, Niels, Marjolein, Cees, Ralph, Koen, Tim, Annemiek, Alex, Ruud, David, Jimmy, James, Ellen, Xin, Emmanuel, Nurul en ieder ander die ik ben vergeten te vermelden.

Als laatste, dank lezer, dat je (delen van) dit boekje hebt willen lezen!

Jan Klok Wageningen, April 2015

About the author

Johannes Bernardus Maria (Jan) Klok was born on October 15, 1983 in Delft (The Netherlands). He finished his high-school education (VWO) in 2001 at "Het Reynaertcollegeïn Hulst. He started in the same year the study of bioprocess technology at Wageningen University. For his thesis, he worked at the Systems and Control group on desinfection of water with UV radiation which also was the topic of his internship at KWR Water Research Institute. In may 2009, he started his PhD research at the Sub-department of Environmental Technology of Wageningen University. From July 2013, he continued working on the biological desulfurization process at Paqell.

The research described in this thesis was financially supported by Shell (Amsterdam, the Netherlands).

Photographs cover: Yvonne Mos, Paqell

Cover design by Luuk Schouten